DELINEATION OF GOLD MINERALIZATION ZONE AT AHAFO APENSU SOUTH CONCESSION, NEWMONT GHANA GOLD LIMITED, USING CROSS BOREHOLE INDUCED POLARIZATION AND ELECTRICAL RESISTIVITY METHODS.

by

ALFRED AGYEI BERKO , BSc Geological Engineering (Hons)

A Thesis Submitted to the Department of Physics,

Kwame Nkrumah University of Science and Technology

in partial fulfillment of the requirements for the degree

of

MASTER OF SCIENCE (GEOPHYSICS)

College of Science

Supervisor: Dr. K. Preko
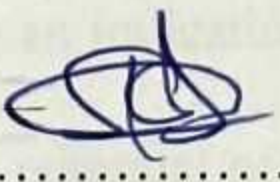
© Department of Physics

October, 2013

DECLARATION

I hereby declare that this submission is my own work towards the award of MSc. Geophysics degree and that, to the best of my knowledge, it contains no material previously published by another person or material which has been accepted for the award of any other degree of the University except where due acknowledgement has been made.

ALFRED AGYEI BERKO 4/11/13

Student   Signature   Date

Certified by:

DR K. PREKO 4/11/13

Supervisor   Signature   Date

Prof. S K Danuor 5/11/13

Head of Department   Signature   Date

Abstract

Hole-to-hole IP/resistivity method was used to explore the zone of gold mineralization at depth on the Newmont Apensu-South Concession to improve the dependability and quality of the subsurface data which led to effective utilization of the drill holes and provide Induced Polarization/Resistivitydata at depth which cannot be obtained in ground IP/resistivity surveys. Pyrite logging of all the drill cores from the holes established the presence of disseminated sulphides (pyrite) in all the drill holes which is the key signature mapped in the IP data in the project area. Chargeability measurements carried out on selected drill holes showed very good correlation with the gold values at depth with a strong positive correlation between chargeability and gold grade with correlation coefficient of 0.83. Laboratory resistivity measurements carried out on some selected drill cores on hand showed poor negative correlation between gold assay value and resistivity value with correlation coefficient of -0.37. The chargeability model from the hole to hole survey aided in the mapping of the gold mineralized zone using a threshold value of 8.5 ms. The model from the chargeability data was very successful in delineating the zone of high chargeability at a depth of about 300 m giving an indication of deep zones of gold mineralization within the study, hence showing a high potential of underground mines. The resistivity data from the hole-to-hole survey could not delineate the gold mineralized zone at depth.

Contents

KNUST

List of Tables

List of Figures

List of Symbols and Acronyms

ϕ	Fraction of the rock filled with the fluid
ρ and ρ_w	Rock resistivity and Fluid resistivity
σ	Conductivity of the medium
J	Current density
E	Electric field intensity
r	Distance of a point in the medium from the electrode.
r_{C1} and r_{C2}	Distances of the point from the first and second current electrodes
P1 and P2	Potential electrodes
C1 and C2	Current electrodes
ρ_a	Apparent resistivity
k	Geometric factor
V and M	Voltage and Chargeability
V_o and V_p	Observed voltage and Overvoltage
A	Area under curve
$\rho_{.0}$	Apparent resistivity at low frequency
$\rho_{.1}$	Apparent resistivity at high frequency
R	Resistance
FE and PFE	Frequency effect and Percentage frequency effect
MF and S	Metal factor and Distance between two drill holes
D and B	Drill hole depth and IP probe location in drill hole

Acknowledgments

I am very grateful to the Department of Physics K.N.U.S.T for the opportunity to upgrade myself with this program. I also offer my sincere gratitude to all my lecturers during this period especially Dr. Kwasi Preko and Mr. David Dotse Wemegah who were my direct supervisors for making this work what it is today. How can I forget my employers, Newmont Ghana Gold Ltd for giving me unrestricted access to both the site and the tools to complete the field work and the data as well. To Jeremy Cook, Chief Geophysicist-Operations, Newmont Ghana Gold Ltd for the idea to work on this project for my thesis work. Thank you very much Dave Wynn for being with the group right throughout the whole field work and working on the data as well. My heartfelt gratitude goes to Mr. Thomas Tsiboah (Supervising Geophysicist- Newmont Ghana Gold Ltd) for his inspiration, support and corrections before, during and up until now. There were times I thought you were making things tougher for me but it really added weight to my work. I salute you sir. How can I forget you Mr. Kwaku Takyi-Kyeremeh for taking time to go through this work and offer your thoughts. Also, I express my sincere thanks to my course mates and colleagues at work who were with me throughout the field work especially George Annan and Augustine Nsiah.

Finally, to my beautiful wife Mrs. Akua Agyei Berko, I say well done for always pushing me to get on when it seemed difficult at times and all my family for the prayers and support that has brought me this far. May the almighty God richly bless you.

CHAPTER 1

INTRODUCTION

Electric IP (Induce Polarization)/resistivity surveying along the Earth's surface is a well-known geophysical exploration technique. Due to its conceptual simplicity, low equipment cost and ease of use, the method is routinely used in mineral exploration. Borehole IP/resistivity tomography, in which both current electrodes and potential electrodes placed in two boreholes can provide detailed information about IP/resistivity distribution between the boreholes (Daniels and Dyck, 1984). Daniels and Dyck (1984) demonstrated a variety of applications of borehole resistivity measurements to mineral exploration. Unfortunately, these early case histories did not include an inversion of the data. Conventional mise-a-la-masse types of measurements are carried out by placing a current electrode in a conductive zone and measuring the potential field distribution in one or more boreholes (Mwenifumbo, 1997). The recently enhanced computing resources and capabilities have created the environment for the increasing interest to construct tomographic images through geophysical inversions (Loke and Barker, 1996) since this makes it possible for large data set to be processed. The use of borehole resistivity imaging goes a long way to lead to the effective utilization of these holes. In this measurement quality data is obtained if the boreholes under consideration are water filled as the electrode array couples to the rock formation and current also needs to pass through the water medium.

1.

Geophysical borehole logging is the recording of rock characteristics at regular intervals along the depth of a drill hole. The tools used are called geophysical probes which detect the rock's natural radioactivity, porosity, density, electrical resistance and many other physical properties. The probe thus used depends on the physical property of interest. Among other things, the logs from drill holes provide information on one of the following;

- Rock layer boundaries.

- Changes in rock type like the 'clayeyness' of a rock formation.

- Zone of mineralization and their thickness.

- Depth to the water table and where aquifers are located down the hole.

The cross borehole IP/resistivity configuration was developed to increase the detection radius around the drill holes being surveyed compared to the detection radius that can be achieved with a classical borehole IP/resistivity. The classical borehole IP/resistivity like the ground IP/resistivity is used to map disseminated sulphides in the proximity of the drill hole. Data inversion and interpretation techniques can help in the mapping of the distribution of polarizable material surrounding the drill hole. However, due to the limited radius of penetration the classical borehole IP/resistivity method, only limited directional information about the mineralized zone can usually be obtained.

The desire to overcome these limiting factors of classical borehole logging led to the development of the cross borehole IP/resistivity method. This method utilizes two potential electrodes in two distinct holes; therefore, the in-hole mineralization has less effect on the detection radius. A target horizon near the bottom of the hole can be mapped because the potential electrodes can be lowered to the bottom of the holes. Again, many hole-pairs may

2

be read and simultaneously processed to deliver an integrated interpretation with an inversion providing a 3-D image of the target (Berube and Wasylechko, 2010).

The use of the cross borehole IP/resistivity tomography in the delineation of gold mineralized zone is the latest addition to the array of geophysical methods employed by Newmont Ghana Gold in its quest for gold exploration in Ghana. Being at the forefront in the use of geophysical methods; namely IP/resistivity, ground gravity, ground magnetic, EM in its exploration activities in Ghana and the rest of Africa, it is with keen interest that this research work was carried out to see if it can be added to the company's long list of geophysical methods.

The Ahafo South concession of Newmont Ghana Gold limited is one of the main ongoing mining projects in Ghana with much attention to expand the existing deposits. The Apensu South deposit is one area work is ongoing to expand the strike length of the deposit. The area has been extensively explored using many geophysical techniques including ground gravity, ground magnetic, IP/Resistivity (both 3-D and gradient array) and TEM. However, not much work has been done in this area using classical borehole logging making this survey very imperative.

This research work will help delineate the gold mineralized zone of the area and help improve the IP and resistivity model of the subsurface while coming up with new model of the project area. A lot of drilling has also been carried out on this concession with most of the drill holes cased which makes it a better site for this research work. Chargeability anomalies mapped especially in the 3-D IP model should be confirmed with the IP downhole logging after drilling.

1.1 Study Area

1.1.1 Regional Setting

The Newmont Ahafo Project is located in south-western Ghana, approximately 300 km northwest from the Capital of Accra (Figure 1.1). It is 107 km northwest of Kumasi, and 40 km south of the regional capital of Sunyani. The currently known reserves and resources at Ahafo, as well as significant extensions to the strike length of the Ahafo mineralized zones, are secured by the Yamfo-Kenyase and the Rank mining Lease.
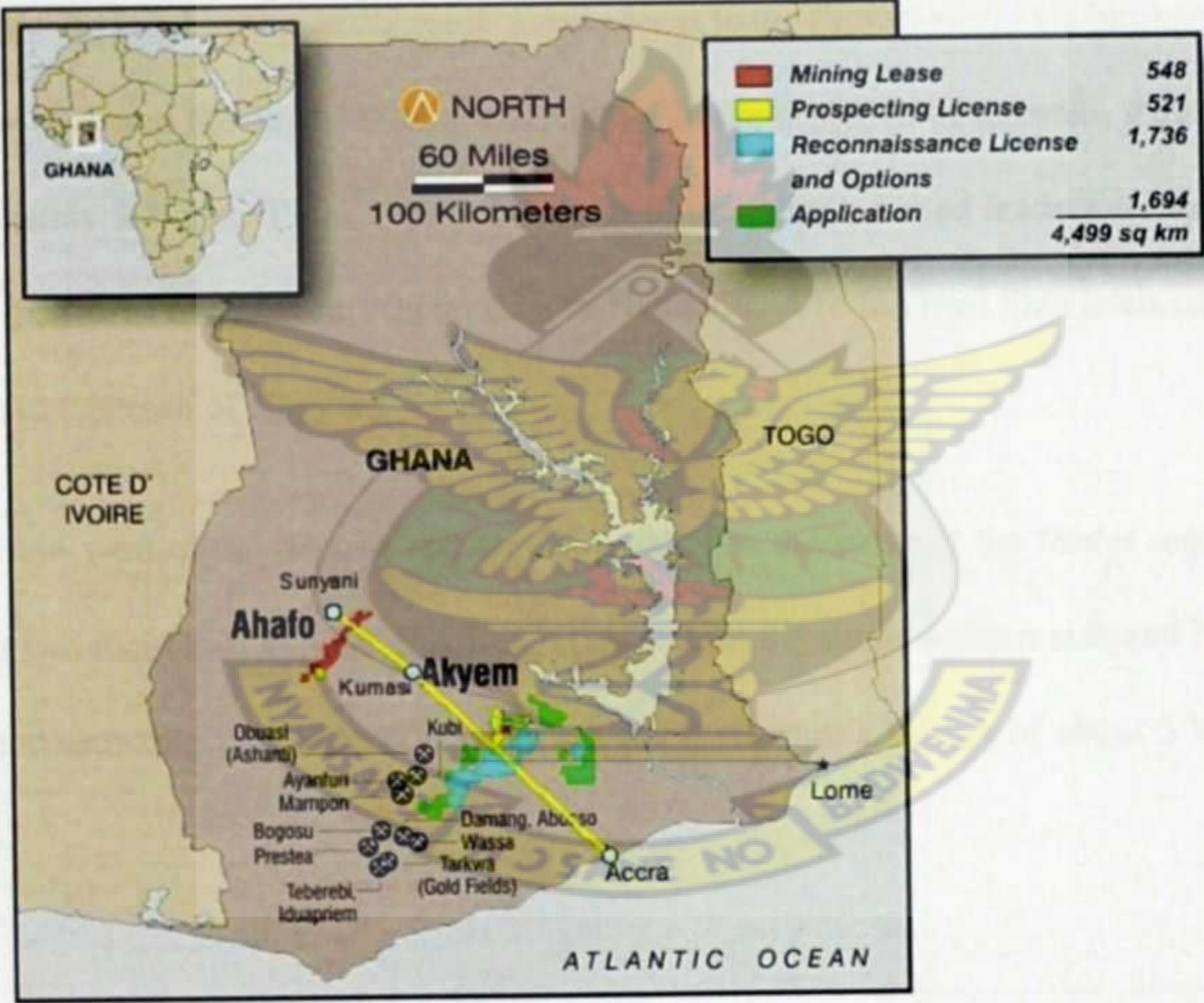
Figure 1.1: Map of Ghana showing Ahafo, the location of Newmont Ahafo project.

The Project is being developed in two phases, Ahafo South Area (Phase One) and Ahafo North Area (Phase Two). Ahafo South area (Phase One) is where Apensu south is located.

In addition, a number of reconnaissance and prospecting licenses cover areas immediately towards the west, south and east of the main mineralized structure.

1.1.2 Location and Accessibility

The Apensu-south gold property is located between the towns of Kenyase and Ntotorosoin the Brong-Ahafo Region (Figure 1.2). Road access to the Project site is via bitumen sealed road from Accra to the Tepa Junction via Kumasi in the direction of Sunyani, a distance of approximately 300 km northwest of Accra. It is 107 km northwest of Kumasi, and 40 km south of the regional capital of Sunyani. Road access to the Project site is via bitumen sealed road from Accra to the Tepa Junction via Kumasi in the direction of Sunyani, a distance of approximately 300 km. From Tepa Junction, a bitumen sealed road leads west for 39 km through the towns of Tepa and Akyerensua to Hwidiem. A tarred road then leads northwest for 8 km to the town of Kenyase.

About 1 km west of the deposit and almost parallel to the strike is the feeder road which connects two main towns in the area,Kenyasi No. 2 on the south western side and Ntotroso on the northern side. This road runs through Kwakyekrom, a village of about 5 km from Ntoroso.

1.1.3 Physiographic Settings and Climate

The Project area comprises low rounded hills with elevations ranging from 110 m to 540 m above mean sea level. Seasonal streams and tributaries of the Tano River basin drain the broad, relatively flat valleys.

5
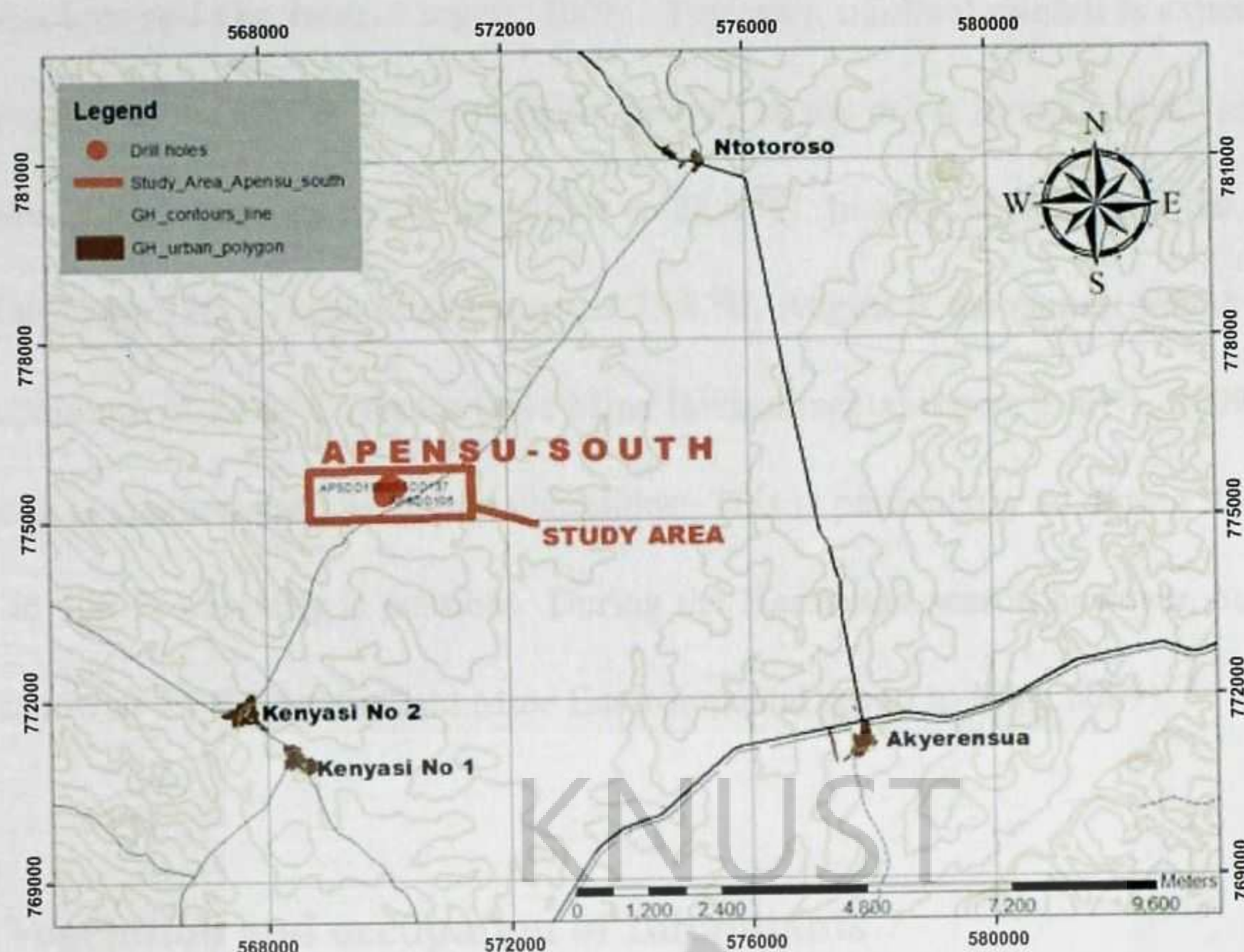
Figure 1.2: Map showing the location of Apensu-south deposit.

The Ahafo Project Area falls within the wet semi-equatorial climatic zone of Ghana and is characterized by an annual maximum rainfall pattern occurring in the months of May to July and from September to October. The climate of the area is determined by movement of air masses which differ in air moisture and relative stability rather than temperature (Ahafo Gold mine Environmental report to EPA, 2007). The two air masses, namely the southwest monsoon and the northeast trade winds, come into contact along the Inter-Tropical Convergence Zone (ITCZ). The ITCZ which passes over the area twice yearly is responsible for the annual succession of seasons. The northern air masses locally called 'Harmattan' coming from the sub-tropical Azores anticyclone and its extension over the Sahara Desert bring hot and dry weather from December, to February (Newmont Ahafo Gold mine environmental report to EPA, 2008).

Mean annual rainfall for the Project area is between 1354 and 1400 mm (Newmont Ahafo

6

Mineral resource and Ore reserve report, 2008). Typically, minimal rainfall is experienced from December to the end of February, with January as the driest month. Mean monthly temperatures within the area range from 23.9 to 28.4 ^{0}C. In general, March is the hottest month of the year with a mean temperature of 27.8 ^{0}C. August is the coolest month with a mean temperature of 24.6 ^{0}C (Ahafo Gold Mine Environmental report to EPA, 2009). The rainy season is characterized by humid conditions. This is particularly so during the night, when 95 to 100 % humidity is possible. During the Harmattan season however, humidity drops to as low as 25 % (Ahafo Gold Mine Environmental report to EPA, 2009).

1.1.4 Vegetation and occupation of Inhabitants

Vegetation in the Project area is composed of a mixture of natural plant communities in early stages of ecological succession, crops, and plantations, patches of second growth forest, and riparian communities along rivers and streams. The natural vegetation in the Project area has been extensively fragmented as a result of agricultural activities, fire, and removal of timber and, consequently, has little resemblance to the native forest communities once typical of the region. Following extensive nation-wide fires in 1983, areas previously dominated by trees and shrubs have been taken over by dense stands of elephant grass (Ahafo Gold Mine Environmental report to EPA, 2006).

The Ahafo Project area shares a boundary with the Bosumkese Forest Reserve, and the AmomaShelterbelt Forest Reserve bisects the Project. The Bosumkese and Amoma Shelterbelt Forest Reserves contain remnants of the Eastern Guinean Forest that at one time covered extensive areas of central Ghana including the project area.

7

The project area consists primarily of subsistence farms with small-scale commercial farming intermingled with areas of forest regrowth and remnants of secondary forest. The major agricultural land users are cocoa, food crop and rice farming. South of the Bosumkese Forest Reserve cocoa farming is the major activity while to the north maize farming dominates.

1.2   Geological Setting

1.2.1   Regional Geology

Large parts of south-western Ghana are covered by Palaeoproterozoic rocks (ca. 2.2 Ga) of the Birimian Supergroup and the overlying clastic sedimentary Tarkwaian Group. The Birimian Supergroup has been divided into the metasedimentary unit (Lower) and metavolcanic(Upper) unit (Junner, 1935; 1940).

The Birimian metasediments comprise a volcanosedimentary assemblage composed of volcaniclastics, wackes, feldspathic sandstones, argillites, and some chemical sediment including Mn-rich formations. The Birimianmetavolcanics is made up of basalts and some interflow sediment. The classical subdivision of the Birimian was reinterpreted by Leube and Hirdes (1986) and Leube et al. (1990). These authors regard Birimianmetasediments and Birimianmetavolcanics as a coeval sequence in which the volcano-sedimentary assemblage (sedimentary basins) represents a distal facies of volcanic belts.

The Tarkwaian formation is a fluviatile consisting of coarse-clastic sedimentary rocks, including conglomerates which are locally gold-bearing (Banket series), as well as

8

sandstones and minor shales. The supracrustal sequences were folded and metamorphosed under greenschistfacies conditions during the Eburnean tectonothermal event at about 2.1 Ga (Leube et al., 1990; Hirdes et al., 1992; Taylor et al., 1992).

Structural investigations by (Eisenlohr, 1989), revealed that Birimian and Tarkwaian rocks were deformed jointly during a single progressive event which involved an initial regionally penetrative low-strain phase producing S1 foliation. This was followed by the formation of high-strain zones (S2) which are commonly located close to the basin/belt contacts. Major thrusts and shears resulting from the deformational events acted as channel ways for mineralizing hydrothermal fluids.
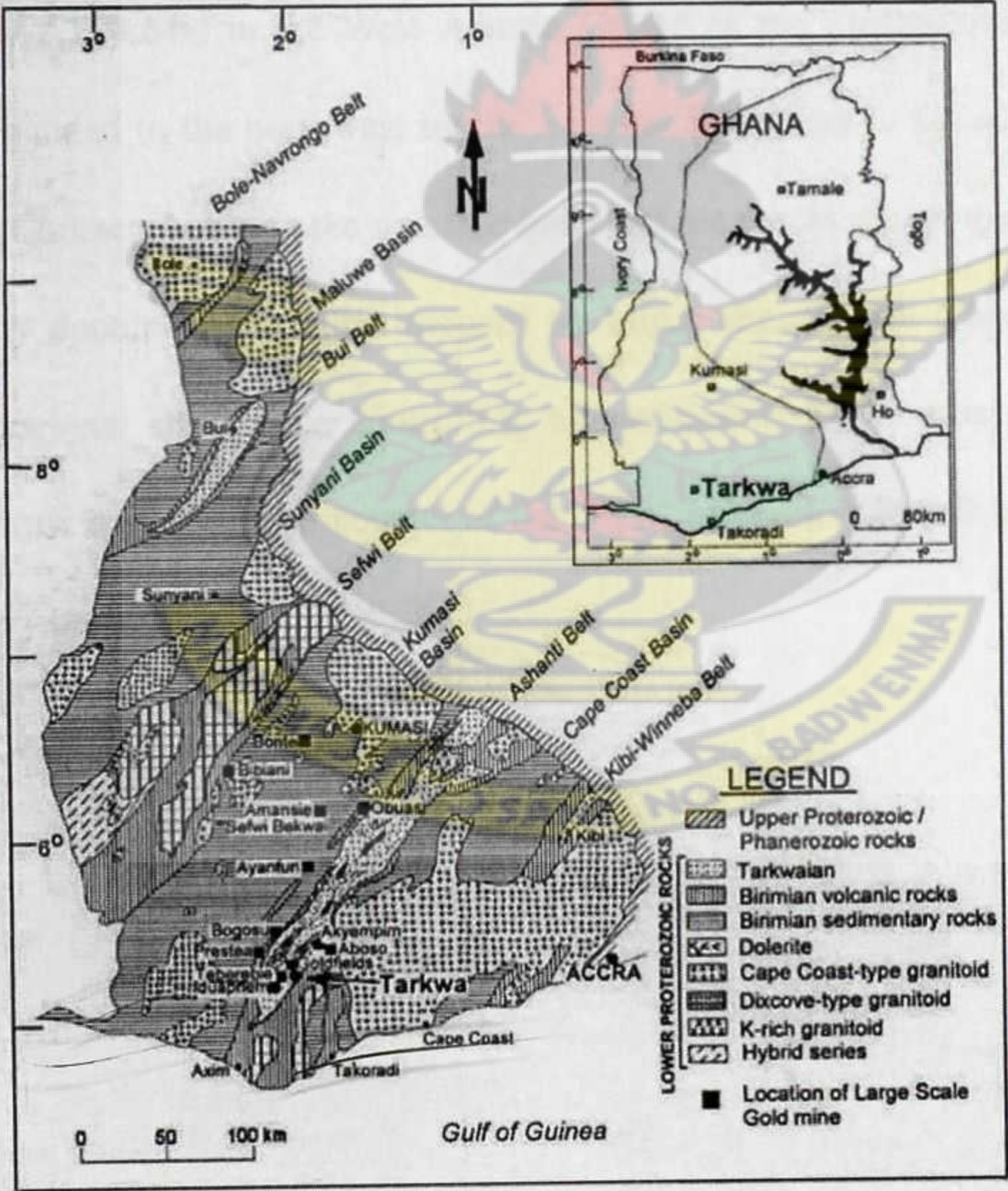
Figure 1.3: Geology map of Ghana showing the gold belts (modified from Leube et al., 1990).

9

The volcanic belts and the sedimentary basins are intruded by igneous rocks mainly granitoids. The granitoids are the belt-type granitoids in the volcanic belts, and the basin-type granitoids in the sedimentary basins (Figure 1.3). These geological events took place at different time intervals between 2180-2170 Ma and 2116-2088 Ma, respectively (Hirdes et al., 1992).

1.2.2   Local Geology

The Apensu-South project is located in the Sefwi Belt and is one of the five NE-SW trending Birimian volcanic belts exposed in south western Ghana. It lies within the Eburnean Tectonic Province (1,800-2,166 Ma) in the West African Craton of the Precambrian Shield. The Sefwi belt is bounded to the northwest by the Sunyani Basin and to the southwest by the Kumasi Basin. Contacts between the volcanic belts and the basins are all major shear zones characterized by ductile fabrics superimposed by brittle shear zones (Griffis and Agezo, 2000). The Regional shear zone controlling mineralization in the area is the Kenyase Thrust. The thrust is the western contact of the Sefwi metavolcanic belt and the Sunyani metasedimentary basin.

10
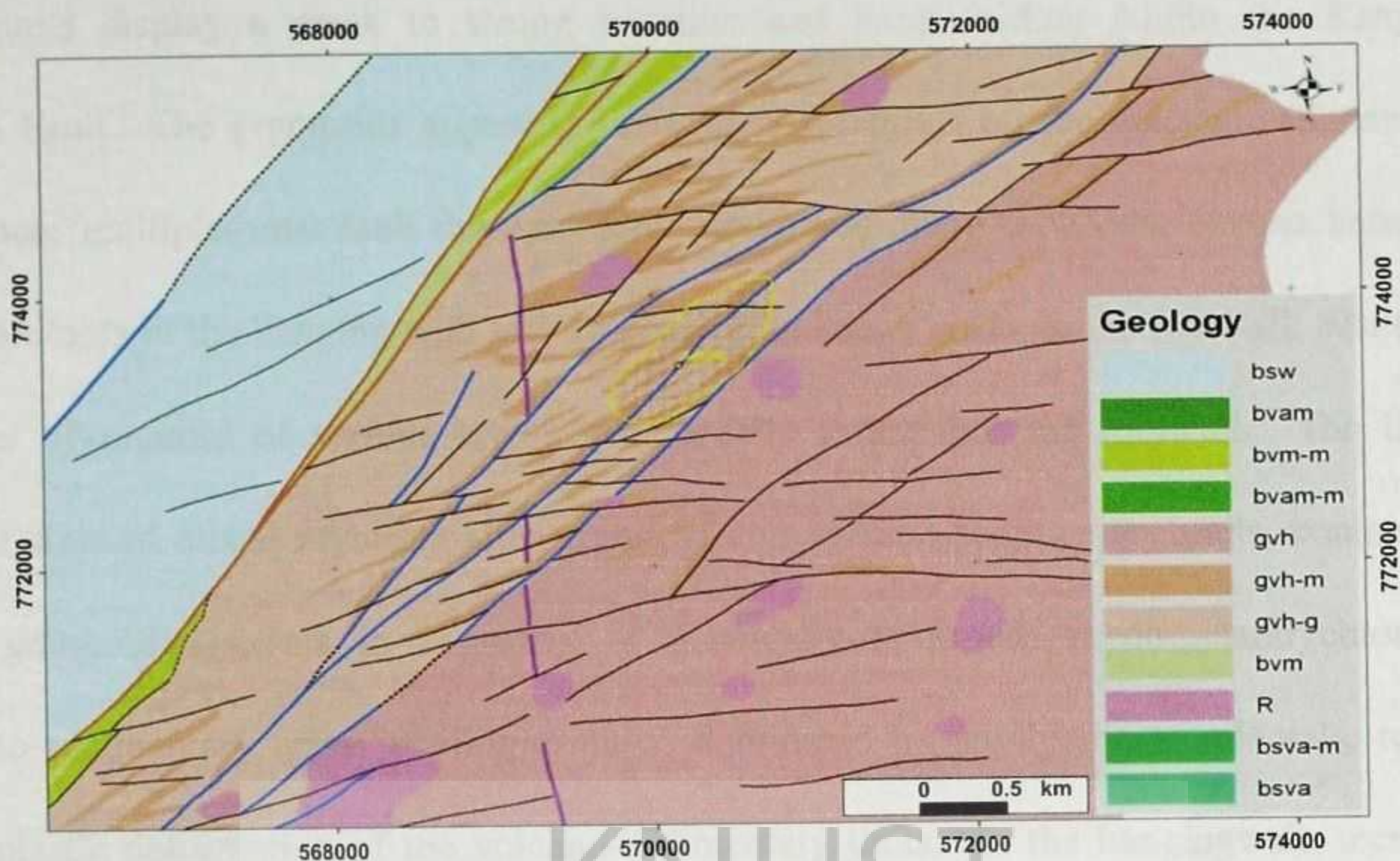
Figure 1.4: Geology of the study area (modified from Cook 2007) bsw - Sedimentary basin domain wackes; gvh - Volcanic belt domain (belt granitoids); R - Discove granitoid and bvm - Birimian metavolcanics basalt.

The Apensu deposit is one of the four Ahafo South deposits and is located on the main Kenyase Thrust Fault zone at the southern edge of the Ahafo trend. It is considered to be a Kenyase-style deposit, localized in a left-hand jog in the thrust fault. The thrust is the western contact of the Sefwi metavolcanic belt and the Sunyani metasedimentary basin (Figure 1.4)

1.2.2.1 Kenyase-style mineralization

Six lithologies and/or litho-structural units have been recognized in the Kenyase-style zones,consisting of: Weakly foliated mixed (meta)-pelitic sedimentary rocks and (meta)-maficvolcanic units attributed to the lower Birimian volcano-sedimentary sequence occur in the footwall of the Kenyase Thrust Fault; Dixcove Suite granitoids form the hangingwallto the thrust. Rocks within the suite vary in composition from granitic to granodioriticto tonalitic and dioritic; locally, 'mylonite after granitoid' can occur. The

11

rock units display a weak to strong foliation and local folding within the Kenyase Thrust Fault. The granitoids appear to have been overthrust on the volcano-sedimentary sequence; multiplethrust fault duplexes have developed along the thrust contact between the granitoids in the hanging wall and volcano/sedimentary rocks in the footwall. Multiple wedges ofgranitoid of various scales were locally thrust into the footwall. The latter form a zone of mixed mylonite after granitoid and volcano-sedimentary units, containing rigid granitoidfragments in a matrix of plastically-deformed, predominantlychloritic, volcano-sedimentary units; phyllonite units, dominated by phyllosilicate minerals, result from plastic deformation of the volcano-sedimentary units. In the hangingwall, tectonic breccias (cataclasite) and finely-crushed rock form within the granitoid units by local, brittle reactivation on or near the Kenyase Thrust Fault.

These rock units have been strongly weathered to a depth of about 50 m, resulting in development of duricrust and saprolite. The duricrust ranges from 1 m to 7 m thick, comprising zones of iron pisolites and iron cement that represent transported material. Most areas are not covered by duricrust. The underlying saprolite is characterized by a complete oxidation of the original sulphides that may locally extend a few meters into the primary bedrock. Partial oxidation of primary sulphides is found as much as 15 m below the boundary of complete oxidation. The partially oxidized zone is rather regular (horizontal) at the deposit scale but oxidized fingers locally extend downwards along joints and fractures into the primary rock.

Hydrothermal alteration in Kenyase Style deposits is characterized by alteration of primary chlorite to sericite-silica, and the addition of silica, iron carbonate, pyrite and local albite to the host rock. Alteration has been characterized and logged as weak, moderate, or strong. Alteration within the Kenyase-style zones has been subdivided into three styles, weak,

12

moderate, and intense: Moderate alteration forms a broad halo in the brittle granitoid unit and a much narrower halo in the less permeable footwall units, primarily focused in slightly more brittle and permeable mixed mylonites. Strong alteration occurs in the cataclasite unit.

Deposits considered to be representative of Kenyase-style mineralization are, from south to north, Apensu (formerly called Kenyase Central), Awonsu (Kenyase East), Amoma (Bosumkese) and Line 10 deposits, Amoma, Awonsu and Apensu. Although the Line 10 deposit is not located exactly on the Kenyase Thrust Fault, Newmont considers that it exhibits all the other features of the Kenyase-style deposits.

1.2.3 Lithology

In chronological order from oldest to youngest, the various lithological units of the Kenyase Style deposits are characterized as follows.

1.2.3.1 Meta-sediments and meta-volcanosedimentary units

The footwall of the Kenyase Thrust contact is comprised of mixed (meta)-peliticsediments and (meta)-mafic volcanic units that are presumably of the Birimianvolcano-sedimentary sequence (grey in Figure 1.5). The units contain a pervasive weak foliation, possibly associated with the various structural events in the Birimian.

13

1.2.3.2 Dixcove Suite granitoids

In the hanging wall of the Kenyase Thrust zone and overlying the volcano-sedimentary units are the Dixcove Suite granitoids (orange in Figure 1.5). The nature of the granitoid varies between deposits, from acidic at Apensu to more granodioritic at Awonsu, tonalitic at Amoma and dioritic.

1.2.3.3 Myonite after granitoid

The granitoids were thrust over the volcano-sedimentary units, most likely during the D2 Eburnean orogenesis, and a series of additional units were created by deformation during the emplacement of the thrust. Near the fault contact the deformed granitoid generated a local 'mylonite after granitoid' with a weak to strong foliation and local folding. This mylonite after granitoid is focused in the Kenyase fault where multiple duplex splays also developed.

1.2.3.4 Zone of mixed mylonite

Multiple duplexes developed along the thrust contact between the granitoids in the hanging wall and volcanic/sediments in the footwall and multiple wedges of granitoid of various scales were locally thrust into the footwall. The latter formed a zone of mixed mylonite after granitoid and volcano-sedimentary units containing rigid granitoid fragments in a matrix of plastically deformed predominantly chloritic volcano-sedimentary units.

1.2.3.5 Phyllonite

Plastic deformation of the footwall units also resulted in the formation of phyllonite units (green in Figure 1.5) that are dominated by phyllosilicate minerals (mainly chlorite) and are the result of plastic deformation of the volcano-sedimentary units.

1.2.3.6 Cataclasite

The final and most critical unit is the cataclasite that is formed during a later phase of brittle re-activation on or near the D2 thrust fault zone. Many rock units that were first logged as mylonite after granitoid were later recognized to be cataclasite units (brown in Figure 1.5). It is a product of brittle deformation of the rigid granitoid protolith which literally shattered during the event and formed finely crushed rock with local tectonic breccias. The cataclasite unit occurs directly in the hanging wall of the Kenyase Thrust, although splays of brittle deformation may locally cut into the footwall, especially at Amoma and Awonsu. It is quite likely that this unit formed during the same D3 sinistral strike-slip faulting event described as the ore-controlling feature described at Ashanti by (Allibone et al., 2002). All these lithological units have been subjected to regional Greenschist Facies and locally up to Lower Amphibolite Facies metamorphism.

1.2.4 Weathered Lithologies

The Kenyase Style deposits at Ahafo are intensely weathered and the weathering profile generally consists of:

15

1.2.4.1 Saprolite

Primary lithologic units that are weathered and intensely oxidized to a depth from 20-50 m and containing leached clays and quartz fragments.

1.2.4.2 Duricrust

Zones of transported alluvial fragments that locally overlie the saprolite zone and vary in thickness from 1-7 m and consist of iron pisoliths and iron cement. All of the saprolite features a complete oxidation of the original sulphides and this may locally extend a few meters into the primary bedrock. Partial oxidation of primary sulphides is found up to 15 m below the boundary of complete oxidation. The partially oxidized zone is rather regular (horizontal) at the deposit scale but oxidized fingers locally extend downwards along joints and fractures into the primary rock.

1.2.5 Mineralization

1.2.5.1 Kenyase Style gold mineralization

The Kenyase Style deposits Amoma, Awonsu and Apensu deposits are associated with the regional thrust contact between the Dixcove Suite granitoids and the footwall volcano-sedimentary units. This sheared contact zone is locally termed the Kenyase Thrust and a typical section through this type mineralization is provided in Figure 1.5.

16
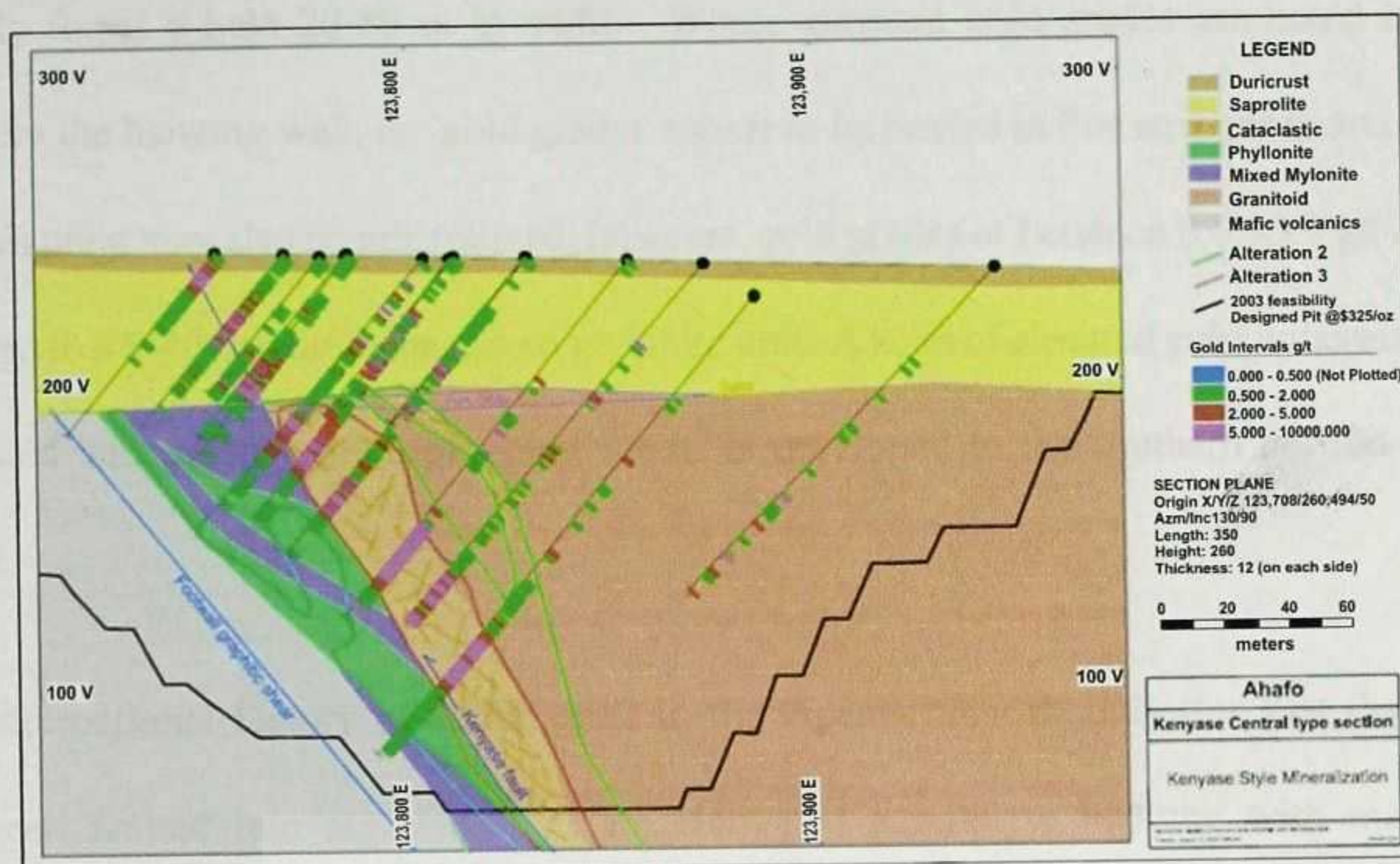
Figure 1.5: A typical section through the Kenyasi style mineralization (Ahafo mineral reserve and resources report, 2008).

Mineralization is developed in mylonitic to cataclasite units along the sheared contact between footwall Birimian volcano-sedimentary units, and hanging wall granodiorite. Footwall units include phyllonite, meta-volcano-sedimentary units and mixed mylonitic volcano-sedimentary units. Late-stage fine-grained aplite dykes that are sub-parallel to the Kenyase Thrust Fault have been logged but may represent fine-grained mylonite zones. To date, the deposit has dimensions of 3.8 km x 600 m, and has been tested to 500 m vertical depth. It remains open at depth

The shear zone varies in width from about 10-75 m in true width, with gold mineralization grading above 0.5 g/t Au ranging from 30-150 m in width. Higher gold grades (>5 g/t Au) are hosted in, or immediately adjacent to, strongly altered cataclasite that is quartz-calcite veined. The veins range from veinlets of 0.1-3.0 cm in width to silica-rich veins that range from 2-10 cm in width. Gold grades of about 0.5-1.5 g/t Au are more commonly developed in the fractured, moderately-altered hanging wall granodiorite. The lower-grade material

17

typically forms a halo 20-80 m in width. Where elevated gold grades are noted in drill core from the hanging wall, the gold grades appear to be hosted in fine stringer quartz veins. Footwall units may also be mineralized; however, gold grades of between 0.01-3.0 g/t Au are restricted to a 5-40 m halo in the mixed mylonite unit. A zone of elevated gold mineralization associated with steeply south-plunging shoots is developed in the southern portion of the deposit.

The deformational history of some veins in the Apensu deposit indicates that the veins have been faulted into segments that are elongated parallel to bedding with increased concentrations of pyrite and carbonates along their margins. Such veins occur in moderately- to strongly-altered zones of host rock.

Six structural components have been identified within the deposit. From oldest to youngest, these are: A zone of plastic deformation in the footwall mixed mylonite zones, graphitic and meta-volcanosedimentary units; Three hanging wall splays off the Kenyase Thrust, named S1, S2 and S3, forming zones of mylonite that display brittle reactivation; A splay fault in the footwall that is interpreted as a plastically-deformed, locally anastomosing shear zone and is marked with graphite; A cataclasite unit, formed by brittle deformation and re-activation of the rigid granitoid forming finely-crushed rock with local tectonic breccias.

Four types of alteration have been recognized, from least to most altered:

Code 0: greenschist minerals including chlorite, calcite and rare pyrite but no evidence of hydrothermal alteration;

Code 1: slightly bleached due to the alteration of some chlorite to paler micas; contains ankerite and rare siderite plus calcite veinlets and patches of pyrite (less than 1%) and rare thin milky quartz veins (1-3 cm width) with occasional associated visible gold;

18

Code 2: grayish to yellowish massive silica and sericite patches that are 1-10 cm in width and are controlled by small brittle shears or mylonitic zones;

Code 3: pervasively silicified rock with strong sericite, rare iron carbonate veinlets, local albite as disseminated crystals, and the complete destruction of chlorite.

1.3 Justification

The high cost of drilling makes it imperative to get optimum use of drill holes once they are drilled. One sure way of doing this is the acquisition of borehole base geophysical data by employing cross borehole tomography. The availability of these drill holes provide an opportunity to get additional and in situ IP/resistivity data to be compared with the subsurface data for better understanding of gold mineralization. The successful utilization of ground based IP/resistivity data in the delineation of gold mineralized zones within the various Newmont Concessions gives credence to the choice of this method. It is known from the subsurface resistivity/IP data that the gold values compare very well with the IP signatures and it is therefore of great interest to investigate at depth how the IP/resistivity hole-to-hole method can aid in the delineation of potential gold mineralization zones.

1.4 Objectives

The main objective of this work was to delineate the gold mineralized zones at various depths below 200 m deep using hole-to-hole resistivity/IP method. Other objectives were:

19

- To determine the importance of resistivity/IP signatures in modeling gold mineralized zones at depth.

- To measure in-situ resistivity and IP data by employing the hole-to-hole method.

- To get more geophysical data at depth where subsurface data is limited in order to aid in gold exploration in the study area.

- To make use of available drill holes to add up data to available geophysical data on one of Newmont's deposit at Ahafo south.

1.5 Literature Review

Various geophysical surveys have been carried out at all Newmont concessions in search of gold deposit. Amongst the numerous ground geophysical surveys carried out over the years are ground magnetics, gravity, Induced polarization, EM, Resistivity, Hole-to-hole down hole survey, etc. An integrated geophysical study was carried out on the Subika gold deposit to aid in studying the physical properties and also to delineate and model the zone that hosts the gold deposit.

During the summer of 2006, several single borehole Vertical Resistivity Profiling (VRP), borehole-to-borehole, and borehole-to-surface resistivity tomography (BRT) data sets across three different massive sulfide deposits were collected. Results from the Nash Creek Zn-Pb-Ag deposit, New Brunswick, Canada are discussed. The Nash Creek Zn-Pb-Ag deposit is located along the western margin of the Jacquet River Graben in northeastern New Brunswick (Canada). Ordovician to Devonian age strata form part of the Tobique Volcanic Belt (Dostal et al., 1989) and comprise a succession of intra-cratonic, rift-related

20

bimodal mafic to felsic volcanic rocks with interstratified sedimentary strata. Sulfide mineralization occurs as stratabound and laterally continuous zones of matrix filling or replacement style mineralization, as fracture filling within flow or pyroclastic units, and as discrete breccia zones. The mineralized environments are charcterized by strong clay alterations, silification and carbonitization. At Nash Creek, wide spread brecciation and alteration zones (often associated with a pyrite-rich matrix) pose a problem for conventional electromagnetic exploration methods: high-grade sulfides (good conductors) are imbedded in laterally extensive alteration envelopes (moderate conductors). The boreholes were water filled and borehole to borehole separation varied from 40 m to 180 m. The data acquisition system was developed by Geoserve in Germany for near surface archaeological and hydrological applications. What is unique about the borehole resistivity system is its electrode and borehole cable design, which allow seamless integration of borehole and surface measurements. The use of borehole cables with up to 24 electrodes each allows the system to acquire more than one thousand resistance readings per hour. The configuration for cross borehole resistivity tomography was proposed by Zhou and Greenhalgh (2000). In this configuration, the current electrodes and potential electrodes straddle the two boreholes (EAGE 69th Conference and Exhibition - London, UK, 11 - 14 June 2007).

Hole-to-hole Resistivity / IP survey was carried out as a part of the Regcourt Projectlocated in the Vauquelin Township, Abitibi, Québec on behalf of Galahad Metals Inc. The objectives of this campaign were to assess the potential for gold mineralization and to propose a follow-up program on the most interesting targets. From December 2 to 11, 2010, a total of 17 independent pairs of receiver holeswere surveyed over the property. Survey specifications, instrumentation control, data acquisition, processing and interpretation were all successfully performed within our quality system framework. The three-dimensional image 3D inversion

21

proposes a possible 3D geometry for the gold mineralized feature of the Regcourt Property. Overall, the 3D inversion allowed the identification of 13 polarizable featuresreaching 10 - 70 mV/V. Among these features, five were considered unknown zones and classed as first priority. For the remaining IP features have either already been intercepted by the drill holes or either represent the Regcourt deposit itself. A follow-up drilling program has been proposed in this geophysical study on the basis of the 3D IP inversion results (Abitibi Geophysics report on Regcourt project, 2011).

At the request of Newmont Mining Corporation, Abitibi Geophysics has produced chargeability and resistivity inversion models from data acquired during a hole-to-hole IP / resistivity survey conducted as a part of the Subika Project in Ghana, Africa. Two current injection bipoles were used in the survey, thus creating two different array geometries. Both of these bipoles surveyed the same 5 receiver hole pairs independently, so we were able to produce models from each bipole and a model from both bipoles together. The resulting models highlight the importance of current bipole orientation relative to the drill holes being surveyed (Abitibi Geophysics report on Newmont Subika project, 2011).

Induced polarization (IP) imaging is a promising tool in engineering and environmental studies. Application of this technique for near-surface investigations has previously been limited by incomplete understanding of the physicochemical controls on the IP response, together with a lack of appropriate methods for data inversion. As laboratory studies have shown, description of IP in terms of complex electrical conductivity enables access to various structural characteristics pertinent to practical issues such as subsurface lithology definition, hydraulic permeability estimation, or hydrocarbon contaminant mapping. In particular, analysis in terms of real and imaginary conductivity components offers improved lithological characterization, since surface polarization effects are separated from electrolytic

22

and surface conduction effects. An Occam-type IP inversion algorithm based on complex algebra is described which accounts for these advances in IP interpretation by directly solving for complex conductivity. Results from crosshole applications at two case study sites demonstrate the suitability of the IP imaging approach for subsurface characterization. In the first case study, the imaging results correlate with the observed complex sequence of Quaternary sediments at a waste disposal site. Characterization of the polarizability of these sediments offers significant value in lithological differentiation. In the second case study, the results of IP imaging at a hydrocarbon-contaminated site illustrate the potential of the method in environmental studies. The hydrocarbon location is clearly evident from the IP image, and a markedly different response is observed at an uncontaminated region of the site. By adopting empirical structural-electrical relationships, images of textural and hydraulic properties are estimated as a step toward improved quantitative characterization. The success of the method for these contrasting applications supports further investigation into understanding the physical and chemical processes that control observed IP (Kemna et al, 2004).

The resistivity data delineated the magic fracture zone as a narrow discrete resistor with a strike length of 2 km and the pole dipole data inversion mapped the zone up to 100 m beneath the surface with a width ranging from 30-60 m. The ground magnetic datasets also mapped the zone as a narrow magnetic anomaly. Petrological and mineralogical analysis on the selected samples from the pit revealed that low magnetic susceptibilities obtained across the mineralized zones were due to processes such as carbonitization, sericitization, silicification and chloritisation resulting from hydrothermal alteration. 3D aeromagnetic modeling also picked up the zone that hosts the deposit. The mineralized zone dips at 50^0 southeast with a strike of N 40^0 E. Geophysical data integration helped in producing a 3-D model of the zone

23

that hosts the deposit and also contributed to the understanding of the physical properties of the mineralized zone (Takyi-Kyeremeh, 2010).

Ground penetrating radar (GPR) survey was conducted over the Subenso-north gold deposit a property of Newmont Ghana Gold Ltd. (NGGL) to delineate the possible fracture zones of mineralization. The Mala GPR equipment with 25 and 50 MHz rough terrain antennae frequencies were used to conduct the survey. The Maximum exploration depth of approximately 925 m corresponding to 50 m was probed. The survey was conducted over a 1 km square block with a total of 21 profiles with a 50 m profile interval. The profiles ran from north-west to south-east. The common offset data collection mode was used. This technique allowed the collection of useful geologic data, for example the upper duracrust which overlain the thick saprolite was imaged with an average thickness between 0 and 8 m. Different radar responses were also obtained from the saprolite indicating the presence of highly weathered zones where complete oxidation includes all of the saprolite. Two sets of inferred structural patterns were established. The structural patterns were S1 and S2. The S1 inferred structures were found between the depth range of (12 m and 42 m) and the S2 also between (31 m and 48 m) for 25 MHz RTA. 50 MHz RTA also recorded S1 structures at the depth range of (14 m and 34 m) and that of the S2 at the depth range of (27 m and 38 m). These sets of inferred structures are potential zones of gold mineralization (Manu, 2011).

Hole-to-Hole Downhole IP/Resistivity was carried out over the Subika deposit to test the effectiveness of mapping mineralized zone at depth. Six drill holes with depth more than 400 m were used in this test survey. The drill holes pairs used ranged from 400 to 800 m in depth. The instruments used for the data collection were mainly an ElrecPro receiver and a VIP 5000 transmitter. The process as used by Abitibi (Berube and Wasylechko, 2010), a geophysical company uses only a single potential dipole running between two holes with

24

the potential electrode located at the same depth in each hole. When the end of one hole is reached, that electrode remains stationary while the other electrode continues to move.

Two orthogonal current bipoles were used for each pair of holes, taking readings from one on the way down the hole, and the other on the way up for this test survey. A depth of 400 to 800 m was given as the depth of interest for the survey. The potential electrodes were incremented by 40 m from the surface to 200 m down the hole, and then from 200 to 400 m down the hole, the increment was reduced to 20 m. The increment was reduced to 10 m through the zone of interest to get better resolution.

The survey was also modified to incorporate two 'reference' electrodes at the surface. These were used for a couple of things. First, channel 1 in the receiver measured between the two references electrodes. This 'trigger' dipole was the same for the entire survey, and provided a constant sign orientation for the other channels measured. It also provided a good check as to which bipole was in use (we used two), and it was successful in using it to correct the other channels for variations in transmitter current, thereby improving measurement repeatability. The idea was ultimately to see how well two of these 'pole' measurements, when summed together, can reproduce the equivalent cross-hole measurement. The advantage of this approach would obviously be that each hole would only need to be read once, instead of multiple times for each desired pair, which could easily be an order of magnitude faster for surveys containing lots of holes. Measuring from a hole to the reference electrodes also allowed determining where one of the electrodes stopped moving just by looking at the data, another useful check.

The chargeability model was able to delineate the mineralized zone using a threshold value of 9.0 ms very well at depth of around 400 to 800 m making this test survey a success.

The success of this survey at Subika project area of Newmont called for the method to be replicated on other deposits and this resulted in carrying out this project at Apensu South.

1.6 Structure of Thesis

The thesis write up consists of five chapters. The content of the chapters are described below. Chapter 1 gives an introduction to the research work and brief description of the study area and its geological setting. The study objectives and justification are also considered. Chapter 2 describes the various theoretical background of the methods used in this work. Chapter 3 describes the materials and the field procedures as well as drill hole selection used in this research work. Chapter 4 talks about the results and findings of the research work. Chapter 5 gives the conclusion and recommendations of the work.
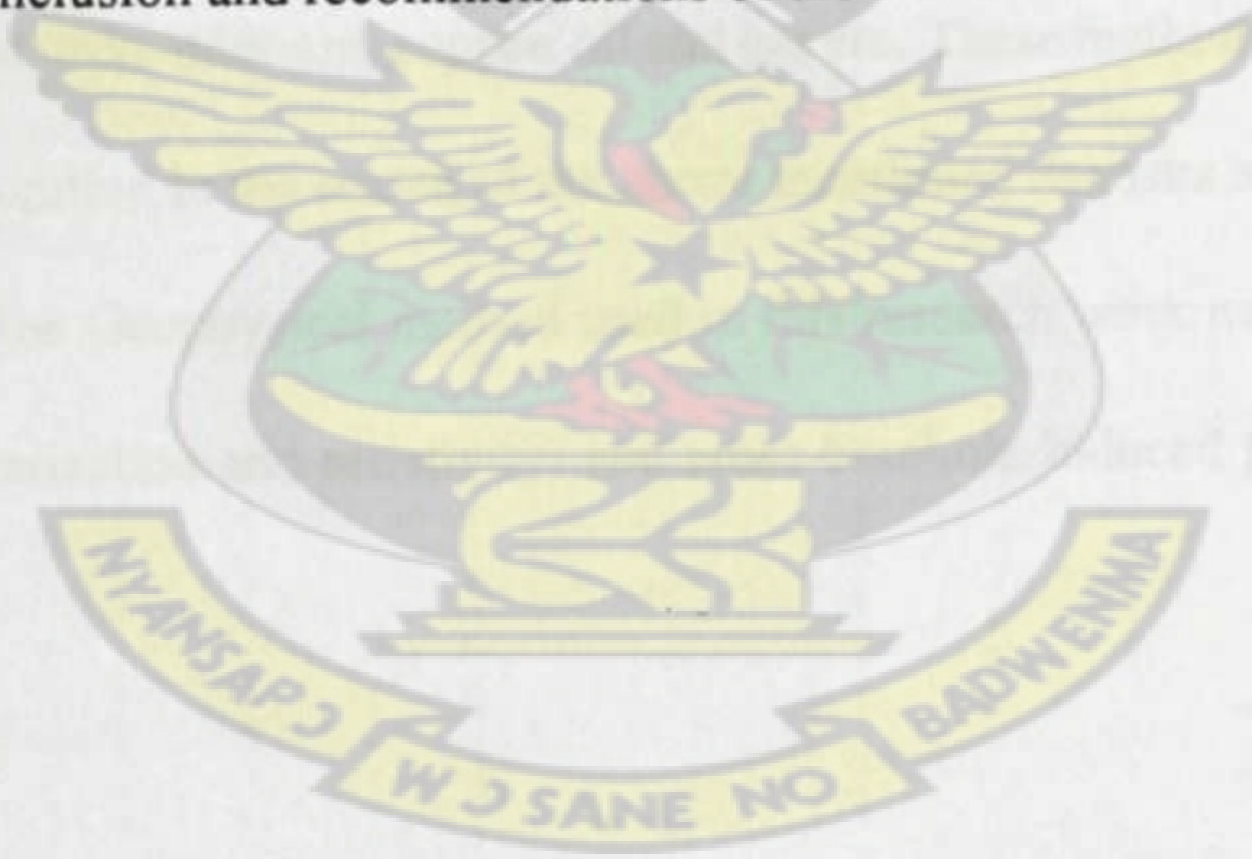
CHAPTER 2

THEORETICAL BACKGROUND

Geophysical prospecting involves mapping the physical properties exhibited by rocks and other subsurface structures. The physical properties of rocks that are mapped out in geophysical surveys are elasticity, density, magnetic-susceptibility, electrical resistivity or conductivity, radioactivity and thermal conductivity. These physical properties have been used to devise geophysical methods that essentially detect discontinuity thus where one region differs from the other in some physical property. These have led to the discovery of many deposits like gold, iron, uranium, copper, oil and gas etc. These methods continue to be useful in mineral exploration in the search of the above mentioned deposits and many more. The basic theories of the Geophysical method used in this research work namely electrical methods (induced polarization and resistivity) and cross-borehole induced polarization are discussed.

2.1 Resistivity Method

2.1.1 Resistivity of Rocks and Minerals

Electric current flows in earth materials at shallow depths through two main methods. They are electronic conduction and electrolytic conduction. In electronic conduction, the current

27

flow is via free electrons, such as in metals. In electrolytic conduction, the current flow is via the movement of ions in groundwater. In environmental and engineering surveys, electrolytic conduction is probably the more common mechanism. Electronic conduction is important when conductive minerals are present, such as metal sulfides and graphite in mineral surveys.

The resistivity of rocks is greatly dependent on the degree of fracturing, and the percentage of the fractures filled with groundwater. Thus a given rock type can have a large range of resistivity, from about 1000 to 10 million Ωm, depending on whether it is wet or dry. This characteristic is useful in the detection of fracture zones and other weathering features. Sedimentary rocks which are usually more porous and have higher water content, normally have lower resistivity values compared to igneous and metamorphic rocks.

The resistivity values of sedimentary rocks range from 10 to about 10000 Ωm. Unconsolidated sediments generally have even lower resistivity values than sedimentary rocks, with values ranging from about 10 to less than 1000 Ωm. One simple equation that gives the relationship between the resistivity of a porous rock and the fluid saturation factor is Archie's Law. It is applicable for certain types of rocks and sediments, particularly those that have low clay content. The electrical conduction is assumed to be through the fluids filling the pores of the rock. Archie's Law is given by:

$$\rho = a\rho_w\phi^{-m} \tag{2.1}$$

Where ρ is the rock resistivity, ρ_w is fluid resistivity, ϕ is the fraction of the rock filled with the fluid, while 'a' and 'm' are two empirical parameters (Keller and Frischknecht, 1966).

For most rocks, 'a' is about 1 while 'm' is about 2. For sediments with significant

28

clay content, other more complex equations have been proposed (Olivar et al., 1990).

The resistivity value of a particular ore body can differ greatly from the resistivity of the individual crystals. Other factors, such as the nature of the ore body (massive or disseminated) have a significant effect. The resistivities of various types of minerals, rocks and ores are shown in table 2.1. Metallic sulphides (such as pyrrhotite, galena and pyrite).

Table 2.1: Resistivities of some rocks and minerals. (Keller and Frischknecht, 1966; Daniels and Alberty, 1966; Telford et al., 1990)

Rocks, Minerals, Ores	Resistivity [Ohm.m]
Sediments	50-150
Chalk	1-100
Clay	100-5000
Gravel	100-5000
Limestone	$50-10^7$
Marl	1-100
Quartzite	$10-10^8$
Shale	10-1000
Sand	500-5000
Sandstone	$1-10^8$
Igneous and metamorphic rocks	
Basalt	$10-10^7$
Gabbro	$1000-10^6$
Granite	$100-10^6$
Marble	$100-10^8$
Schist	$10-10^4$
Slate	$1-10^7$
Minerals and Ores	
Silver	1.6×10^{-8}
Graphite, massive	$10^{-4}-10^{-3}$
Galena (PbS)	$10^{-3}-10^2$
Magnetite ore	$1-10^5$
Sphalerite (ZnS)	10^3-10^6
Pyrite	1×100
Chalcopyrite	$1\times10^{-5}-0.3$
Quartz	$10^{10}-2\times10^{14}$
Rock salt	$10-10^{13}$

2.1.2 Basic Resistivity Theory

The purpose of electrical surveys is to determine the subsurface resistivity distribution from measurements on the ground surface. From these measurements, the true resistivity of the subsurface can be estimated. Electrical resistivity surveys have been used for many decades in hydrogeological, mining and geotechnical investigations.

The fundamental physical law used in resistivity surveys is Ohm's Law that governs the flow of current in the ground. The equation for Ohm's law in vector form for current flow in continuous medium is given by:

$$\vec{J} = \sigma \vec{E} \qquad (2.2)$$

where σ is the conductivity of the medium, $\vec{J}$ is the current density and $\vec{E}$ is the electric field intensity.

In practice what is measured is the electric field potential. In Geophysical surveys the medium resistivity which is the reciprocal of conductivity $\rho = \frac{1}{\sigma}$ is commonly used. The relationship between the electric field potential and the field intensity is given by:

$$\vec{E} = -\nabla \Phi \qquad (2.3)$$

Combining equations (2.2) and (2.3) we obtain:

$$\vec{J} = -\sigma \nabla \Phi \qquad (2.4)$$

In resistivity surveys the current sources are in the form of point sources in the form of current electrodes either stainless steel rods or aluminum foils. A homogeneous subsurface

30

and a single point current source on the ground surface is shown in figure (2.1)
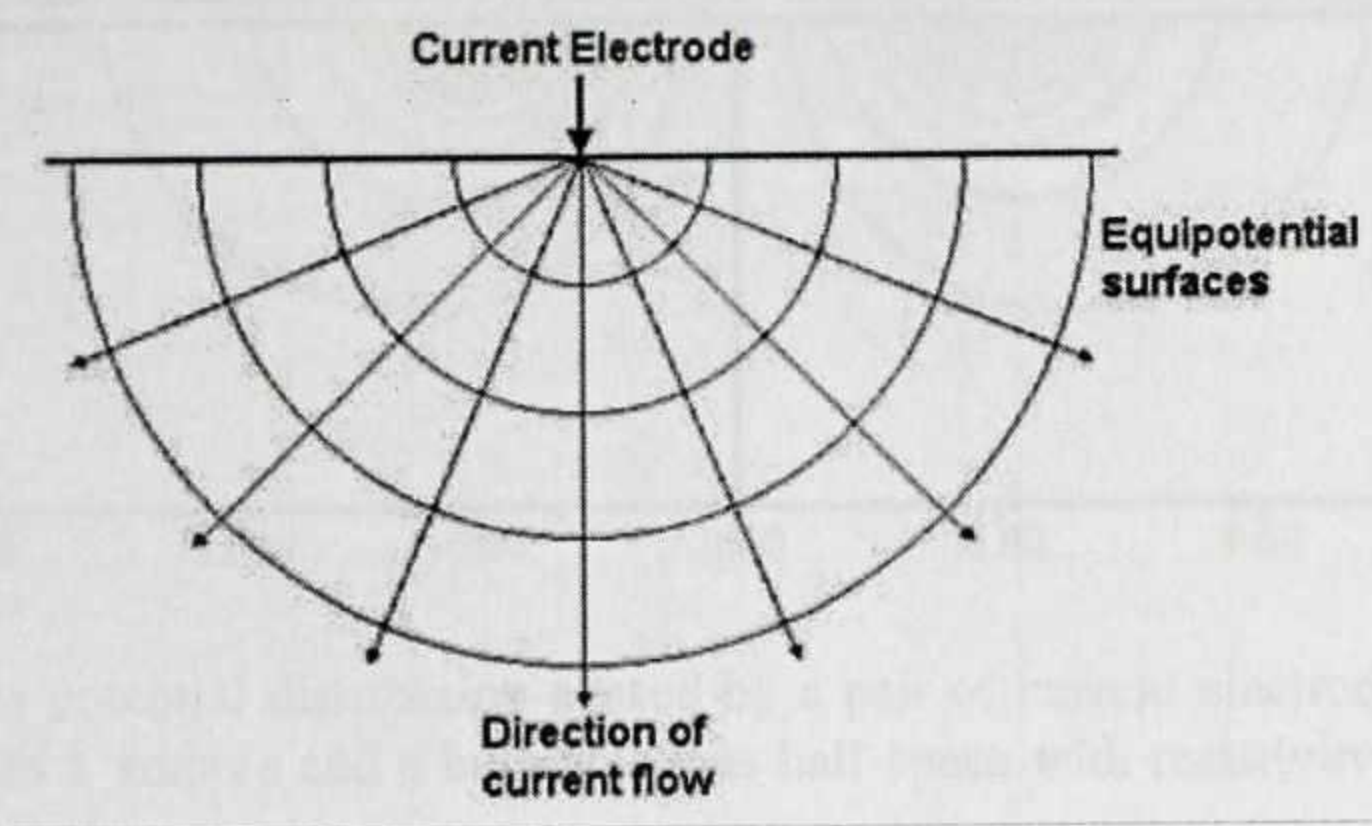
Figure 2.1: The flow of current from a point current source and the resulting potential distribution (Loke, 2004).

In this case, the current flows radially away from the source and the potential varies inversely with distance from the current. The equipotential surfaces have a hemisphere shape and the current flow is perpendicular to the equipotential surface. The potential in this case is given by:

$$\Phi = \frac{\rho I}{2\pi r} \qquad (2.5)$$

where r is the distance of a point in the medium from the electrode. In practice, all resistivity surveys use at least two current electrodes, a positive current (source) and a negative current source (sink).
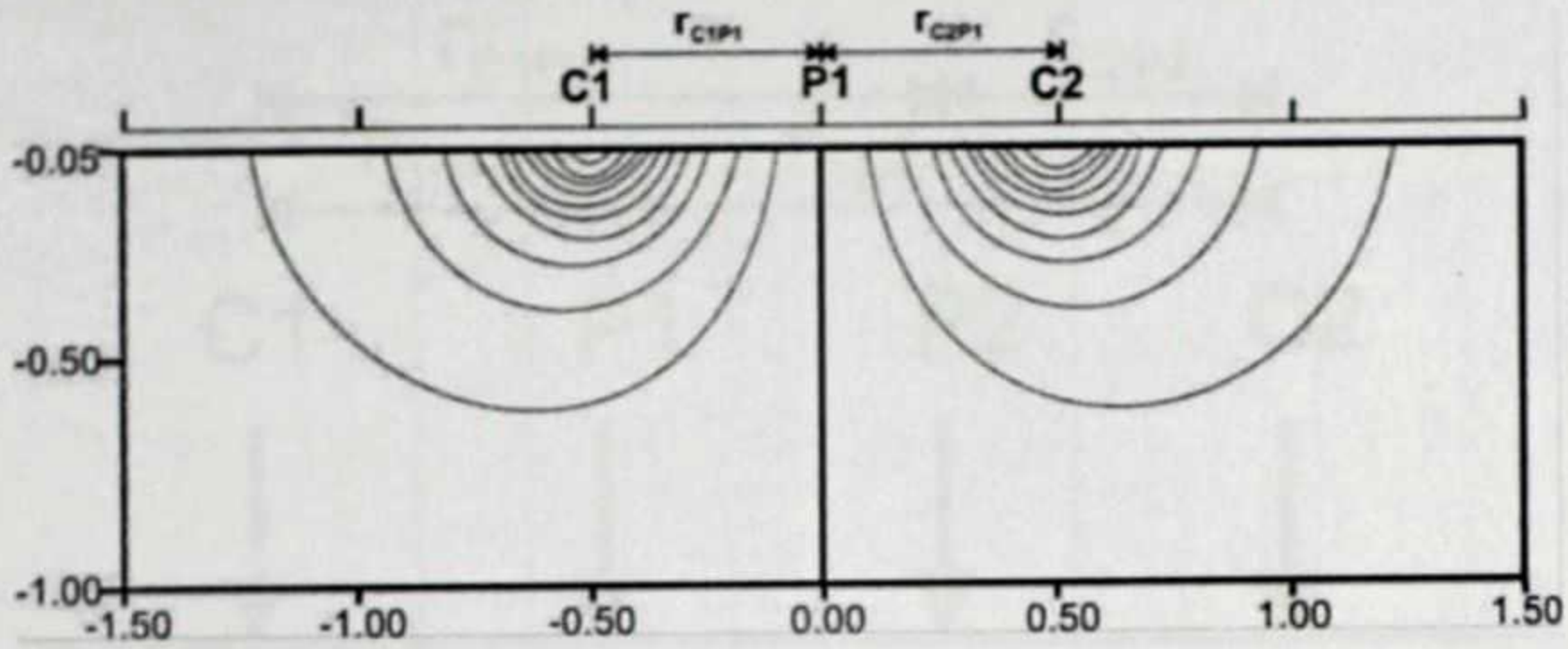
Figure 2.2: The potential distribution caused by a pair of current electrodes 1 meter apart with a current of 1 ampere and a homogeneous half-space with resistivity of 1 Ωm (Loke, 2004).

Figure 2.2 shows the potential distribution caused by a pair of current electrodes. The potential values have a symmetric pattern about the vertical place at the mid-point between the two electrodes. The potential value in the medium is given by:

$$\Phi = \frac{\rho I}{2\pi}\left(\frac{1}{r_{C1}} - \frac{1}{r_{C2}}\right) \qquad (2.6)$$

where r_{C1} and r_{C2} are distances of the point from the first and second current electrodes. In all resistivity surveys, the potential difference between two points on the ground surface is measured by a pair of current and potential electrodes. A typical arrangement with four electrodes is shown in figure 2.3 where P1 and P2 are potential electrodes and C1 and C2 are the current electrodes.
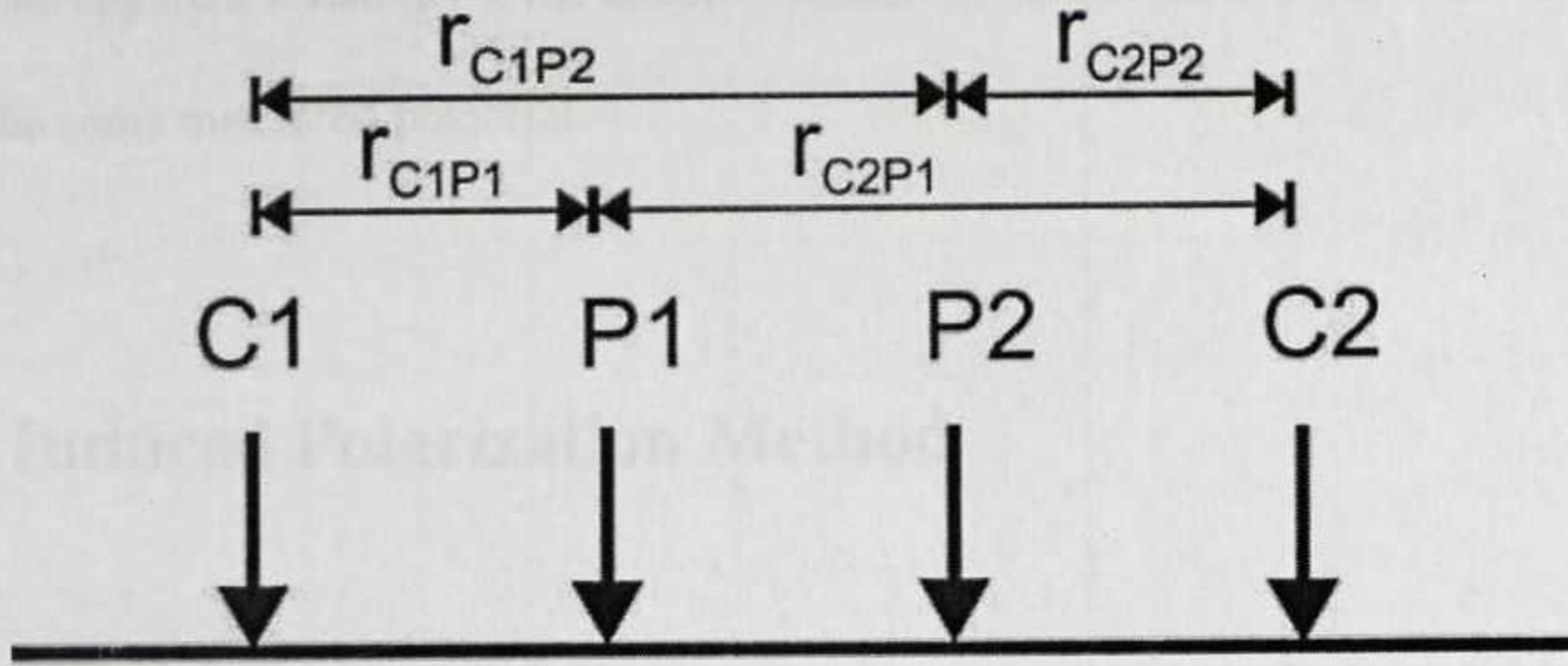
Figure 2.3: A conventional array with four electrodes to measure the subsurface resistivity (Loke, 2004).

The potential difference is given by the difference in the values between the two potential electrodes.

$$\nabla\Phi = \frac{\rho I}{2\pi}\left(\frac{1}{r_{C1}P_1} - \frac{1}{r_{C2}P_1} - \frac{1}{r_{C1}P_2} + \frac{1}{r_{C2}P_2}\right) \tag{2.7}$$

Equation 2.7 gives the potential that would be measured over a homogeneous half space with a four electrode array. Actual field surveys are invariably conducted over an inhomogeneous medium where the subsurface has a 3D distribution. The resistivity measurements are still made by injecting current into the ground through current electrodes C1 and C2 in figure 2.3 and measuring the resulting voltage at potential P1 and P2. From the current I and potential $\nabla\Phi$ values, an apparent resistivity ρ_a value is calculated.

$$\rho a = \frac{k\nabla\Phi}{I} \tag{2.8}$$

where

$$k = \frac{2\pi}{\left(\frac{1}{r_{C1}P_1} - \frac{1}{r_{C2}P_1} - \frac{1}{r_{C1}P_2} + \frac{1}{r_{C2}P_2}\right)} \tag{2.9}$$

is a geometric factor that depends on the arrangement of the four electrodes (Loke, 2004). The calculated resistivity value is not the true resistivity of the subsurface, but an apparent

33

value. The apparent resistivity is the effective resistivity of a uniform earth which would give

rise to the same measured potential.

2.2 Induced Polarization Method

The phenomenon of induced polarization (IP) is reported to have been noted by Conrad

Schlumberger as early as 1912. The induced polarization method has been used since the

late 1940s, having been developed during the Second World War by William Keck and David

Bliel as part of a US Navy project to detect mines at sea (Grow, 1982). One aspect of IP,

known as the overvoltage effect, has been known about since the nineteenth century. In

the 1980s there were considerable advances in instrumentation, and sophisticated techniques

such as complex resistivity and spectral IP (Pelton et al., 1978) were developed, although

there is still much research to be done to relate geological causes to the observed geophysical

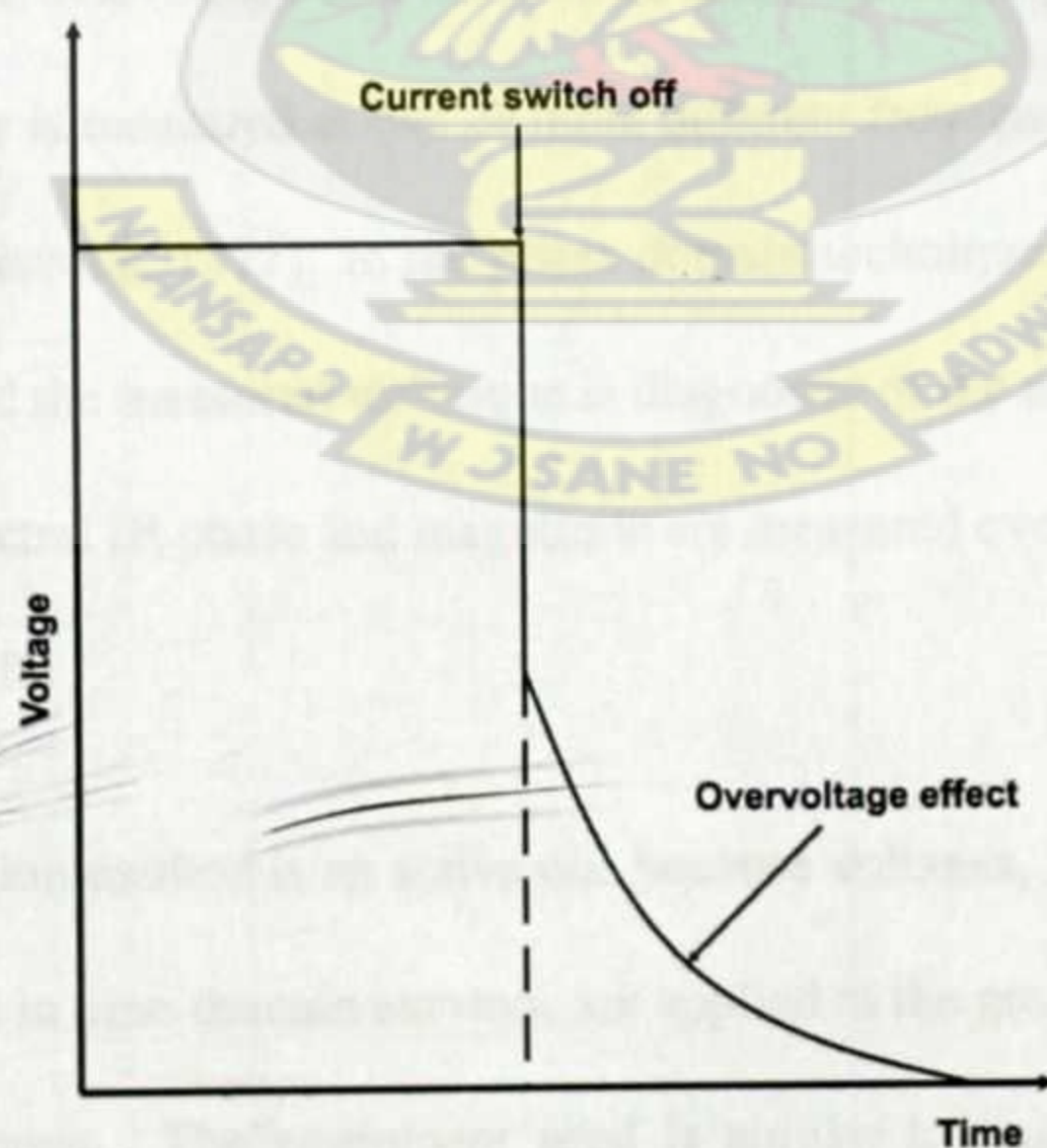data. Thus, there are difficulties in attempting quantitative interpretation.

Figure 2.4: The overvoltage effect after an applied current is switched off (Reynolds, 1997).

34

The main current application of IP prospecting is in the search for disseminated metallicores and, to a lesser extent, groundwater and geothermal exploration. Since the early 1990s, there has been an increased interest in the possible use of IP methods in environmental application. Measurements of induced polarization are made using conventional electrical resistivity electrode configurations involving two current and two non-polarizable potential electrodes. When the applied current is switched off, the voltage between the potential electrodes takes a finite and measurable time (seconds to several minutes) to decay to zero (Figure 2.4) because the ground temporarily stores charge (i.e. becomes polarized) and acts somewhat like a capacitor. When the current is switched back on, the voltage does not peak instantaneously but builds up over the same time period (the rise-time) to its maximum applied value. The voltage decay and rise-time are dependent upon both instrumental and geological factors, and are thus diagnostic of the nature of the ground.

There are four systems of induced polarization measurement namely; Time Domain, Frequency Domain, Phase Domain and Spectral IP. Time domain (or pulse transient) techniques measure the overvoltage as a function of time; and in frequency domain methods the apparent resistivity is measured at two or more different frequencies (usually lower than 10Hz-Patella and Schiavone, 1977). In the phase domain technique, the phase-lag between the applied current and the measured technique is diagnostic of the nature of the sub-surface mineralization. In spectral IP, phase and magnitude are measured over a range of frequencies from 10^{-3} to 4×10^3 Hz.

The induced polarization method is an active one because voltages, which can be as high as several thousand volts in time-domain surveys, are applied to the ground in order to generate measurable over voltages. The equipment used is similar to, but much more elaborate than, that employed in electrical resistivity work. The induced polarization method excites

35

(induces) a response in the ground which is dependent upon the distribution and nature of mineral grains present, and is most effective when the mineral grains are disseminated rather than combined in a massive form.

The exact causes of induced polarization phenomena are still unclear, but the two main mechanisms that are reasonably understood are grain (electrode) polarization (overvoltage) and membrane (electrolytic) polarization, both of which occur through electrochemical processes.

2.2.1 Grain (Electrode) Polarization

Grain or electrode polarization occurs by the same process that results in self-potentials. If a metal electrode is placed in an ionic solution without a voltage being applied, charges with different polarities separate, resulting in the establishment of a potential difference between the electrode and the solution. When a voltage is applied, the ionic balance is disturbed; this causes a current to flow, which in turn changes the potential difference between the electrode and the solution. When the applied voltage is removed, the ionic balance is restored by the diffusion of ions.

In the geological situation, current is conducted through the rock mass by the movement of ions, within groundwater, passing through interconnected pores or through the fracture and micro-crack structure within the rock. When an electronically conducting grain (e.g. a metal sulphide) blocks a flow channel, charge builds up (Figure 2.5) as in the electrochemical cell; this opposes the current flow and the grain becomes polarized, so creating a potential difference across the grain. On switching off the applied voltage, the ions diffuse back through the electrolytic medium and the potential difference across the grain reduces to

36

zero in a finite time, giving the characteristic overvoltage decay measured in time-domain systems.
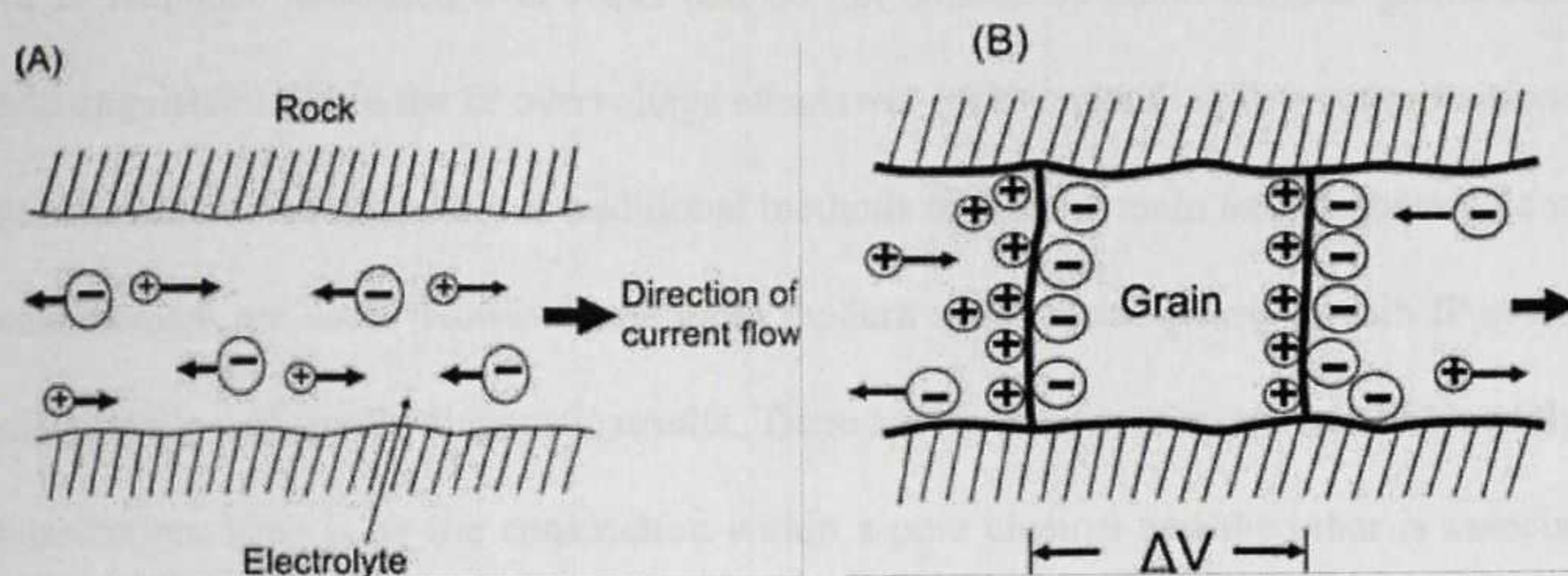
Figure 2.5: Grain (electrode) polarization. (A) Unrestricted electrolyte flow in an open channel. (B) Polarization of an electronically conductive grain, blocking a channel (Reynolds, 1997).

Grain polarization is essentially a surface phenomenon and this is why disseminated ores (with correspondingly large total surface areas) produce a significant IP response. Sometimes an IP response is obtained over a halo of disseminated ore around a massive orebody. Although it is the individual electronically conducting mineral grains that become polarized, complete zones with significant concentrations of ore will also take on a net polarization; this results in a macroscopic polarization current flow in the ground which is measured as the IP response. The factors affecting the rate at which the ionic balance is restored are extremely complex and may depend upon the pore shape and size, rock structure, permeability, electrolytic conductivity and ionic concentration, and on the electronic conductivity of the mineral grain. Bornite, cassiterite, chalcopyrite, galena, graphite, limenite, magnetite, pyrite, pyrolusite and pyrrhotite, all exhibit strong IP responses as they have high electronic conductivities. The sulphides sphalerite, cinnabar and stibnite have low electronic conductivities and do not produce significant IP responses. For the same reason, they tend to produce only minimal, if any, self-potentials.

37

2.2.2 Membrane (Electrolytic) Polarization

An IP response measured over rocks that do not contain sulphide mineral grains can be indistinguishable from the IP overvoltage effect over rocks containing low concentrations of disseminated ores, especially if traditional methods of time-domain and frequency-domain measurement are used. However, the more modern spectral and phase-domain IP systems may provide sufficiently diagnostic results. There are two causes of membrane or electrolytic polarization. One is by the constriction within a pore channel and the other is associated with the presence of clay within pore channels, such as in impure sandstone. There is a net negative charge at the interface between most rock minerals and pore fluids. Positive charges within the pore fluid are attracted to the rock surface and build up a positively charged layer up to about 100 μm thick, while negative charges are repelled. Should the pore channel diameter reduce to less than this distance, the constriction will block the flow of ions when a voltage is applied. Negative ions will leave the constricted zone and positive ions will increase their concentration, so producing a potential difference across the blockage (Figure 2.6). When the applied voltage is switched off, the imbalance in ionic concentration is returned to normal by diffusion, which produces the measured IP response.

The second cause of membrane polarization is the presence of clay particles or filaments of fibrous minerals, both of which tend to have a net negative charge. Positive ions are attracted to them, producing a positively charged cloud within the pore space. When a voltage is applied, positive charges can move between these similarly charged clouds but the negatively charged ions are blocked, which produces a difference in ionic concentration (Figure 2.6 B). When the applied voltage is switched off, the imbalances in ionic concentration decay to normal levels by diffusion, so causing a measurable IP response.
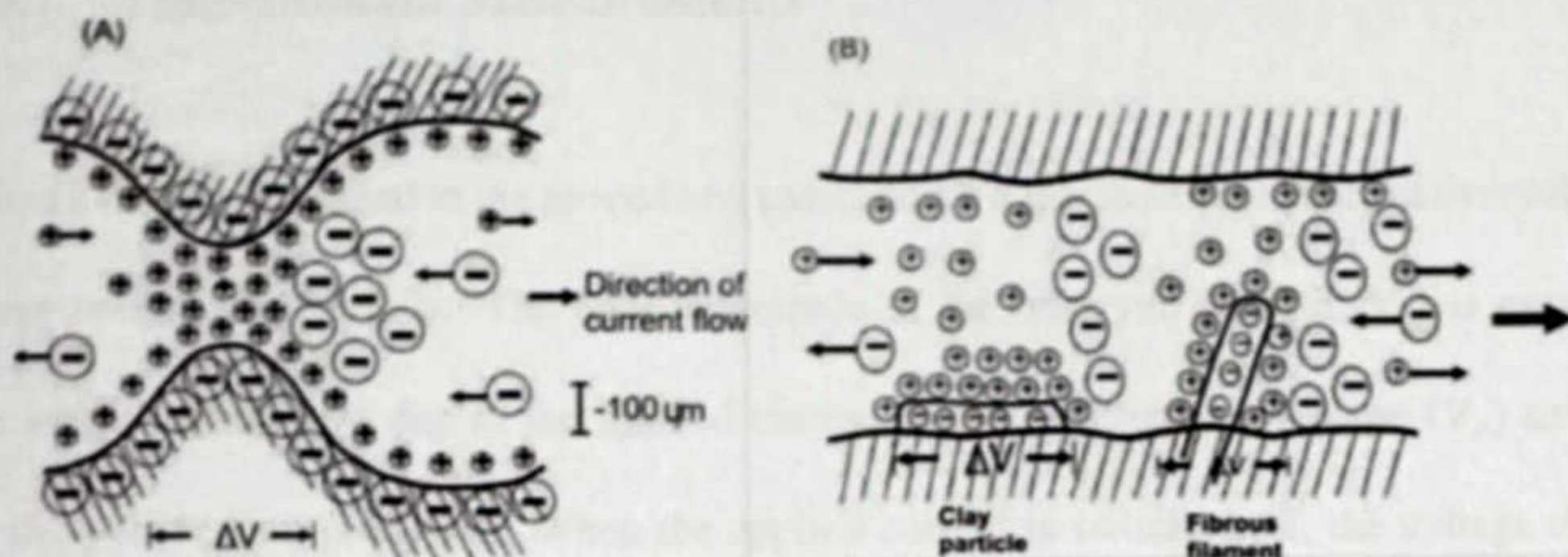
Figure 2.6: Development of membrane polarization associated with (A) a constriction within a channel between mineral grains, (B) negatively charged clay particles (Reynolds, 1997).

2.3 Measurement of Induced Polarization

Current is applied to the ground by means of two current electrodes, and the induced-polarization effect is measured between two potential electrodes, most commonly in a dipole-dipole, Wenner, Schlumberger (gradient) and pole dipole arrays. Electrode spacings are commonly tens to several hundred meters, but in broad reconnaissance surveys for which the Schlumberger array tends to be used, the spacings can be even larger. The type of equipment used is bulkier and more elaborate than that used for resistivity surveys, and also depends on the type of IP survey being conducted. A transmitter is used to generate the applied current input into the ground, and the polarization effects are detected by a receiver comprising non-polarizable porous-pots connected to the potential electrodes. Profiles are undertaken with fixed electrode spacings in much the same way as in the constant-separation traversing of electrical resistivity surveys.

2.3.1 Time-Domain Measurements

When a current is applied to the ground and switched off a few moments later, an overvoltage decay results (Figure 2.7). The total magnitude of the observed voltage (V_o) is equal to the actual voltage (V) due to the applied current plus a polarization voltage (V_p) caused by the polarization processes. When the applied current is switched off, the voltage drops instantaneously by the amount V, leaving a residual voltage (the overvoltage) (V_p) which decays with time. One measure of the IP effect is the ratio V_p/V_o which is known as the Chargeability and is usually expressed in terms of millivolts per volt or percent.

Instrumentally, it is extremely difficult to measure V_p at the moment the current is switched off, so it is measured at a fixed time (typically 0.5 s) after cut-off. Measurements are then made of the decay of V_p over a very short time period (0.1 s) after discrete intervals of time (also around 0.5 s). The integration of these values with respect to time gives the area under the curve (Figure 2.7), which is an alternative way of defining the decay curve. When the integral is divided by V_o, the resultant value is called the chargeability (M) and has units of time (milliseconds) (Figure 2.8).

The true chargeability is virtually impossible to measure in a field situation as each layer within the ground will have its own absolute value of chargeability and of true resistivity. What is measured is a complex function of all the true resistivities and absolute chargeabilities for all the media being sampled within the range of the equipment. A short charging period will produce a lower IP response than a long charging period.

The major advantage of integration and normalizing by dividing by V is that noise from cross-coupling of cables and from background potentials is reduced. Care has to be exercised

40

in selecting appropriate time intervals to maximize signal-to-noise ratios without reducing

the method's diagnostic sensitivity.
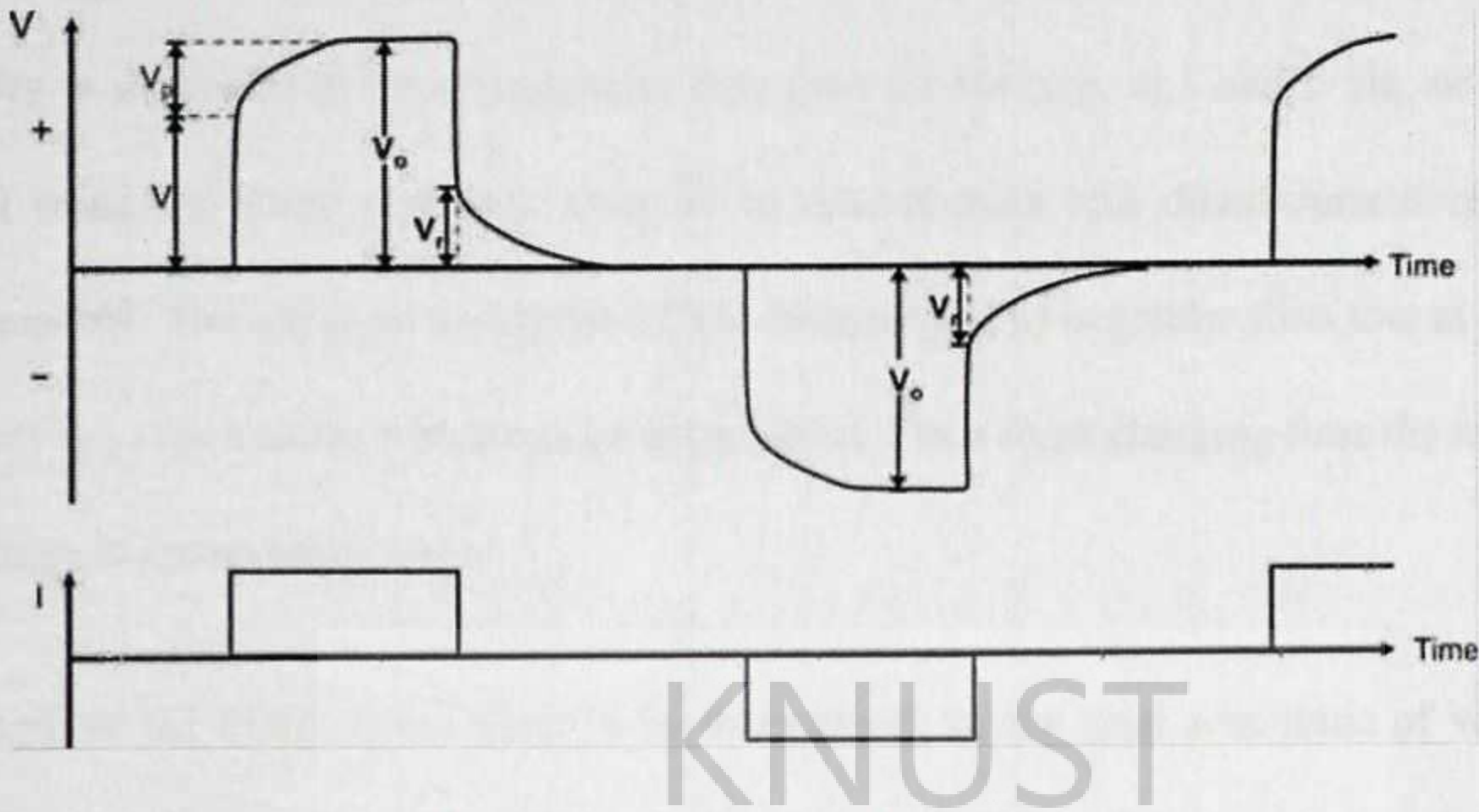
Figure 2.7: Application of a pulsed current with alternate polarity and the consequent measured voitage showing the effect of the overvoltage (Reynolds, 1997).
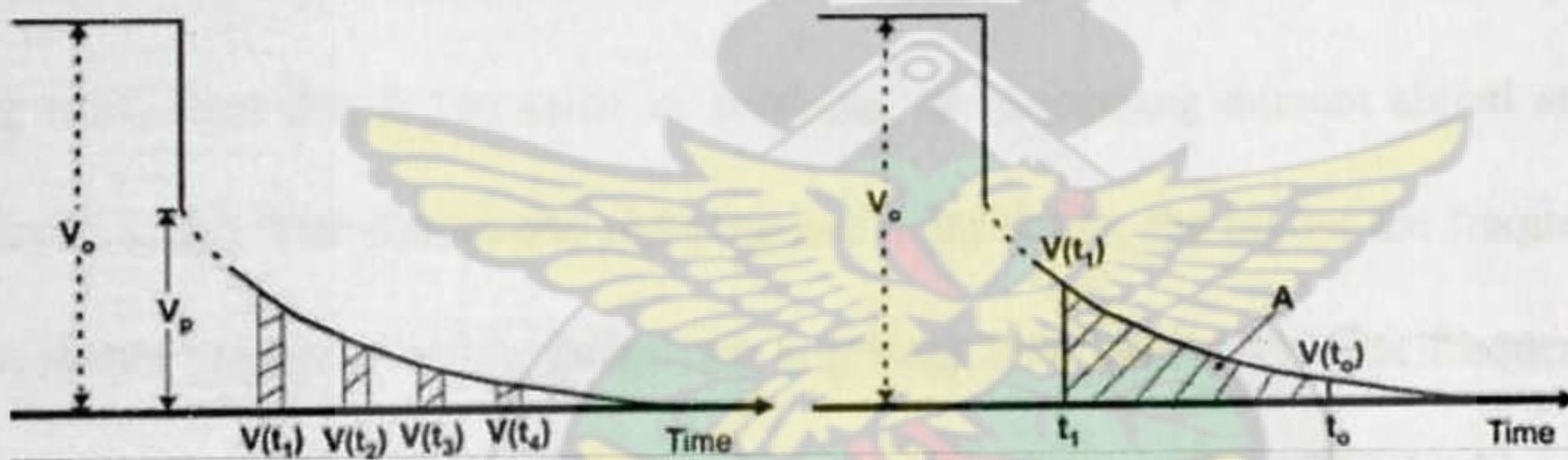
Figure 2.8: Two forms of measurement of the overvoltage at discrete time intervals and by the area beneath the overvoltage curve (A) (Reynolds, 1997).

Chargeability,

$$M = \frac{V_p}{V_o}$$

(2.10)

where V_p is the overvoltage and V_o the observed voltage with an applied current.

Apparent chargeability

$$M_a = \frac{1}{V_o} \int_{t_1}^{t_2} V_p(t)dt = \frac{A}{V_o}$$

(2.11)

where $V_p(t)$ is the overvoltage at the time t, and A is the area under the curve.

41

2.3.2 Frequency-Domain Measurements

In frequency domain (variable frequency) induced-polarization studies, the apparent resistivity is measured at two frequencies less than 10 Hz (e.g. 0.1 and 5 Hz, or 0.3 and 2.5 Hz) using the same electrode array as in time-domain and direct-current resistivity measurements. The apparent resistivity at low frequency ($\rho_{.0}$) is greater than that at a higher frequency ($\rho_{.1}$) for reasons which can be appreciated. For a short charging time the measured overvoltage is appreciably lower.

The length of the decay is too short to be determined, so the total amplitude of voltage is measured with respect to the applied current, giving a value of the resistance (R) which, when multiplied by the appropriate geometric factor, is the apparent resistivity. If the current is switched in polarity, and on and off, with a time delay comparable to the length of the charging time, then this is the same as applying an alternating current signal at a given frequency (f hertz). The shorter the charging and delay times, the higher the frequency, and so the apparent resistivity at low frequency is greater than that at a higher frequency. The two apparent resistivities are used to determine the frequency effect (FE) (unitless), which can be expressed alternatively as the percentage frequency effect (PFE) (units: %)

Frequency effect:

$$FE = \frac{\rho_{.0} - \rho_{.1}}{\rho_{.1}} \tag{2.12}$$

where $\rho_{.0}$ and $\rho_{.1}$, are the apparent resistivities at low and higher frequencies respectively, and $\rho_{.0} > \rho_{.1}$

Percentage frequency effect:

$$PFE = 100\frac{(\rho_{.0} - \rho_{.1})}{\rho_{.1}} = 100FE \qquad (2.13)$$

The frequency effect in the frequency-domain is equivalent to the chargeability in the time-domain for a weakly polarizable medium where FE > 1.

Marshall and Madden (1959) modified the expression involving the frequency effect to produce the metal factor (MF) (or the metal conduction factor). It is thought by some geophysicists that metal factor data delineate disseminated sulphide zones more effectively than frequency effect data.

Metal factor:

$$MF = A\frac{(\rho_{.0} - \rho_{.1})}{\rho_{.1}\rho_{.0}} = A(a_{.0} - a_{.1}) \qquad (2.14)$$

units: siemens/m, where, $a_{.0}$ and $a_{.1}$ are the apparent conductivities ($\frac{1}{\rho}$) at low and higher frequencies respectively; and $0.30 < a_{.1}$; and $A = 2n:\times 10$

Alternatively, the metal factor is given by:

$$MF = A \times \frac{FE}{\rho_{.0}} = A \times FE \times a_{.0} \qquad (2.15)$$

Although disseminated ore bodies can be located using IP data, chargeability, frequency effect and metal factor do not give a good indication of the relative amount of the metallic mineralization within the source of the IP response. It is necessary to go to more elaborate methods such as spectral IP, and even then the estimates obtained are not unambiguous. One further frequency-domain method that has been used but which has been superseded by the

43

spectral IP method is 'phase IP'. Only one frequency is necessary. Induced polarization is identified by the presence of a phase lag between the applied current and the polarization voltage measured.

2.3.3 Hole-To-Hole Induced Polarization and Resistivity

This is the running down of IP probes into drill holes to measure the IP effect. Resistivity is also measured at the same time. It is similar to the ground IP/Resistivity survey in terms of the gear and the set-up except that this one occurs in two drill holes at the same time. The hole-to-hole induced polarization configuration was developed to increase the detection radius around the drill holes being surveyed compared to the detection radius that can be achieved with a classical borehole induced polarization survey. This concept was advanced by Abitibi Geophysics in conjunction with several other gold mining companies.

The classical borehole induced polarization is used to map disseminated sulphides in the proximity of the drill hole. However, due to the limited radius of penetration, only limited directional information about the mineralized zone can usually be obtained. The investigation range is about half the distance between P2 and C1 in a single drill hole.
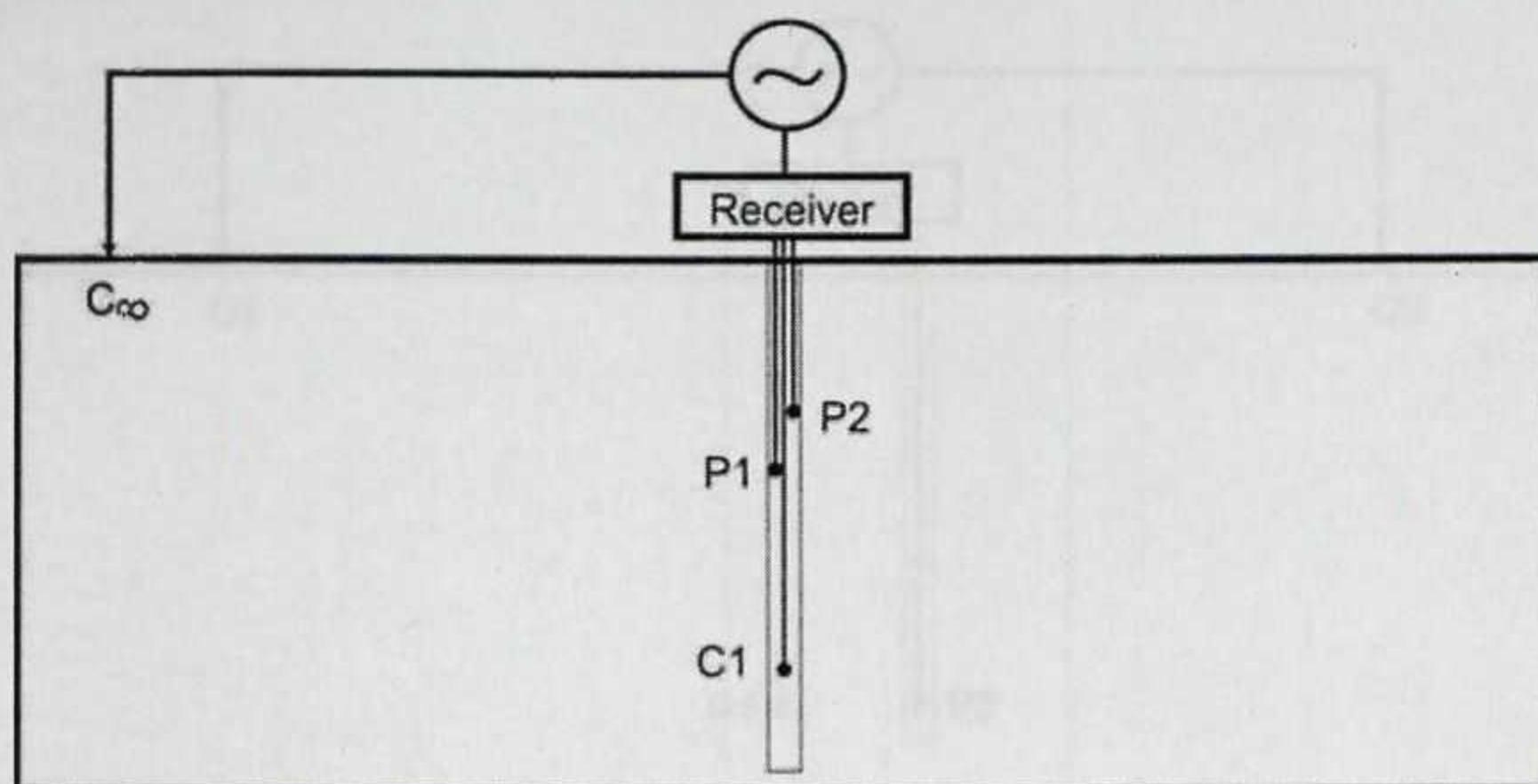
Figure 2.9: Set up of a classical borehole survey (Berube and Wasylechko, 2010).

With this type of set-up, readings cannot be taken up to the end of the borehole with the target horizon often near the bottom of the hole particularly with large electrode spacing. Also, all active electrodes are inside the borehole; therefore the maximum electrode spacing is limited by the borehole length. The detection radius is further limited as it is a fraction of the electrode spacing. The numerous in-hole electrodes increase the sensitivity of the technique to in-hole mineralisation, which negatively impacts the detection radius.

The desire to overcome these limiting factors of classical borehole IP led to the development of the hole-to-hole IP method.
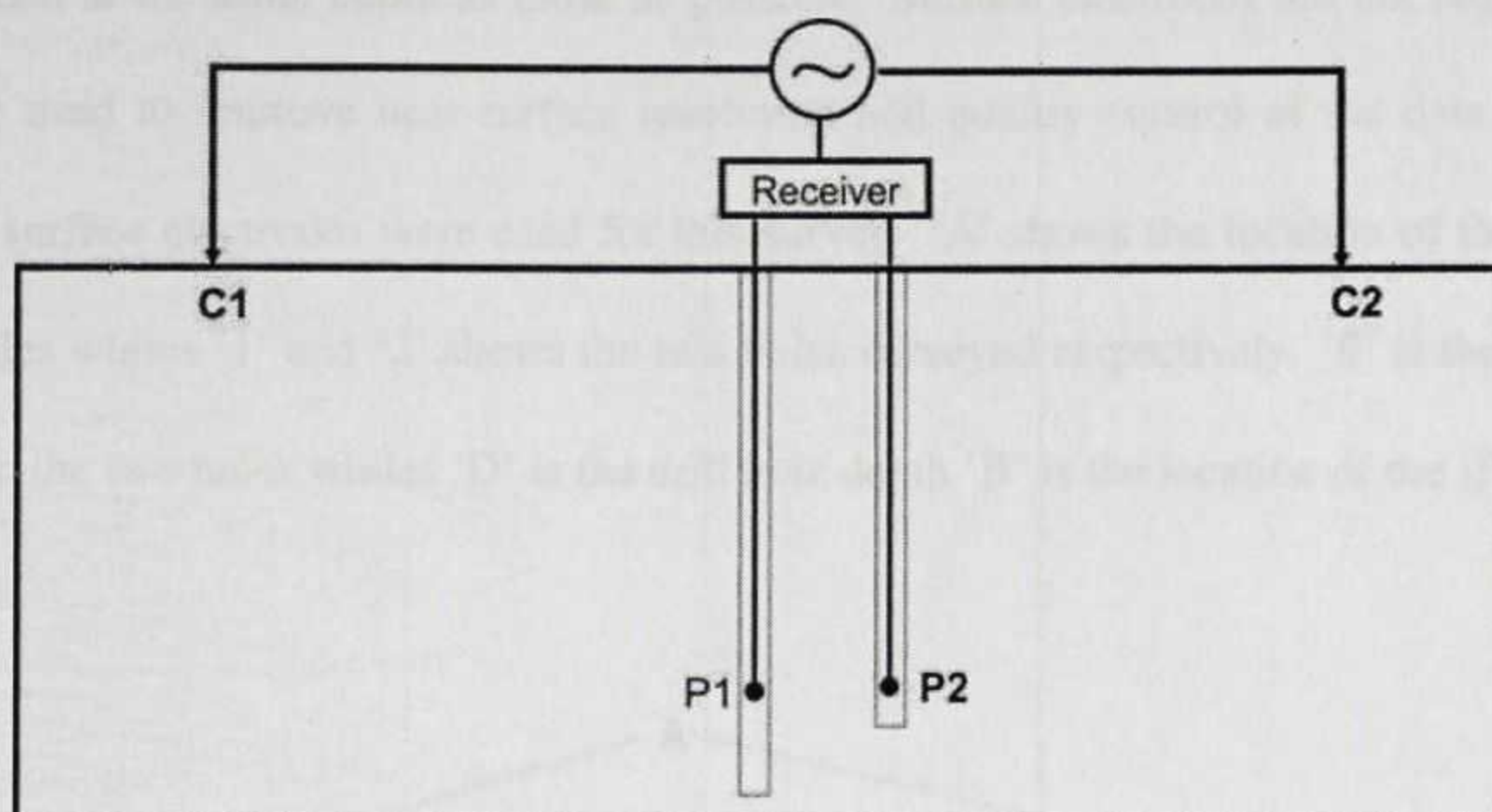
Figure 2.10: Set up of Hole-to-Hole down hole survey (Berube and Wasylechko, 2010).

The P1-P2 spacing which is the distance between the drill holes typically may be between 100 and 1500 meters usually determined by the aspect ratio and should not be too far apart. (Advanced Geosciences, Inc., 2003) The aspect ratio is the relationship between the borehole depth and distance between two boreholes should be equal to or greater than 1.5. The geometry of the set-up is very important. The aspect ratio and electrode spacing are important parameters for a successful survey. The C1-C2 separation should be at least two to three times the average target depth (Berube and Wasylechko, 2010). The detection radius is approximately half the distance between the hole-pairs being surveyed. Only one potential electrode is inside a borehole, therefore, the in-hole mineralization has less effect on the detection radius. A target horizon near the bottom of the hole can be mapped because the potential electrode can be lowered to the bottom of the hole. Many hole-pairs may be read and simultaneously processed to deliver an integrated interpretation with an inversion providing a 3D image of the target.

The aspect ratio, D/S for this survey was averagely 1.6. Electrode spacing can be random; however, for efficient modeling and good resolution, electrodes in different boreholes should

46

be aligned at the same depth as close as possible. Surface electrodes are not required but may be used to improve near-surface resolution and quality control of the data. A total of two surface electrodes were used for this survey. 'A' shows the location of the surface electrodes whiles '1' and '2' shows the two holes surveyed respectively. 'S' is the distance between the two holes whiles 'D' is the drill hole depth 'B' is the location of the IP probe in the hole.
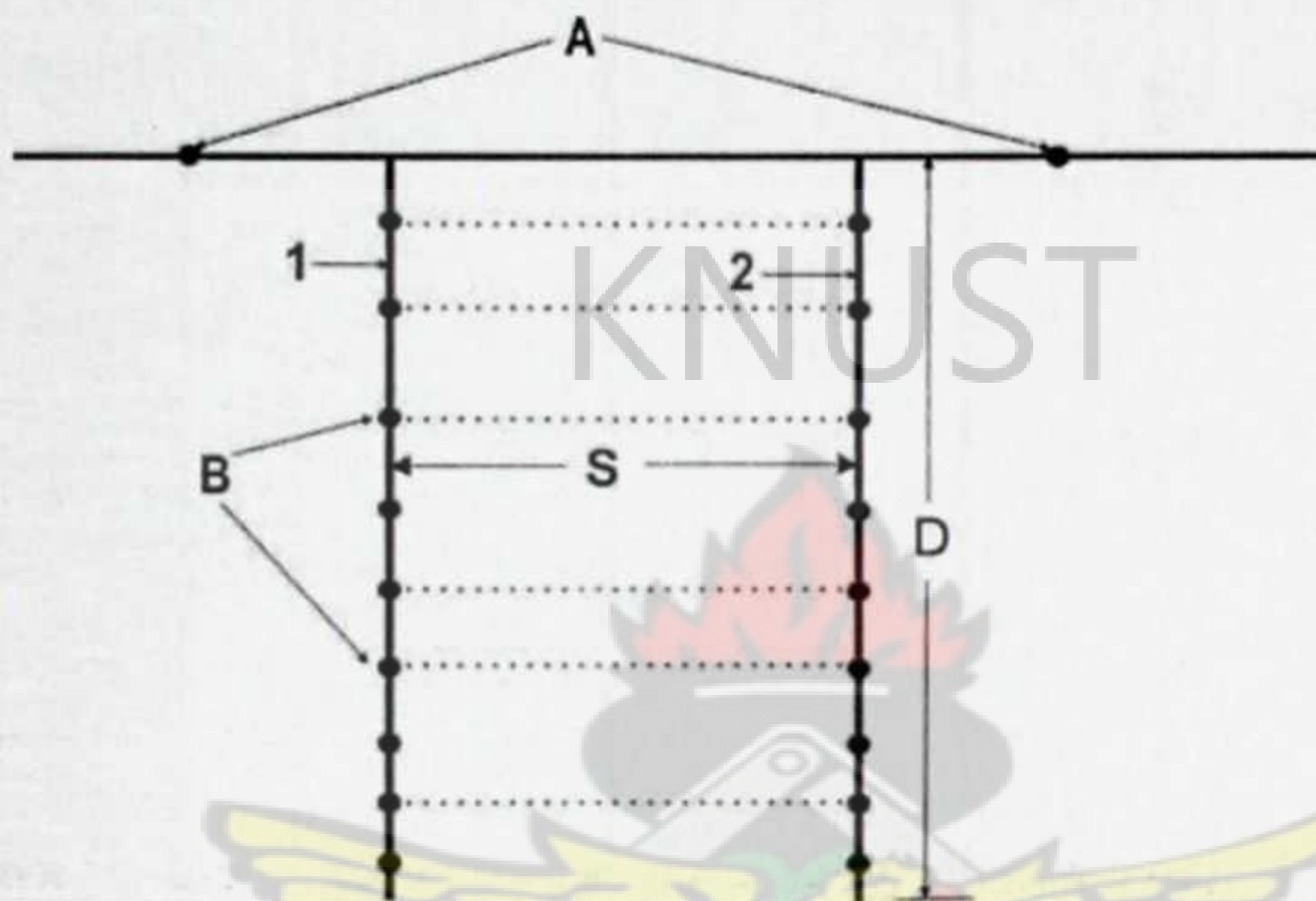
Figure 2.11: Set up parameters of two drill holes (Berube and Wasylechko, 2010).

For a 3D survey like this one, there needs to be a minimum of three boreholes so that a web of measurements is taken as illustrated in figure 2.3. Four boreholes with data collected along six 2D transects (AB, AC, AD, BC, BD, and CD) make a perfect 3D data set. The rectangular size of ABCD (Figure 2:12) can be increased by adding a fifth borehole in the middle. This way the investigated volume can be increased.
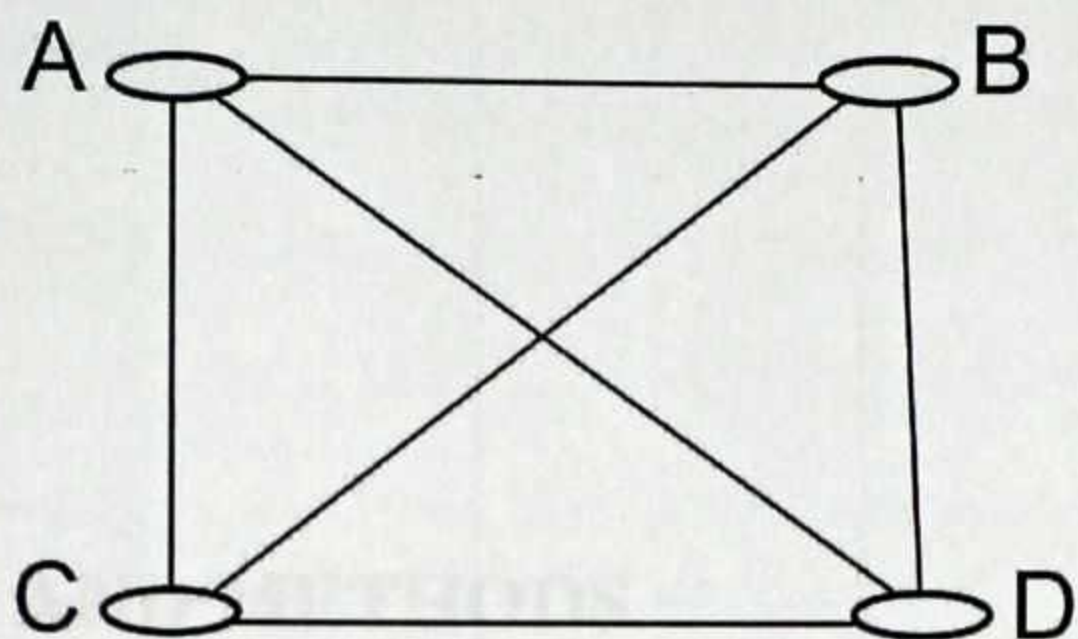
Figure 2.12: Set up parameters of two drill holes (Berube and Wasylechko, 2010).

CHAPTER 3

MATERIALS AND METHODS

3.1 Materials

All materials used for this thesis work were provided by Newmont Ghana Gold Limited right from the data collection through to data processing and interpretation with supervision from my supervisors from K.N.U.S.T. The data collection was carried out with the help of the geophysics crew of the company. The main tools used for this survey were two winches, two pentapods, a VIP 5000 transmitter, an Elrec pro receiver, a Honda generator, an IP probe, a dummy probe, electrode potentials, aluminum foils, current and potential wires.

Geological data from the drill holes including collar (location coordinates of the holes),surveys (that is the azimuth and dip of the drill holes), and rock lithology were acquired from the company database.These helped in the correlation of the chargeable zones, the geology and the gold mineralization in the holes. All software such as Oasis Montaj, ArcGIS used throughout the entire thesis work were also provided by the company.

3.2 Pyrite Logging

This process was carried out to determine the amount and presence of disseminated sulphide in the drill cores. The brassy-yellow metallic color of pyrite has in many cases lead to people mistaking it for Gold, hence the common nickname 'Fool's gold'. Due to its association with gold mineralization within the Birimian gold mineralization, it is considered one of the main path finder minerals for gold. A pyrite logging of all the drill holes surveyed was obtained from Bastillion, a contract group of geologist working for Newmont. This survey gave indications of the percentage of pyrite in cores in all the drill holes. This also made a better understanding of the data as per the abundance of disseminated sulphides (pyrite) in the drill holes. This therefore provides data to help in the determination of the correlation between pyrite (main pathfinder of gold) content with the level of gold mineralization within the study area. This proved to be the case as the results showed some level of pyrite in most of the mineralized rocks in the drill holes.

Figure 3.1: Presence of Sulphide mineralization in diamond drilled split core samples: Left - spots of pyrite; Right - Spots of disseminated sulphide.

The success of the IP effect (chargeability) anomaly in mapping the zone of gold mineralization within the study area was as result of the presence of these disseminated sulphides (pyrite) found in the rocks. This is due to the ions pile up effect produced between

the specific lower resistive metallic interface (pyrite) and highly resistive hosting rocks in the area, thereby giving rise to an increase in resistance to the current flow along the mineral and rock boundary. The polarization takes place at each of the infinite number of solution-metal interfaces in the mineralized rock. Induced polarization effect therefore takes place at those interfaces where the mode of conduction changes from ionic in the solutions filling the interstices of the rock to electronic in the metallic minerals present in the rock (Goudie and Hallof, 1997).

3.3 Selection of Site and Holes

The success of this method on one of the main deposits of Newmont Ghana Gold Limited made it imperative to carry it on other deposits with different geology to see how effective it will be. The process involved getting current drill holes data from geologist at the two sites of Newmont Ghana Gold Limited namely Ahafo North and South. Based on this information, two sites from Ahafo North; Subenso North and Terekyere West deposits were selected initially since the previous survey which was successful was carried out at Ahafo South. Most of the drill holes selected in these two sites were blocked rendering most of them inaccessible. This problem was largely due to the thick saprolite cover in these areas making the drill holes to cave in with time.

Attention was then shifted to Apensu-South at Ahafo South where the drill holes were found to be in good condition for this survey to go on. The selection and determination of the area and drill holes used for this work was based on a number of considerations such as depth of drill holes, accessibility of drill holes, availability of drill holes, separation of drill holes and distribution of the drill holes.

51

The first thing to look out for from a drill hole data was their various depth since the resolution of IP/ resistivity imaging decreases with depth. Therefore, the deeper the drill holes the better since ground IP/resistivity surveys are able to map up structures in the region of about 200 m. The drill holes at these sites were probed to access their availability and suitability after which they were chosen for the survey. The drill holes were selected making sure that they were within reach and available such that they could be interconnected to form the required web. These were done together with the project geologists and so the accessible ones were selected. Collaboration with the geologist around gave information on drill holes which were old and difficult to get to and the most recent ones. Information was gathered from the various project geologists for drill holes which were readily available thereby making the selection process quite easy. This allowed for quick search for the drill holes since the available ones were known already.

The separation of the drill holes was critical in the selection so as to ensure that a good web could be formed out of which a 3D model could be generated. It involved measuring the distances between the drill holes using the aspect ratio. The drill holes were also selected ensuring a good spatial distribution between them.

3.4 Location of Drill Holes

The selected drill holes were located with the help of Garmin hand held GPS. The UTM coordinates of the drill holes were loaded into the GPS to locate them. The area around the drill holes upon location were cleared to prepare the place for the next stage.

3.5 Probing of holes

One of the most important stages of this survey was the probing of the drill holes. This involved running down the drill holes with a dummy probe to find out whether the holes were blocked or opened. This also allowed for the determination of the actual depth of the drill holes from what was acquired from the geologist. This was also very necessary so that the actual probe for the data collection was not stacked into the drill holes.

Figure 3.2: Dummy probe on a winch.

This was done by setting up the pentapod over the drill hole of interest after clearing the area complete of any weeds. A counter was mounted on it and the probe wound onto a winch was lowered down over the counter through a groove to the tip of the drill hole. The counter was set to zero and the probe gently lowered into the hole till it touched the bottom of the hole. In figure 3.1, 'A' is the metal wire on the winch; 'B' is the dummy probe and 'C' is the handle.

Figure 3.3: A counter mounted on a pentapod.

With the counter (Figure 3.2), the depth to which the probe ended was determined. After the end of the hole was reached, the wire was reeled back manually. This process was continued over all the drill holes. During all this processes, the pentapod was firmly held in place by short iron bars with some human touch while keeping close eye on the whole setup to prevent any slip up. The various depths of the drill holes were recorded. All safety standards as required by Newmont were followed as per the Standard Operating Procedure (SOP) for this survey. Probing was done on four different deposits at Ahafo North and South namely Subenso North, Tekyere West, Apensu South and Subika. 'A' is the digital counter which measured the distance of the drill holes and 'B' is the pentapod.

A total of 26 drill holes were probed at Subenso North out of which none could go beyond 30 m making it impossible to carry out the survey over this deposit and Tekyere West was considered. Over 17 drill holes probed at Terekyere West deposit, 6 were opened beyond

54

350 m which were good but their spatial distribution made it impossible to form a web forthe survey to be carried out. They were either too close or too wide apart. Most of the drill holes were blocked at these two sites as most of them had caved in due to the thick saprolite cover in these areas. The drill holes were not cased to the end of the saprolite layer hence this problem.

This prompted attention to be switched to Apensu South and Subika at Ahafo North. With Subika, since previous work had already been done there successfully, it was considered a good spot. Unfortunately out of sixteen drill holes probed, only seven were opened scatted over the area. These were underground holes which would have been very good but most of them were dry due to the excessive pumping of water from the Subika pit which was nearby.

Finally, out of forty-six holes probed at Apensu South, twenty-two were opened spread over the area with the separation and distribution looking very good for five of them. The average depth for these five drill holes was 276 m. Though it would have been great having a longer strike length, the challenges leading to this point made it imperative to run the survey over this area. This was an area close to the Apensu mining pit with not much previous ground geophysical survey information thereby making it very useful. Specifically there was no IP/resistivity data over this area. The gold values of these drill holes at this area were not very good considering its proximity to the Apensu mining pit and so data from these holes were critical in understanding what was happening and to see if more drill targets could be generated. The gold values for hole APSDD105 ranged from (0.03 - 1.93) ppm with average gold value of 0.44 ppm. Gold values for APSDD109 ranged from (0.01-5.4) ppm with average gold value of 0.54 ppm whiles hole APSDD117 had gold values between (0.01-1.08) ppm with an average of 0.23 ppm. Drill holes APSDD124 and APSDD136 had average gold values of 0.14 ppm and 0.23 ppm respectively where APSDD is the abbreviation of Apensu

Table 3.1: Drill holes with their collar coordinates and depth.

No	HOLE_ID	X [UTM]	Y [UTM]	Elevation [m]	Hole Depth [m]	Probed depth [m]
1	APSDD105	570046.862	775477.205	197	330	300
2	APSDD109	570197.381	775571.136	198	355	340
3	APSDD117	570084.478	775642.395	197	278	270
4	APSDD124	569976.843	775550.446	196	250	220
5	APSDD136	569966.394	775397.072	193	278	250

3.6 Pairing of Drill Holes

The selected drill holes were paired in such a way to form a web using the aspect ratio with no particular order. They were paired as follows: APSDD124 and APSDD105; APSDD105 and APSDD136; APSDD124 and APSDD136; APSDD117 and APSDD124; APSDD117 and APSDD105; APSDD109 and APSDD105; APSDD117 and APSDD109; APSDD124 and APSDD109. Based on these pairing, the drill holes were interconnected by ensuring that there was a linkage between them so that wires were connected from one hole to the other. After all the connections were made and paths created to all the drill holes, the area was then ready for data collection.
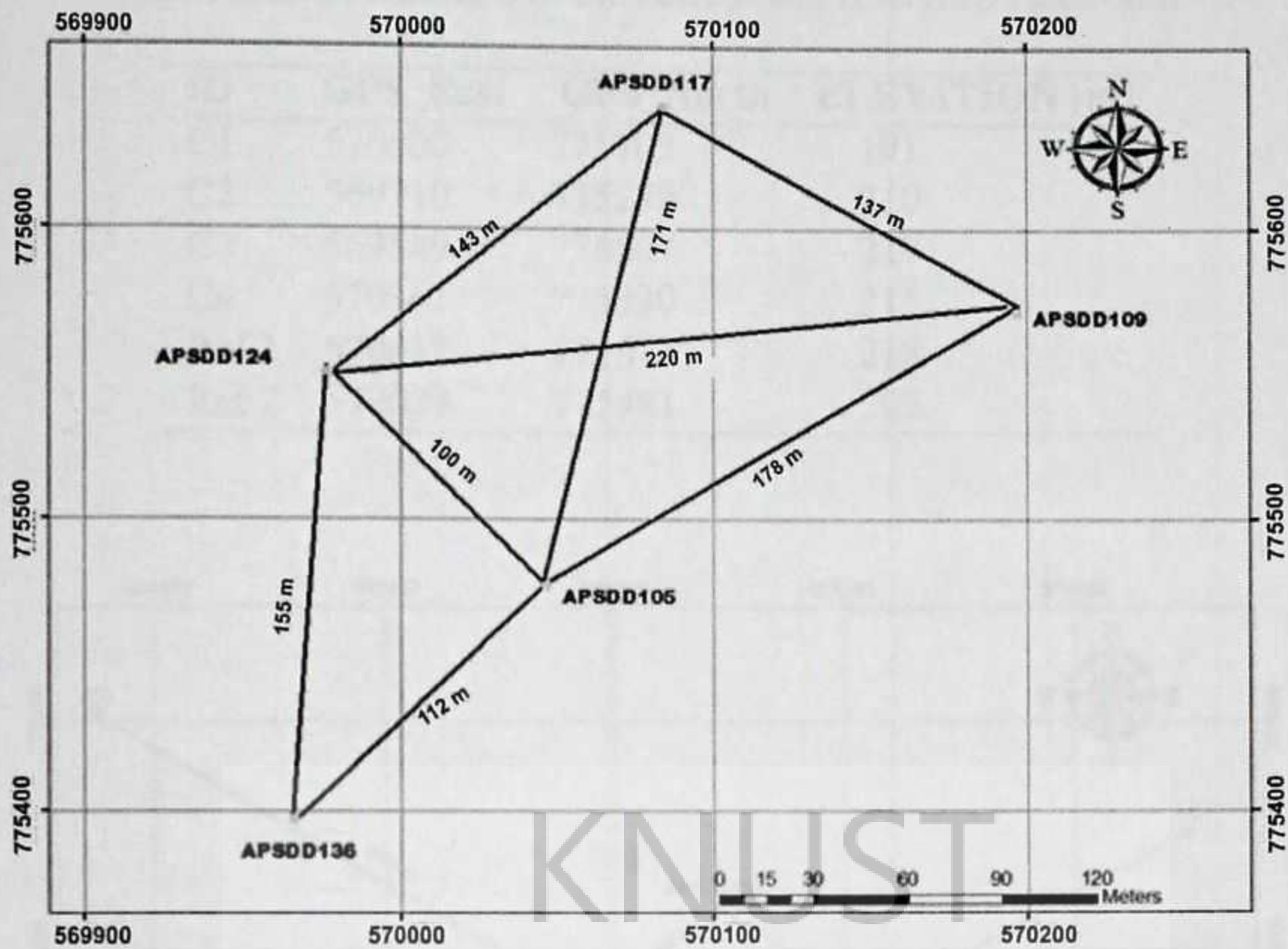
Figure 3.4: Web configurations of the drill holes showing their inter-connectivity.

3.7   Experimental set-up

The setting up involved the creation of the current pits for current transmissions, laying out of the current wires and laying out of potential wires between the drill holes. Before this was done, the current injection points were located with the help of the Garmin GPS. Two pairs of current pits were straddled perpendicular to each other over the drill holes with current electrode separation twice the average depth of the drill holes. One bipole was in NE - SW direction whiles the other was in NW - SE direction. The NE - SW bipole was labeled C1 - C2 whiles the NW - SE bipole was labeled C3 - C4. Ref 1 and 2 were the surface potential electrodes.

57

Table 3.2: Coordinates of the current and reference electrodes.

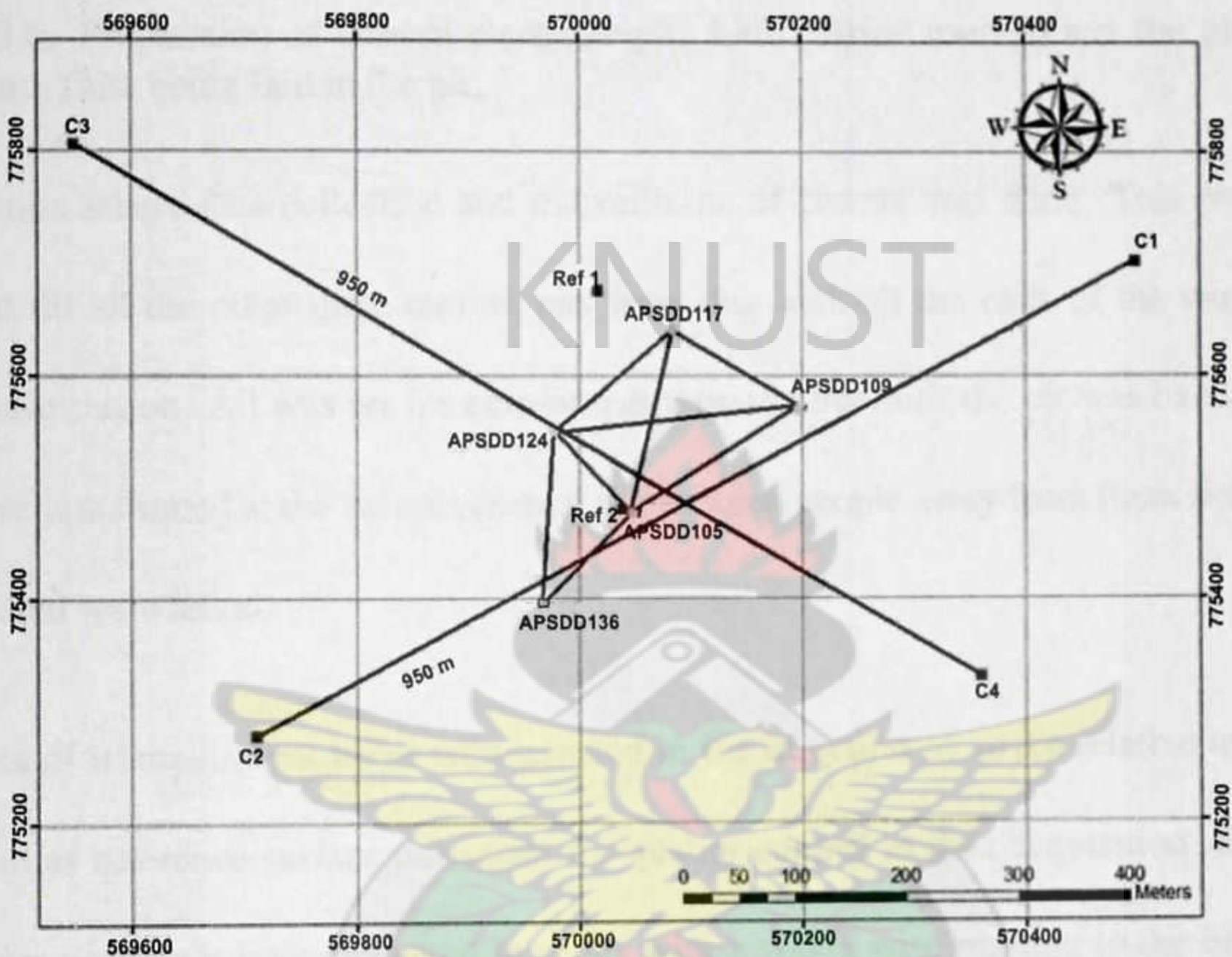| ID	GPS_East	GPS_North	ELEVATION [m]
C1	570500	775703	191
C2	569710	775279	210
C3	569549	775807	217
C4	570361	775330	215
Ref 1	570017	775677	218
Ref 2	570039	775481	203

Figure 3.5: Electrode setup of the survey showing the current injection points.

A 2 m² area was cleared after locating the places for the current pits with the help of a hand

held GPS and prepared for the pits. A 30 cm deep pit was dug with the help of pick-axe

and shovel. The pit was made wet with salt solution (brine) to increase the transmission of

electric current into the ground. Aluminum foil was then laid in the pit to increase the surface

area for the transmission of current.

The exposed end of the current wire was connected to one end of the aluminum foil and

the pit covered with sand and more water poured on the pit. The wire was then laid to a

58

Figure 3.6: Preparation of current electrode pit: Left - Brine used to wet the pit; Right - Aluminum foils being laid in the pit.

base station where data collection and transmission of current was done. This process was repeated till all the other three current pits were dug with all the ends of the wires getting to the base station. All was set for current transmission but until the pit was barricaded and then guards stationed at the various current pits to keep people away from them since current transmitted were lethal.

Two sets of triangular pot holes were created in the direction of strike relative to the holes and used as reference surface potentials for quality control in data acquisition. Each set of triangular pots were interconnected in series with a single wire running to the base station. Three potential electrodes made up each set which were connected in series.

After all these were done, the winches for data collection with the IP probe on it were positioned at the first two drill holes to be surveyed. A potential wire was then attached to each winch at a hole which served as a potential electrode for the holes. The winch with the IP probe and the cable connector to the base station is shown in figure 3.10. 'A' is the IP probe for data collection whiles 'B' is the cable connector.

Figure 3.7: Left - Triangular potential electrode connected in series ; Right - IP probe with the cable connector.

The pentapod with the counter were mounted on the holes and aligned with the winches placed some five meters away along the direction of the holes. The IP probe was lowered through the hexapod to the tip of it just at the entrance of the hole and the counter was set to zero before reading began.

The stage was now set for data collection. The first bipole to be read was connected to thetransmitter at the station which in turn was connected to the generator. Before transmission of current was started, there was clear communication between the crews at the various station and the guards to ensure that everyone was clear of the current pits since the transmitted current was lethal.

Figure 3.8: Left - Connection of the current wires and gen-set cable to the transmitter ; Right - Set- up of the IP probe on a drill hole .

The big black cable was in turn connected to a generator which powers the transmitter. A Honda generator was used. From figure 3.8 (Left), 'A' is the current wires connected to the transmitter from the electrode pits; 'B' is the transmitter cable to the generator and 'C' is the transmitter. Figure 3.8 (Right) shows an operator monitoring the measuring digital counter for the distance travelled by the IP probe into the hole.

3.8 Data Acquisition

The data collection involved transmitting current into the ground by means of a VIP 5000 transmitter and a generator and measuring the primary voltages, resistivity and chargeability. An Elrec pro receiver was used in the data acquisition. The two surface potential electrodes occupied the first channel of the receiver followed by the two electrodes from the two holes at the second channel. With the help of jumper cables, the channels were increased to seven to take readings between hole to reference 1 and reference 2. So the seven channels included data from reference 1 and 2, hole to hole, hole 1 to reference 1, hole 1 to reference 2, hole 2 to reference 1 and hole 2 to reference 2.

The first channel which was the two reference electrodes was used as the trigger channel throughout the data acquisition process. This channel remained constant in terms of the readings for the primary voltages for each pair of hole serving as good quality control check. They were the same because they remained stationary throughout the measurements.
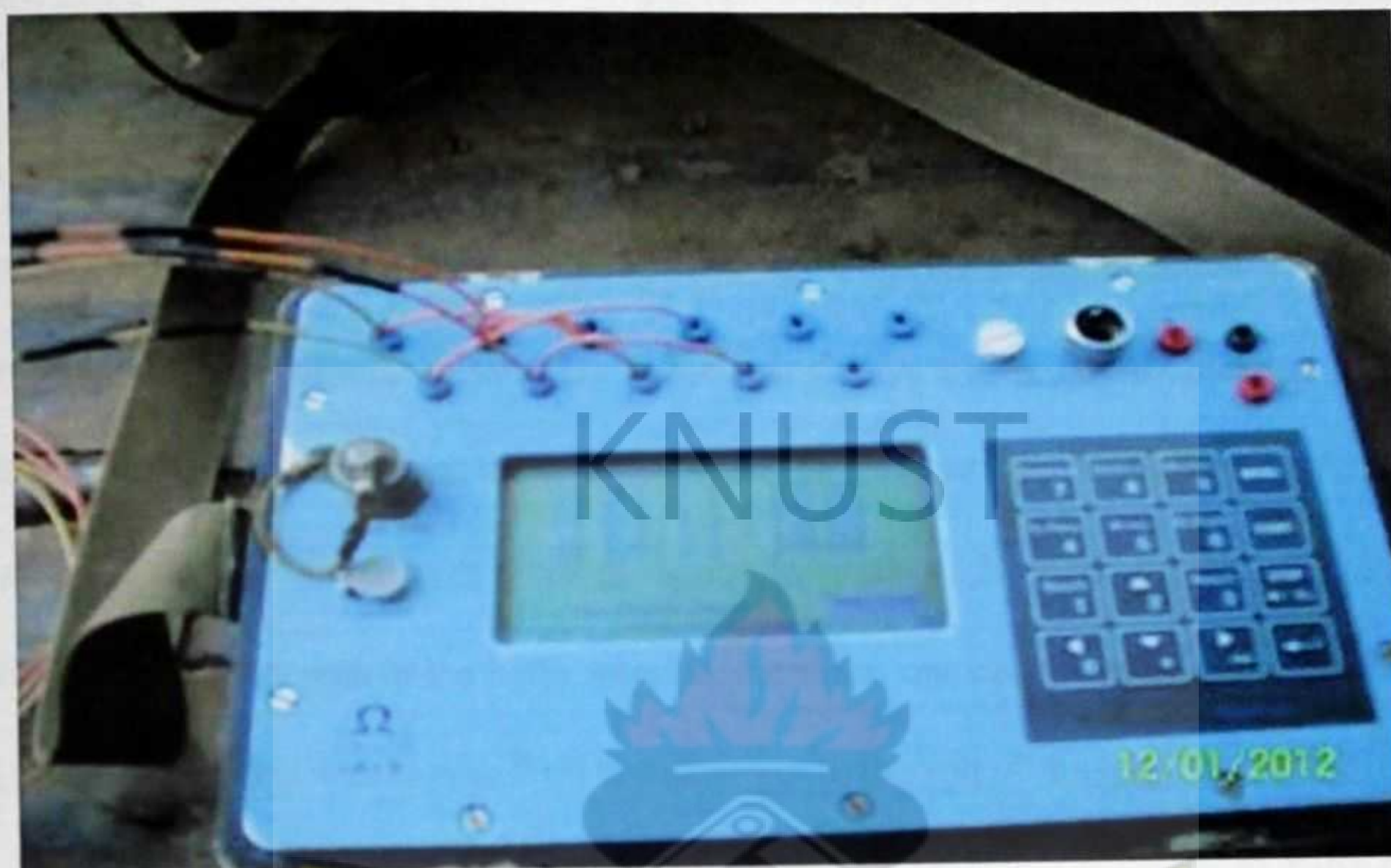

Figure 3.9: Elrec pro receiver with potential electrode cables.

This was how the cables from the two drill holes, surface electrodes and the jumper cables were arranged on the receiver. After these connections were done, the IP probe on each hole was dropped to the first 20 m with the help of the counter after setting it to zero carefully. The drill holes were surveyed at a constant interval of 20 m both down the hole and up the hole. The most northern of the two drill holes relative to each other was named as hole 1 and the other hole 2.The first of the two bipole C1 - C2 which was in NE - SW direction was connected to the transmitter ready for transmission. A filename to distinguish between the two bipoles were used to include the drill hole IDs and direction of bipole. A filename of NE11710501 indicates the use of bipole 1 between drill hole 117 which is the most northern

and drill hole 105 surveying down the hole. NW11710502 will mean reading holes 117 and 105 using bipole 2 surveying up the hole.

All the above drill holes were surveyed both down and up the holes. The average distance between the drill holes was 151 m. When all these parameters were set and fed into the receiver by the operator, the generator was powered for subsequent transmission of current. The amount of current generated depended on the contact resistance between the current bipoles. Beginning from the first bipole, readings were taken simultaneously from both holes after the transmission of current. There was always a clear communication between the operators at the transmitter, the two holes and the receiver to input the right parameters. As stated earlier, readings were taken at regular intervals of 20 m till the end of hole was reached. Since the depths of the holes were not the same, one ended before the other and the one which ended first was kept still till the other got to the end of the hole.

When the ends of hole were reached for both holes, the first bipole was changed for the second and the readings taken on our way up. The last hole to end was surveyed up keeping the other constant at the same constant interval until it got to the same level with the other hole for the two to continue again. All these were done manually with one person on the winch to control the movement and the other on the counter to check the distances.

A record of the hole ID, filename, most northern of the two holes, hole depths were kept. A total of 20 stacks for two good repeated readings were taken for each interval. 40 stacks of three or four readings were taken for noisy data. As a quality control measure, the data for channel 1 remained the same and it was well noted to make sure the right data was acquired. A change in the reading of channel 1 for the primary voltages meant something was wrong. The Elrec pro receiver gave information on the resistivity, chargeability and voltages across

the electrodes. It also had data to noise ratio known as the 'Q values' for quality control on the values churned out of the receiver. All the readings were done in a troop carrier which also served as the base station for easy mobility.

Figure 3.10: Data collection in a troop carrier on the receiver.

One pair of hole was surveyed each day from top to bottom of the hole using one bipole and vice versa using the other bipole. The data was downloaded daily on a laptop after the day's work and ready for processing and synthesizing.

3.9 Data Processing

The basic assumption was that only two potential fields were under consideration, one for each Tx bipole pair. The hole-to-hole method actually measured the change in value of this scalar field between two points (the potential electrodes).

64

By also measuring all potential differences relative to a 'reference' surface electrode, one could then calculate the potential difference between any two points in any of the holes by adding two of the other measurements together (as long as they used the same reference and same Tx bipole).

3.9.1 Data Preparation

The data was taken through a couple of processes to make it ready for the modeling process. Since the Elrec pro receiver was not designed for the hole-to-hole down hole survey, it was imperative to go through these processes to suit the modeling. The direct resistivity and chargeability readings from the field were not used but only after these processes.

First, all the primary voltages (Vp) data were normalized to a current of 1A (divided by the Tx current). This ensured that only two possible potential fields were considered. Also all repeated readings were averaged. This was done for the resistivity readings to normalize it or to bring it to the same base for modeling purposes.

Next the IP measurements were converted to secondary potentials. This was achieved by multiplying the chargeability values and decays by the Vp's where Vs and Vp are the secondary and primary voltages respectively since Chargeability is simply Vs/Vp. This eliminated most of whatever EM coupling may be present in the decays. At this point inversion could then be run on the hole-to-hole data that was actually collected.

3.9.2 Synthesizing Data

The resistivity and chargeability measurements between potential electrodes were calculated. This was done by picking one of the surface reference pots to be the potential reference. Most of the drill holes were used many times and so multiple measurements were obtained from that drill hole to the reference. These repeats were averaged before the next step which was the modeling of the data.

Every combination of data that was measured relative to this reference was added together. The same thing could be done using the other reference, to get an identical data set, which could also be averaged together to improve the noise level slightly. After this stage, the inversion was run on this comprehensive dataset.
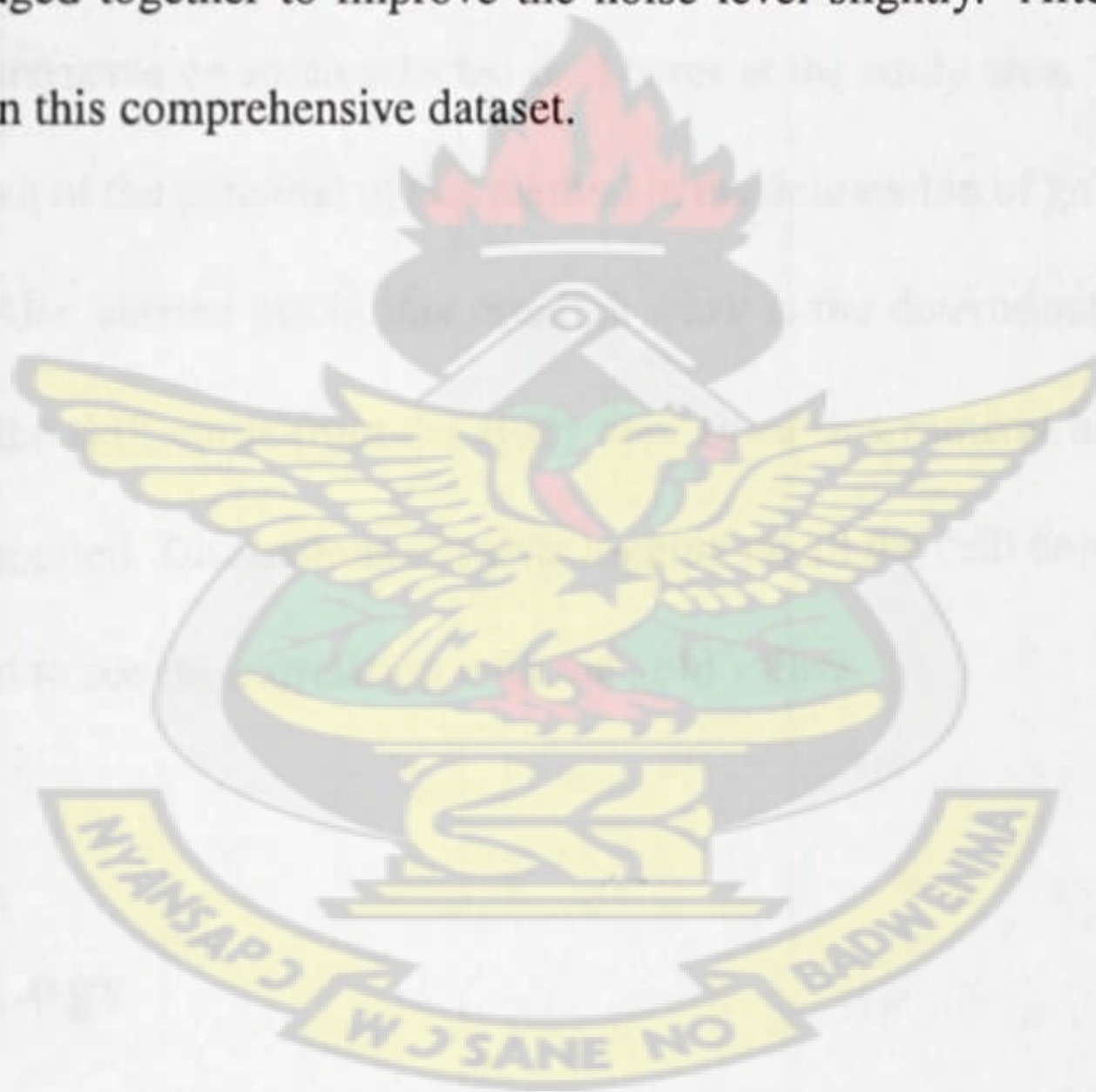
CHAPTER 4

RESULTS AND DISCUSSIONS

Down hole electrical logging was carried out on the Apensu South area of the Newmont Ghana Gold Ahafo Project in Brong Ahafo to determine its usefulness in the delineation of gold mineralization. The datasets processed namely induced polarization and resistivity datasets are discussed. Also considered in this work are results from resistivity and chargeability measurements on some selected drill cores at the study area. This is to help in the full understanding of the potential of this method in the delineation of gold mineralization in the study area. Also carried out in this research work is the determination of the pyrite composition in all the drill cores from the study area since this mineral have effect on the electrical methods applied. Discussions of pyrite logging on all the drill holes surveyed were therefore considered to see the correlation with the gold values.

4.1 Pyrite Logs

The results of the pyrite logging on all the drill cores of the drill holes revealed considerable amount of disseminated sulphide (pyrite) in the project area. The outcome of this showed why the IP data was more useful for this project as the disseminated sulphides are chargeable. A plot of depth interval against the pyrite and gold values from the pyrite logging of all the drill cores from the drill holes showed some correlation between pyrite and the gold values at

67

some of the intervals within the drill holes. Generally, the pyrite percentage was much higher than the gold percentage in all the drill cores making this method very good in this area. This means that there are other factors other than pyrite alone which controls the presence of gold. Some of these factors are alteration, structures, etc.
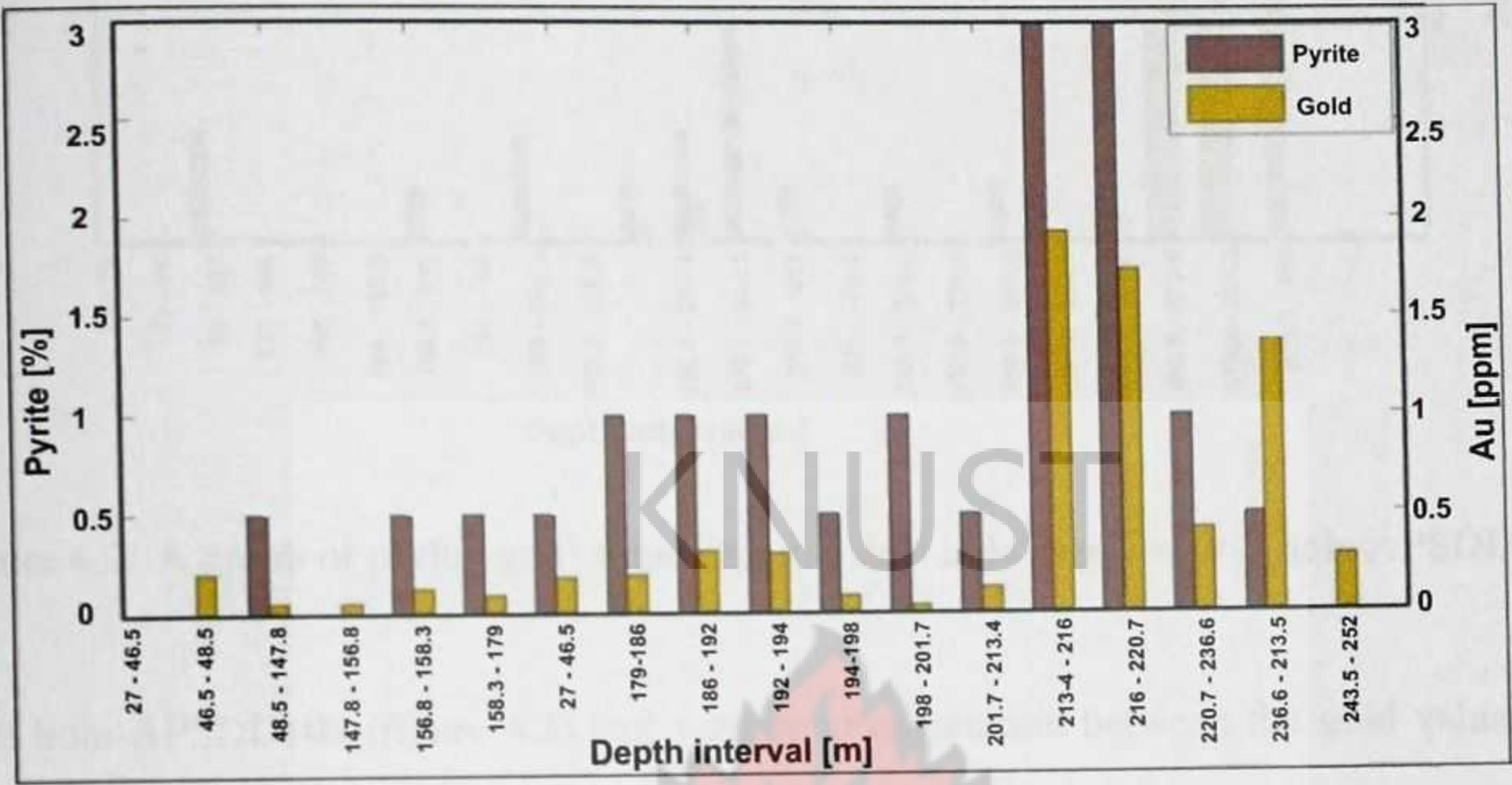

Figure 4.1: A graph of pyrite with gold values for hole APSDD105.

It is observed from figure 4.1 that the pyrite and gold composition are variable within the different depths of the drill hole. Also noted is that all the pyrites logged were associated with some percentage of gold but some of the gold mineralized zones corresponding to depths of (46.5 - 48.5) m, (147.8 - 156.8) m and (243.5 - 252) m were found not to have any notable pyrite composition. The highest percentages of pyrite and gold were found at depth intervals of (213.4 - 220.7) m and (220.7 - 243.5) m. These depths recorded pyrite and gold compositions of 3%, 1.9 ppm (part per million) and 3%, 1.7 ppm respectively giving good indications for the use of this method. It can be observed from figure 4.1 that the pyrite percentage was higher than the gold percentage. The average gold value for this hole was 0.44 ppm.
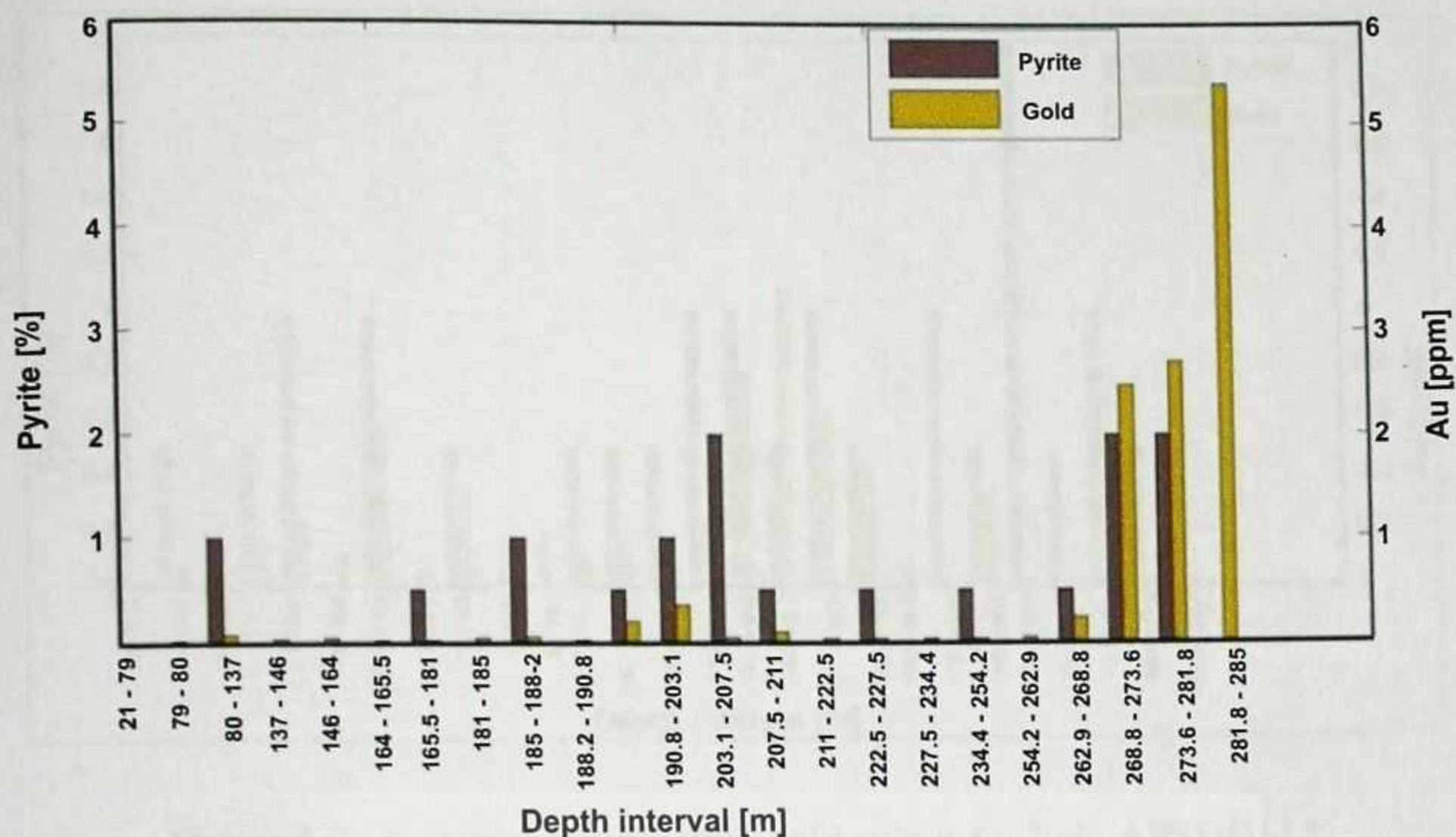
68

Figure 4.2: A graph of pyrite, gold values against drill hole depth of drill hole APSDD109.

Drill hole APSDD109 (figure 4.2) had very good correlation between the gold values and pyrite at depth interval of 268.8 m and 281.8 m. Traces of gold values were found at most areas where there were pyrites. However, there is exception at depth interval of 281.8 m to 285 m which recorded the highest gold percentage composition in the hole with no apparent presence of pyrite. This goes to proof the point that there are other factors other than pyrite alone that control the presence of gold. It may also be attributed to the fact that there were some traces of pyrite but the logger found nothing based on what he saw which makes this process of logging very subjective in areas where the pyrite is not of high percentage. This hole had an average gold value of 0.54 ppm.
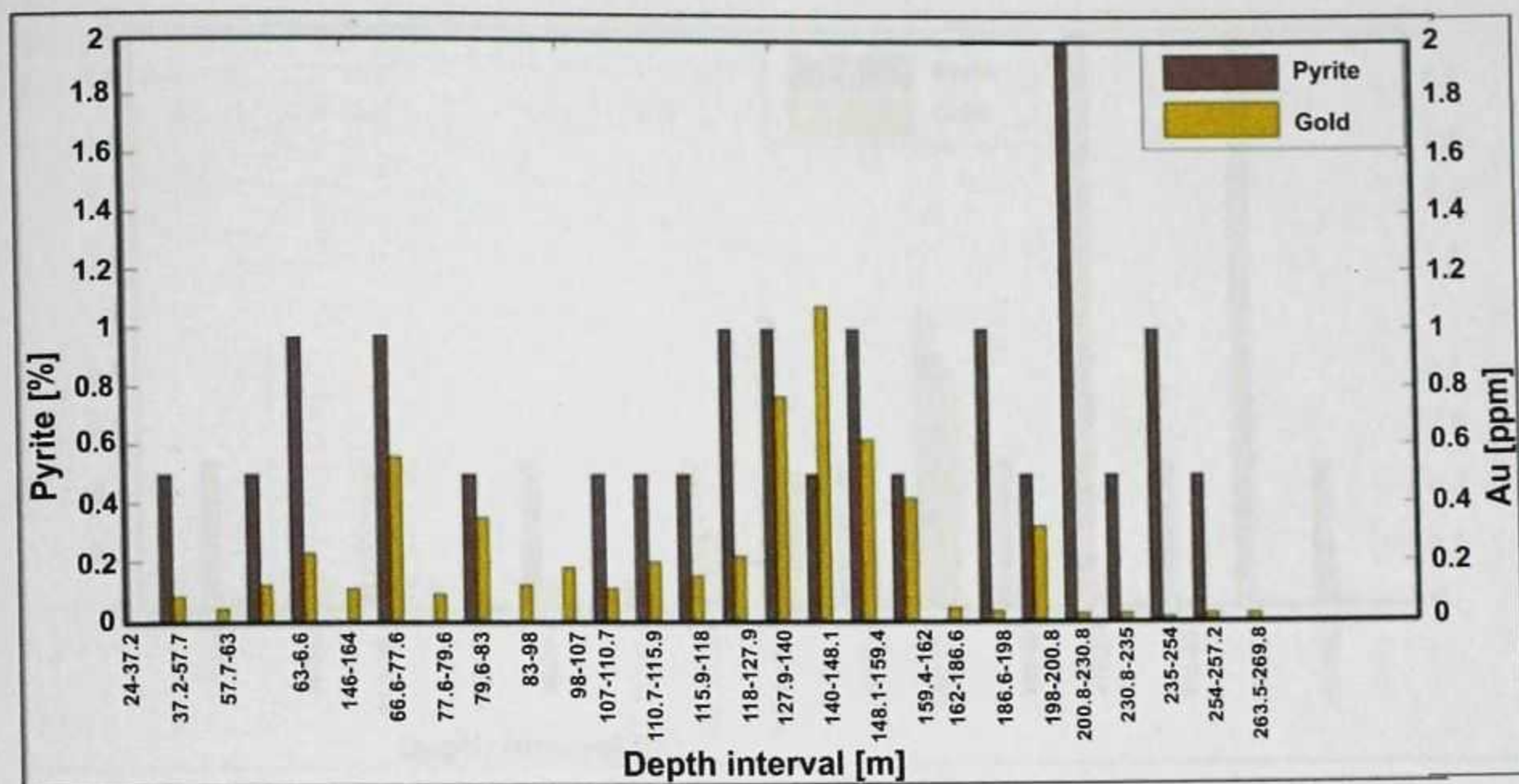
69

Figure 4.3: A graph of pyrite with gold values for hole APSDD117.

Drill hole APSDD117 in figure 4.3 shows relatively high percentage of pyrite among all the drill holes surveyed basically from near surface to the end of the hole. Consequently the amount of gold seems to be higher than all the other holes though the best grade was not from this hole. It also did not have very good gold values at depths between 200 m and 269 m though the highest percentage of pyrite occurred within this range from (200.8 - 230.8) m. This drill hole had a better correlation between the percentage pyrite and presence of gold at all the depths as every interval had some gold associated with the pyrite though range intervals (77.6 - 79.6) m, (83 - 98) m, (98 - 107) m had no pyrite associated with the gold values. The average gold value of this hole was 0.23 ppm
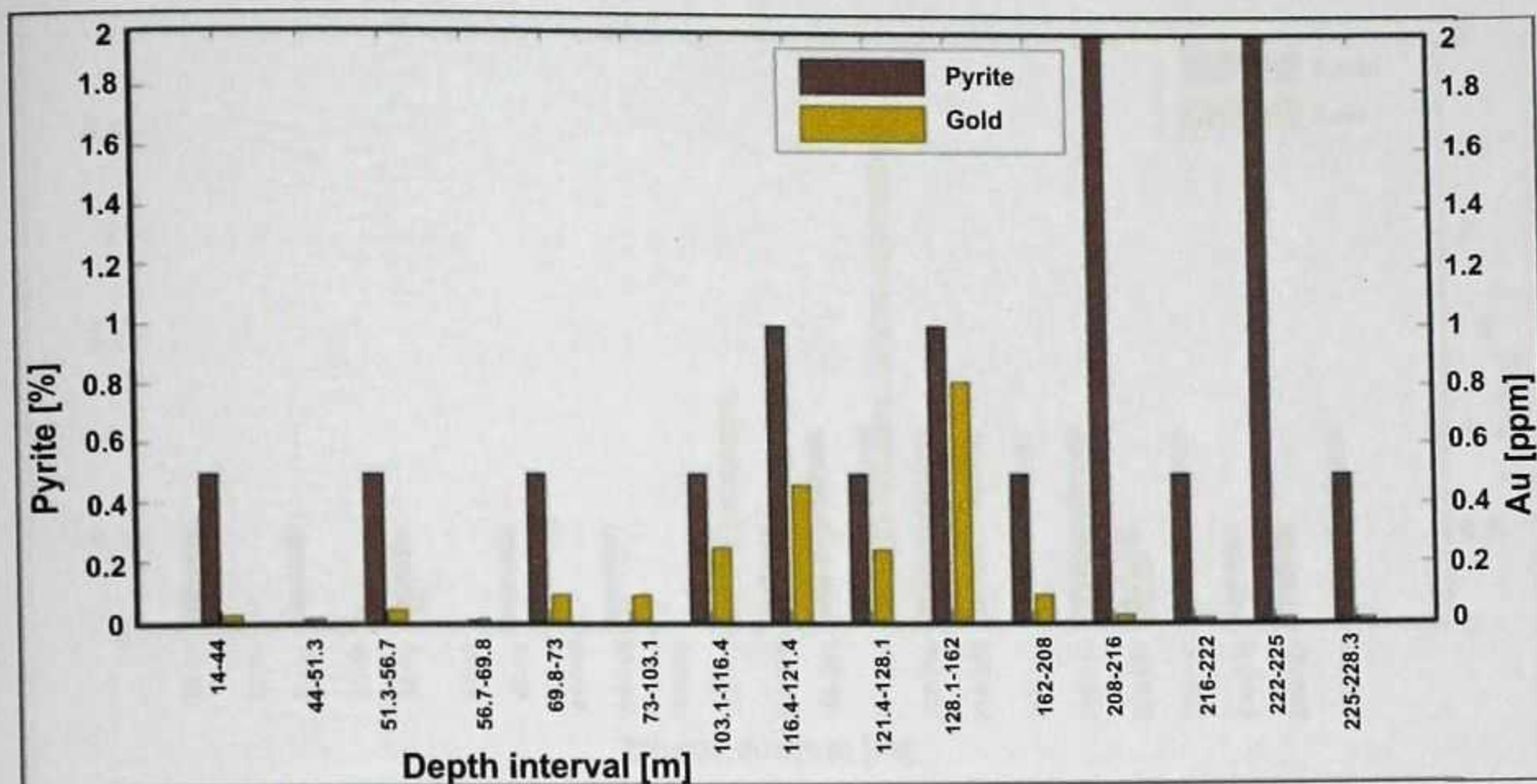
Figure 4.4: A graph of pyrite with gold values for hole APSDD124.

Drill hole APSDD124 (figure 4.4) seems to have the least percentage of pyrite among all the drill holes surveyed and also recorded the least amount of percentage of gold assay values found in all the drill holes surveyed. This hole also did not have good gold values at depth but high amount of pyrite. The good gold values were found also at the mid-section just like the previous drill hole. It had considerable amount of percentage pyrite at all the intervals with the highest occurring at intervals (208 - 216) m and (222 - 225) m. The average gold value for this hole was 0.14 ppm.
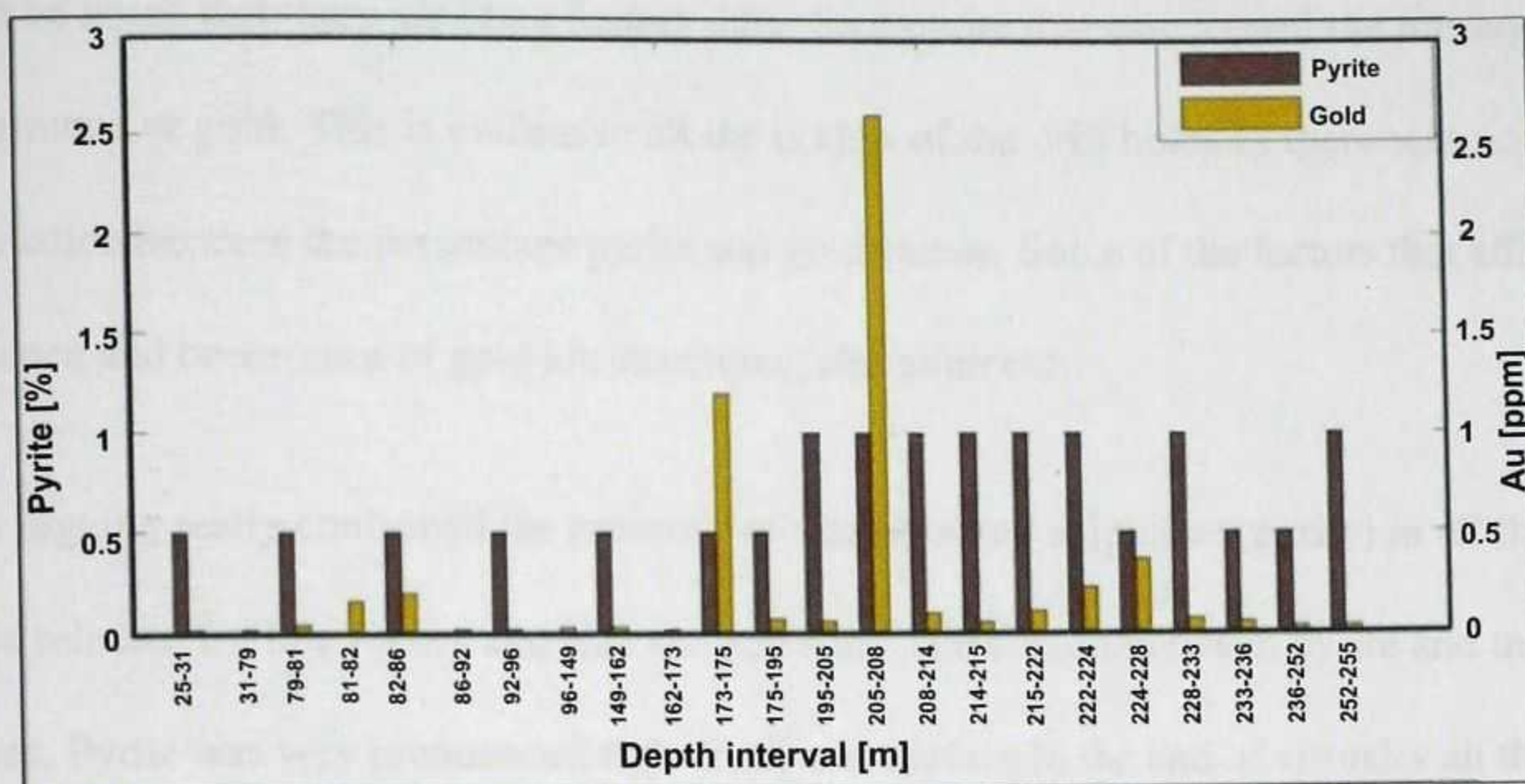
Figure 4.5: A graph of pyrite with gold values for hole APSDD136.

Drill hole APSDD136 in figure 4.5 also had very reasonable amount of pyrite percentage composition almost from the surface to the end of the hole also with the good gold values at the depth intervals of (173 - 175) m and (205 - 208) m within the mid-section of the graph. The highest percentage of gold value was found at the depth interval of 205 m to 208 m with an equal high pyrite percentage composition of 1%, a compositional percentage that is recorded by eight other intervals. This drill hole also had a bit of gold values at depth from 208 m to the end of the hole. This hole had an average gold value of 0.23.

It was observed from the result of the logging that the percentage pyrite did not correspond very well with the gold values throughout the holes. This deviation could be attributed to the subjectivity used in the logging instead of the qualitative geochemical analysis used in the gold composition analysis. In the subjective logging, the logger determines the value to give depending on what is seen on the split surface of the core. In this way a different logger could give a different value to the same observation of pyrite. This could influence the percentage of the pyrite collected. But generally, the higher percentage of pyrite in all the drill cores from the drill holes showed why the IP data was more useful than the resistivity data. It

72

must be noted that there are other factors other than pyrite that can control the presence and occurrence of gold. This is evident in all the graphs of the drill holes as there was no direct correlation between the percentage pyrite and gold values. Some of the factors that affect the presence and occurrence of gold are structures, alteration etc.

This logging really confirmed the presence of disseminated sulphides (pyrite) in all the drill holes selected for this survey and also showed some correlation between pyrite and the gold values. Pyrite was very pronounced right from near surface to the end of virtually all the drill holes with some deviations at some points in the survey area thereby making the IP method very useful and successful.

4.2 Resistivity Data

4.2.1 Laboratory Resistivity Result

Laboratory resistivity measurements carried out on some selected drill cores at the survey area in 2009 showed poor correlation between gold assay values and resistivity values at depth within the study area (Takyi-Kyeremeh, 2010). This seems to be the general trend of the Newmont Ahafo South Project area where my project site falls. With this in mind not much was expected regarding the application of the resistivity data in the mapping of the gold mineralized zone at depth and this was also the case in the first case study of this method at the Ahafo project area. The results of the laboratory measurements on some selected core at the Ahafo project area are shown.

Table 4.1: Results of resistivity measurements on selected drill cores at Subika.

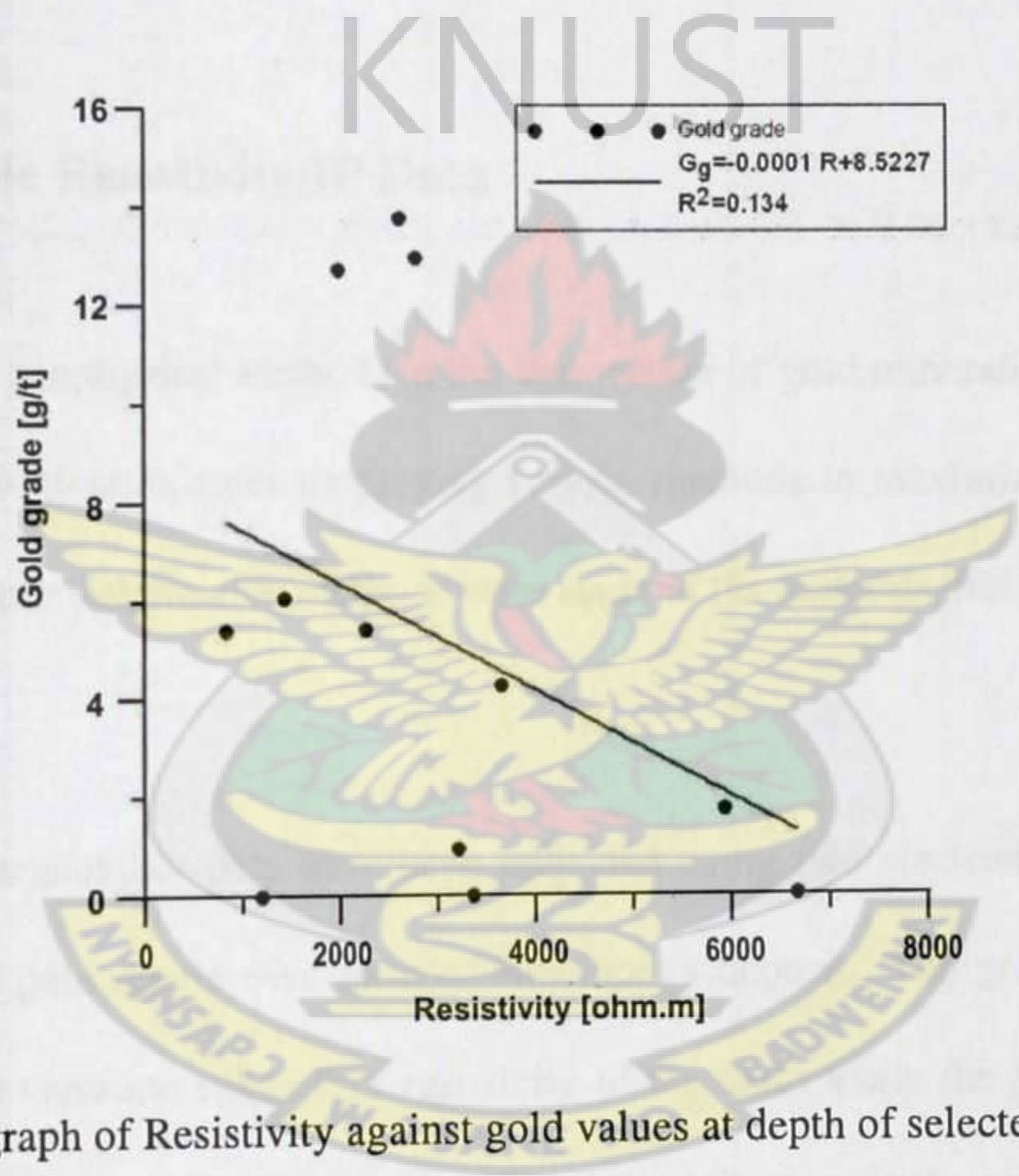| Hole ID	Depth Range [m]	Resistivity [Ohm.m]	Gold grade [g/t]
SKP096	330 - 331	66633	0.03
SKP096	348 - 349	14299	2.060
SKP096	370 - 371	8277	5.4
SKP096	379 - 380	26084	13.81
SKP083	440 - 441	33595	0.005
SKP083	486 - 487	59280	1.76
SKP083	516 - 517	19798	12.73
SKP083	522 - 523	36464	4.3
SKP107	630 - 631	11904	0.005
SKP107	678 - 679	32026	0.96
SKP107	701 - 702	27752	12.98
SKP107	716 - 717	22615	5.42

Figure 4.6: A graph of Resistivity against gold values at depth of selected drill cores.

Figure 4.6 is a gold grade verses resistivity scatter plot of some rock samples at depth in the study area. This is to determine the relationship between the gold mineralization and the resistivity of the samples. The result gives a negative correlation between the gold values and resistivity at depth with a coefficient of correlation of -0.37. This shows a decrease in gold assay values with increasing resistivity in the area. The general decrease in gold assay values

with increase in resistivity shown by (figure 4.6) can be attributed to the pyrite composition of the zone of mineralization that is associated with the Birimian mineralization (Griffis et al., 2002; Kesse, 1985; Ahafo Feasibility Study, 1997). The sulphide (pyrite) in general have a low resistivity while the host rock have a high resistivity, hence its presence in the rock will lower its resistivity. It is also observed from Table 4.1 that there is no correlation of the resistivity with depth of the sample. This indicates that at depth there is no well-defined resistivity signature though there are spot of good gold values hence no correlation with the gold values.

4.2.2 Drill hole Resistivity/IP Data

The application of geophysical methods in the delineation of gold mineralization cannot be over emphasized, with companies employing various methods to maximize their reserves. Resistivity and induce polarization methods were some of the methods that were used in this regard.

Resistivity and chargeability data have been collected using two electrode arrays namely gradient array and pole dipole over most of Newmont's deposit. The gradient array data mapped the lateral variation subsurface resistivity of the earth while the pole dipole array investigated the vertical variation of the subsurface anomalies seen in the gradient array data. Various surveys have shown a good correlation between the resistivity, chargeability and the gold values at surface. It was observed that at depth, the chargeability seemed to work very well from the hole-to-hole survey carried out at the study area as compared to the resistivity method. This could be attributed to the presence of disseminated sulphides with the zone of mineralization hence producing a strong induced polarization effect. The resistivity on the

75

other hand did not produce any good result from the down hole resistivity log at depth.

4.3 Resistivity Data

Figure 4.7 is a 3D block model obtained from the resistivity data collected from the hole-to-hole survey of six pair of drill holes in the study area. It is observed from the block resistivity model that a highly resistive material occurs at the surface which is in agreement with the geology of the area. It is mapped as a granitoid which is highly resistive. This did not give much information in terms of the correlation with the gold values at depth shown by previous ground base survey over the area. This highly resistive body at the surface indicated by 'A' in figure 4.7 confirms the general trend of the geology in the area of the survey. A lesser resistive body was also mapped at depth which is labeled B.
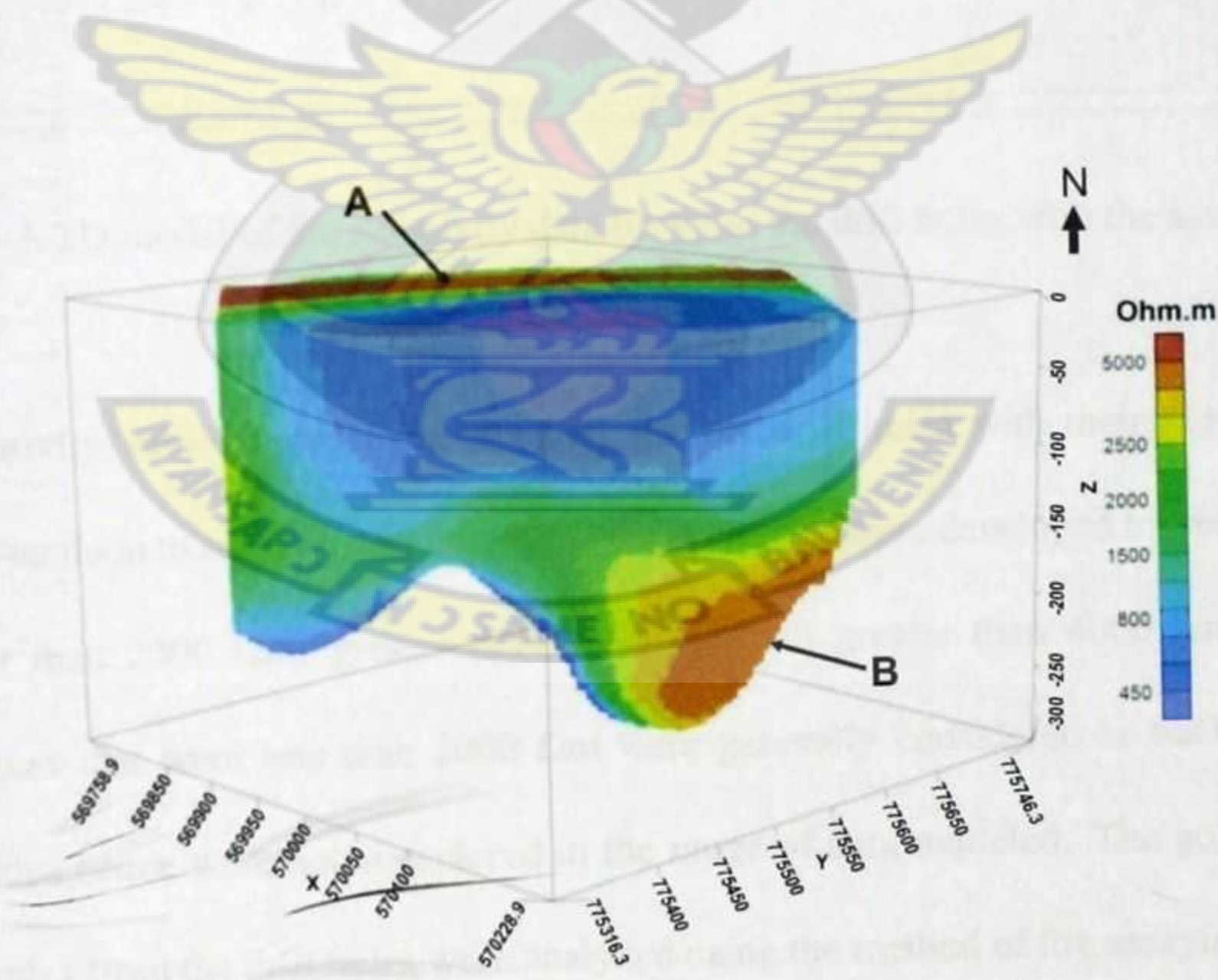

Figure 4.7: A 3D block model of the Resistivity.

All the drill holes with their assays plotted on the 3D resistivity model showed the gold mineralized zone falling out side the highly resistive zones. The mineralized zone fell in the conductive zone labelled 'C' in figure 4.8. This is probably due to disseminated sulphides associated with the mineralized zone. A lesser resistive zone labelled 'C' did not map any gold value.
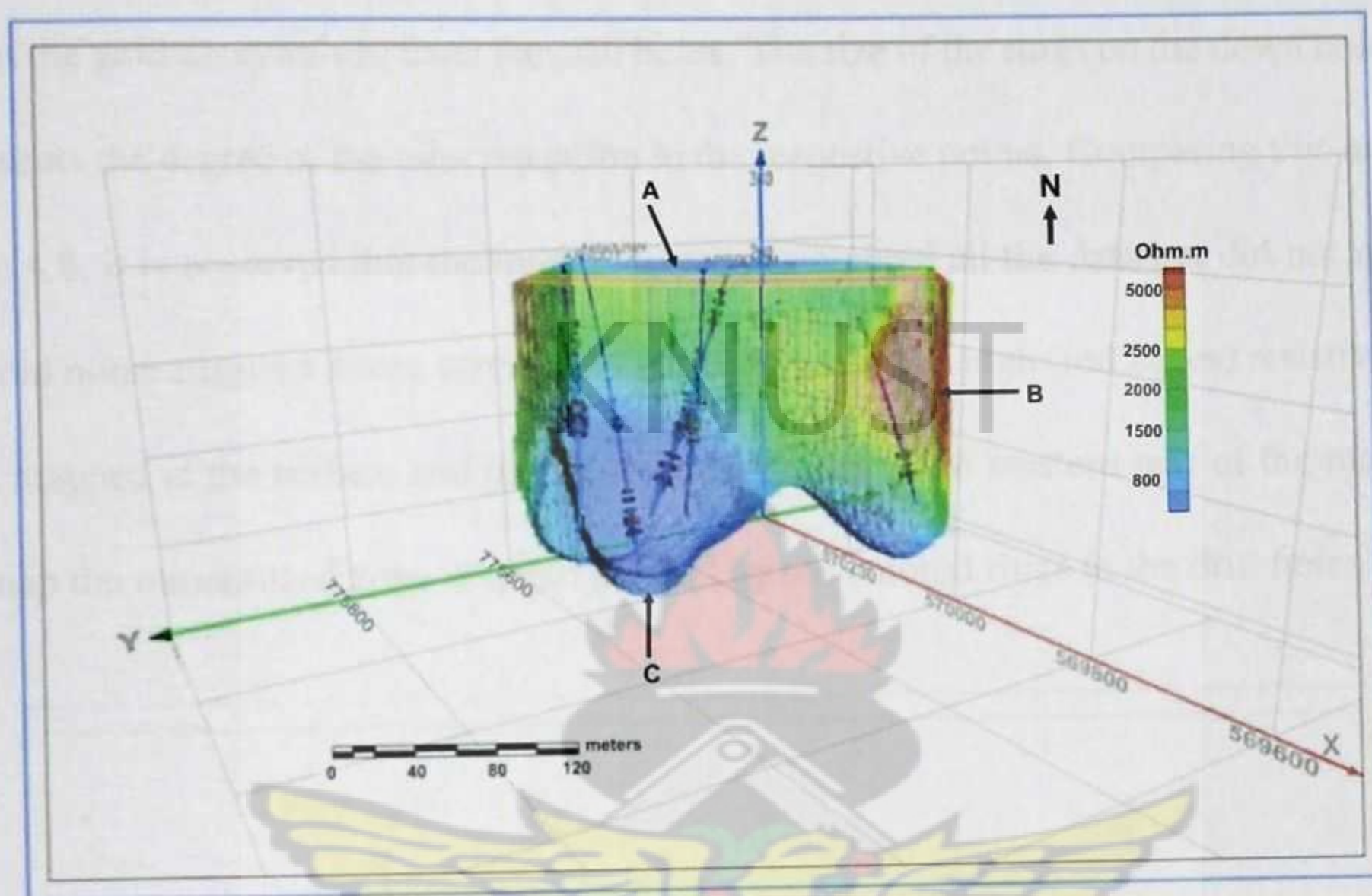

Figure 4.8: A 3D model of the resistivity data showing the drill holes with the assays.

Different resistivity value ranges were modeled and the drill holes with their gold assay values plotted on them to see how they correlate. These models were developed for resistivity values greater than 2000 Ωm; greater than 3000 Ωm and greater than 4000 Ωm. The resistivity values that were less than 2000 Ωm were generally considered as background resistivity values hence were not considered in the range of data modeled. The gold assay values of samples from the drill holes were analyzed using the method of fire assaying at the SGS laboratory at Kenyase. Drill holes with the gold values in it were plotted on the models to find how well they mapped the gold mineralized zones. In order to determine the range of

the resistivity values that clearly delineated the zone of gold mineralization, different ranges

of resistivity data were used in modeling the data.

Figure 4.9 is the resistivity model for resistivity values greater than 2000 Ωm. In this image

the pink parts of the block represent the zones of high resistivity while the light green portions

represent relatively lower resistivity zones. The down hole plots on the other hand are the

plot of the gold assay values from the drill holes. The size of the rings on the down hole strips

represents the degree of the mineralization in the respective points. Comparing this model to

figure 4.8, it is observed that the model virtually contained all the data but did not map out

the gold mineralization zones very well. From these models, high (red zones) resistive zones

were mapped at the surface and part of the eastern and south western part of the model did

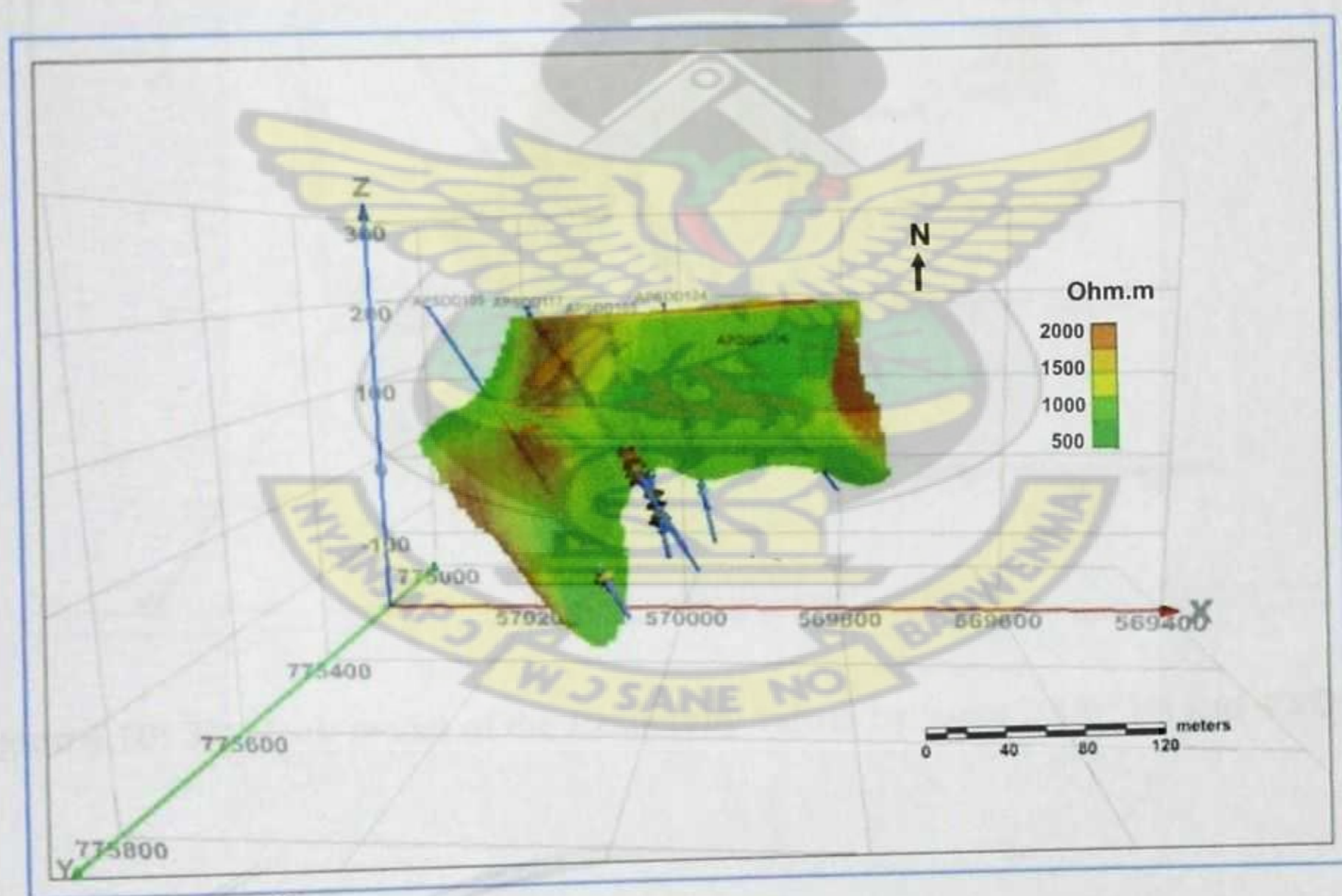not map the mineralized zone at depth marked by the colored rings in the drill holes.

Figure 4.9: 3D block model for Resistivity values up to 2000 Ωm.

From the figure 4.9, most of the gold values in the drill hole fell in the light green part of

the model with gold values in hole APSDD109 falling outside the model at depth with no

78

gold values in the resistive part. Figure 4.10 shows the resistivity model for resistivity values

greater than 3000 Ωm. It can be observed that a highly resistive body is mapped at the surface

indicated by 'A' which maps some gold values in drill holes APSDD117 and APSDD105 at

the surface. The next higher resistive body is mapped at the eastern side of the model labeled

B which clearly misses the gold mineralized zone at depth. Point 'C' shows the least resistive

part of the model which mapped some gold values in drill hole APSDD109 as shown by the

arrow. The ring-type multi-colored portion in the drill holes are the gold values and clearly

this model also missed out in mapping the gold mineralized zone as they all fell outside the
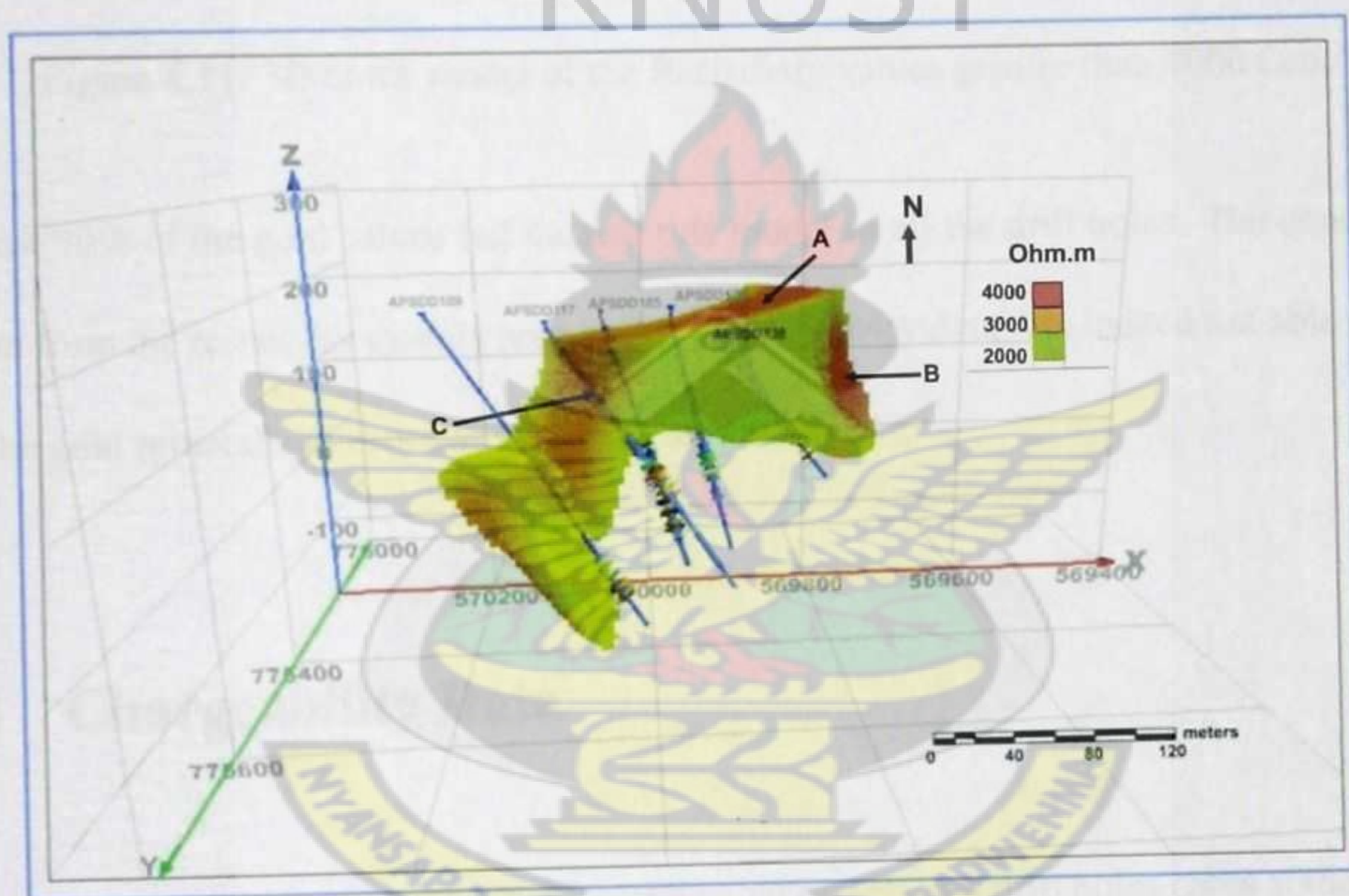
model.

Figure 4.10: 3D block model of the Resistivity values between 2000 Ωm and 4000 Ωm.

Higher resistivity values more than 4000 Ωm clearly missed out on mapping the mineralized

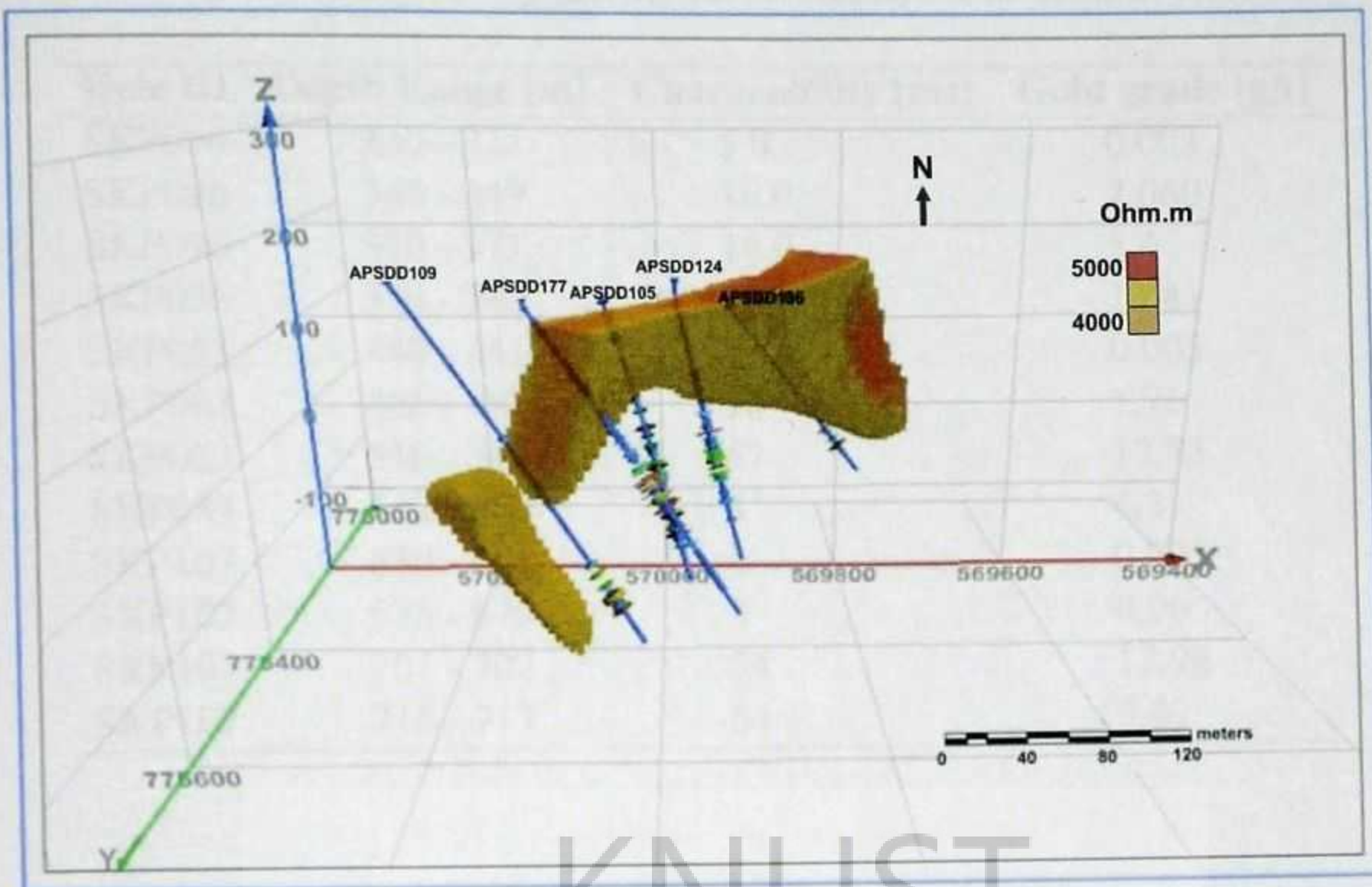zone at depth although it did map out some gold values at the surface in hole APSDD105.

Figure 4.11: 3D block model of the Resistivity values greater than 4000 Ωm.

Almost 90% of the gold values fell outside this model in all the drill holes. The conclusion drawn from the resistivity models proved that the resistivity data was indeed not able to map out the gold mineralized zones as proved in all the models.

4.4 Chargeability Data

Chargeability measurements (Table 4.2) carried out on selected drill holes cores at the survey area wherethe hole-to-hole down hole survey was first tested showed very good correlation with the gold values at depth (Takyi-Kyeremeh, 2010).

Table 4.2: Results of chargeability carried out on selected drill cores at the survey area.

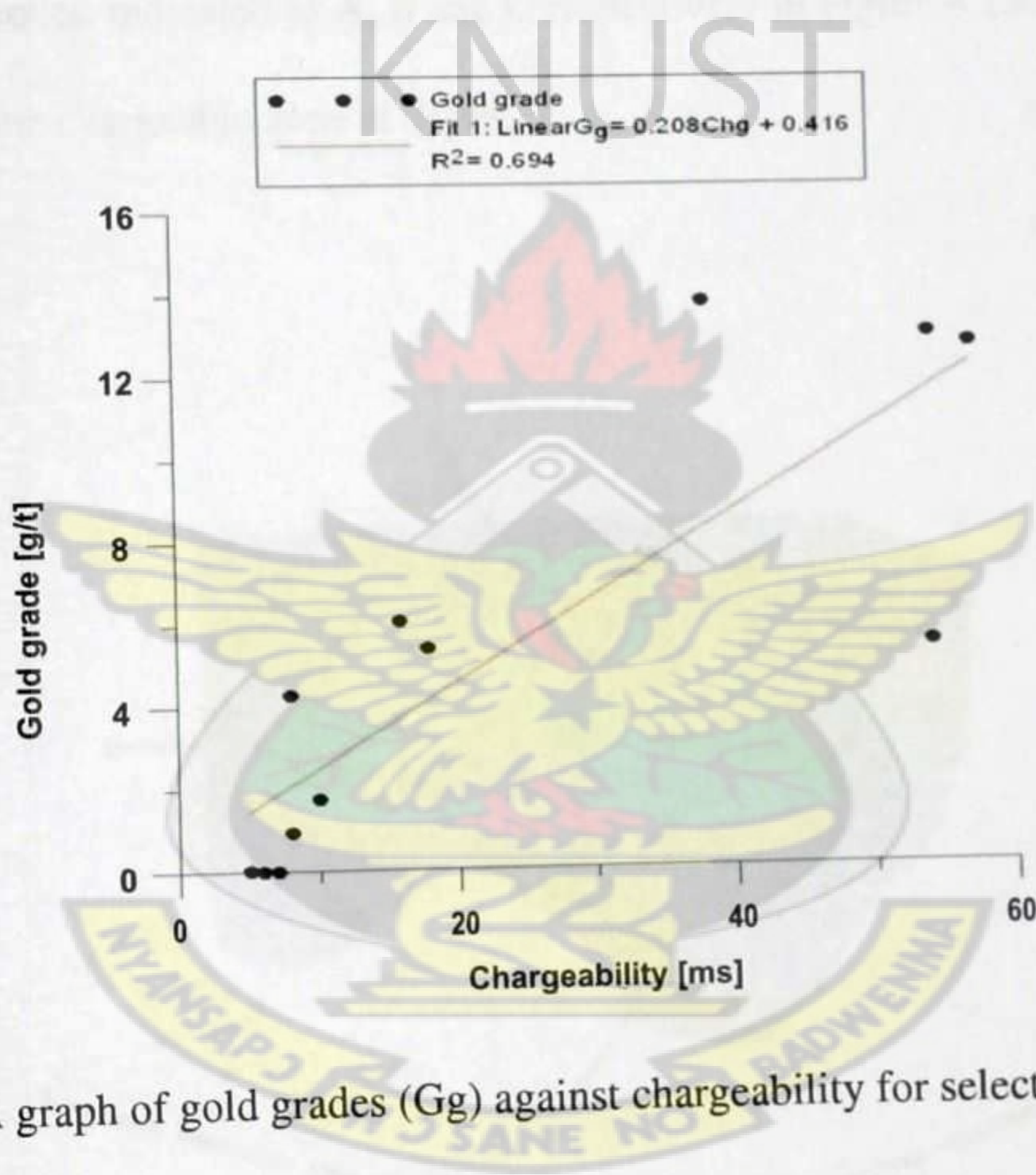| Hole ID	Depth Range [m]	Chargeability [ms]	Gold grade [g/t]
SKP096	330 - 331	5.0	0.003
SKP096	348 - 349	16.0	2.060
SKP096	370 - 371	18.0	5.4
SKP096	379 - 380	38.0	13.81
SKP083	440 - 441	7	0.005
SKP083	486 - 487	10	1.76
SKP083	516 - 517	57	12.73
SKP083	522 - 523	8	4.3
SKP107	630 - 631	4	0.005
SKP107	678 - 679	8	0,96
SKP107	701 - 702	54	12.98
SKP107	716 - 717	54	5.42

Figure 4.12: A graph of gold grades (Gg) against chargeability for selected core samples.

These drill holes were selected based on the depth and the gold values. The results showed a strong positive correlation between chargeability and gold grade with correlation coefficient of 0.83. This gave an indication of a chargeability signature at depth. This really confirmed the test hole-to-hole survey findings carried out over the survey area which really mapped the gold values at depth. This also confirmed the use of the hole-to-hole down hole IP method

81

at depth and giving credence to the pyrite logging as well.

In view of this, further models were made on the chargeability data to try and map the gold values at depth. The previous hole-to-hole survey at the project area gave a very good correlation between the gold values and the chargeability at depth. But picking data right at the source that is in the drill holes gave a better understanding of the whole process and gave a very good correlation between the chargeability and the gold values.

A block model of the chargeability data showed a chargeable zone at the surface, at depth and in the mid-section indicated as A, B and C respectively in Figure 4.13. But of uttermost importance was the chargeable zone at depth.
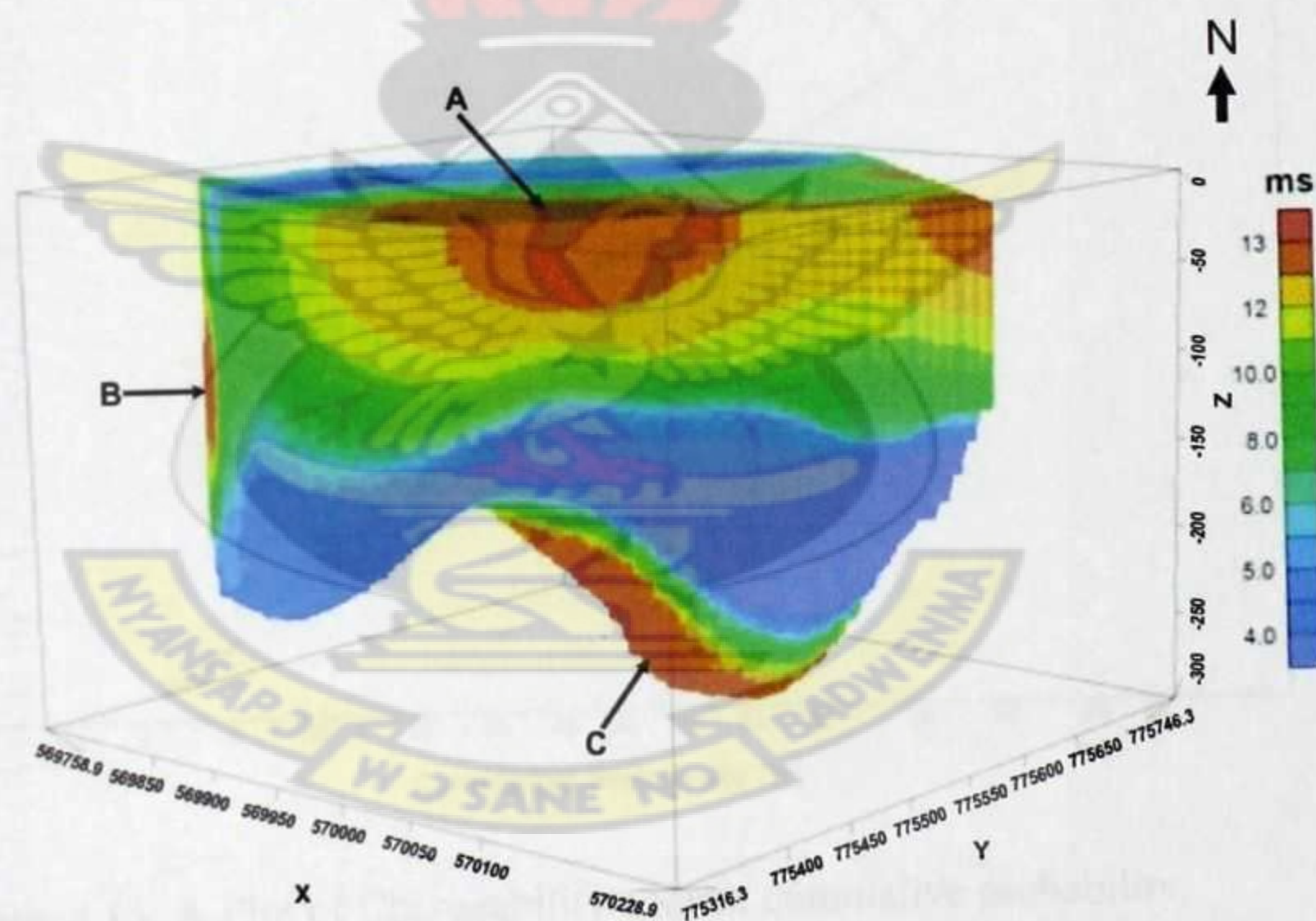

Figure 4.13: 3D Chargeability block model of Apensu-South.

This data was then taken through a series of processes to get the best fit with the gold values obtained from the drill data. The chargeability model was run through the drill hole data to see how it mapped the gold values. By so doing, the threshold chargeability value above which the gold values were clearly mapped was obtained. Iso-surfaces were derived from the model to get the best fit for the data, which is the optimum value range to perfectly map the mineralized zone. Different iso-surfaces were selected till the one that best mapped the mineralized zone was attained. A log - linear plot on the chargeability data (Figure 4.14) showed two natural breaks in the data out of which models were made on them to find which one best fit the data.
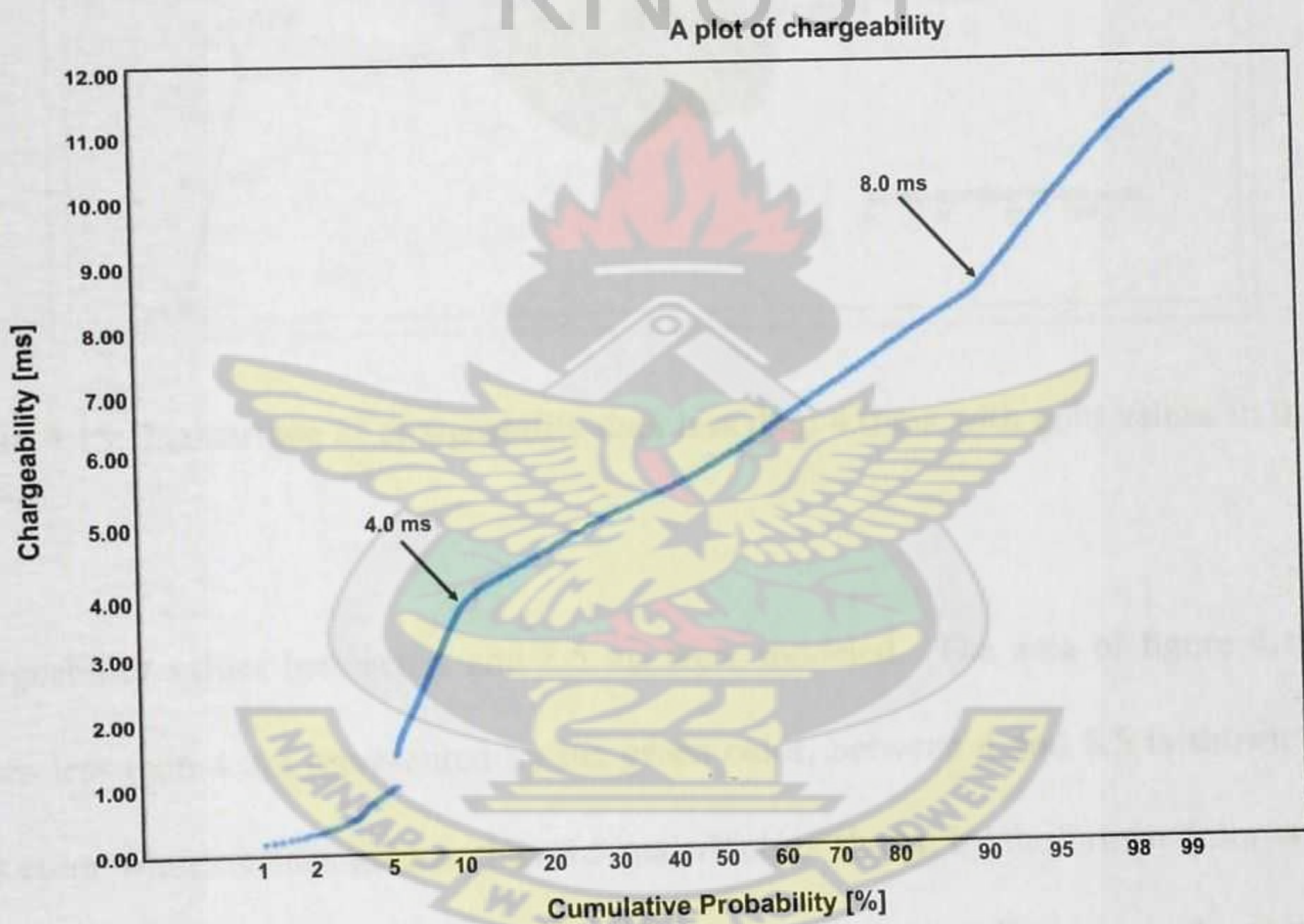

Figure 4.14: A Plot of Chargeability against cumulative probability.

Based on the chargeability plot, iso-surfaces were made for 4.0 ms and less, between 4.0 and 8.5 ms and above 8.5 ms. The drill holes with the gold values were then plotted on these models to find the one that best mapped the gold mineralized zone. The chargeability values

83

less than 4.0 ms were the background values and this was evident in the iso-surface generated for this data set. There was no pattern in it as it covered all the drill holes and could therefore not map the mineralized zone. This is clearly evident in figure 4.15 as there was no pattern in the model generated within this data range.
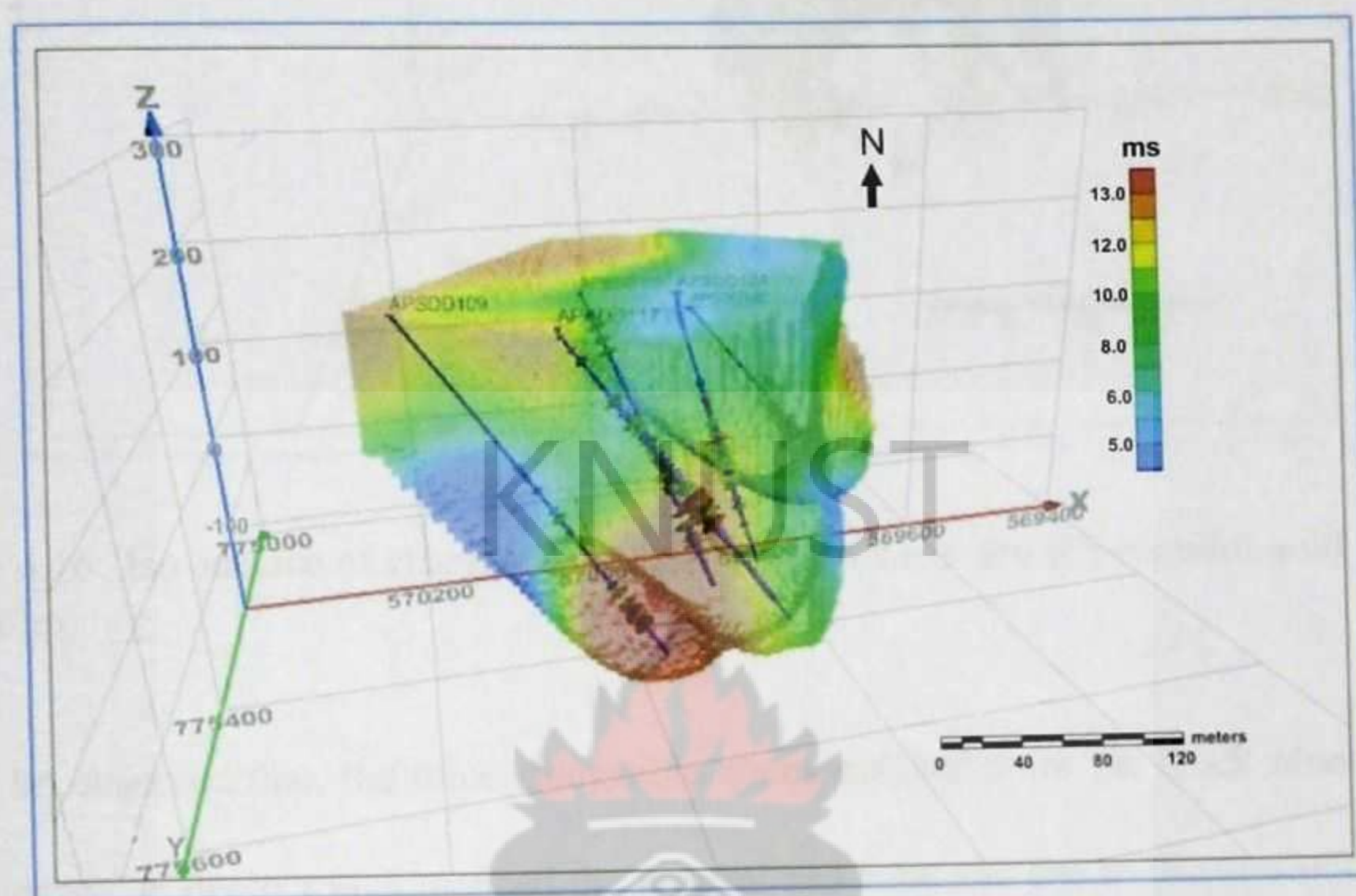

Figure 4.15: Iso-surface of chargeability data less than 4.0 ms with gold values in the drill holes.

Chargeability values between 4 and 8.5 ms were modeled. The area of figure 4.16 with values less than 4 are represented by the green color, between 4 and 8.5 is shown by the blue color whiles values greater than 8.5 ms which is shown by the brown color with the drill holes plotted on them. The different colors of rings in the drill holes are the gold assay values. From figure 4.16, the data range that map out the gold mineralized zone is clearly identified. Chargeability values greater than 8.5 ms were able to map the gold mineralized zone very well at depth as all the gold values in the drill holes fell within this range. Based on this, further models were generated on the chargeability data greater than 8.5 ms.
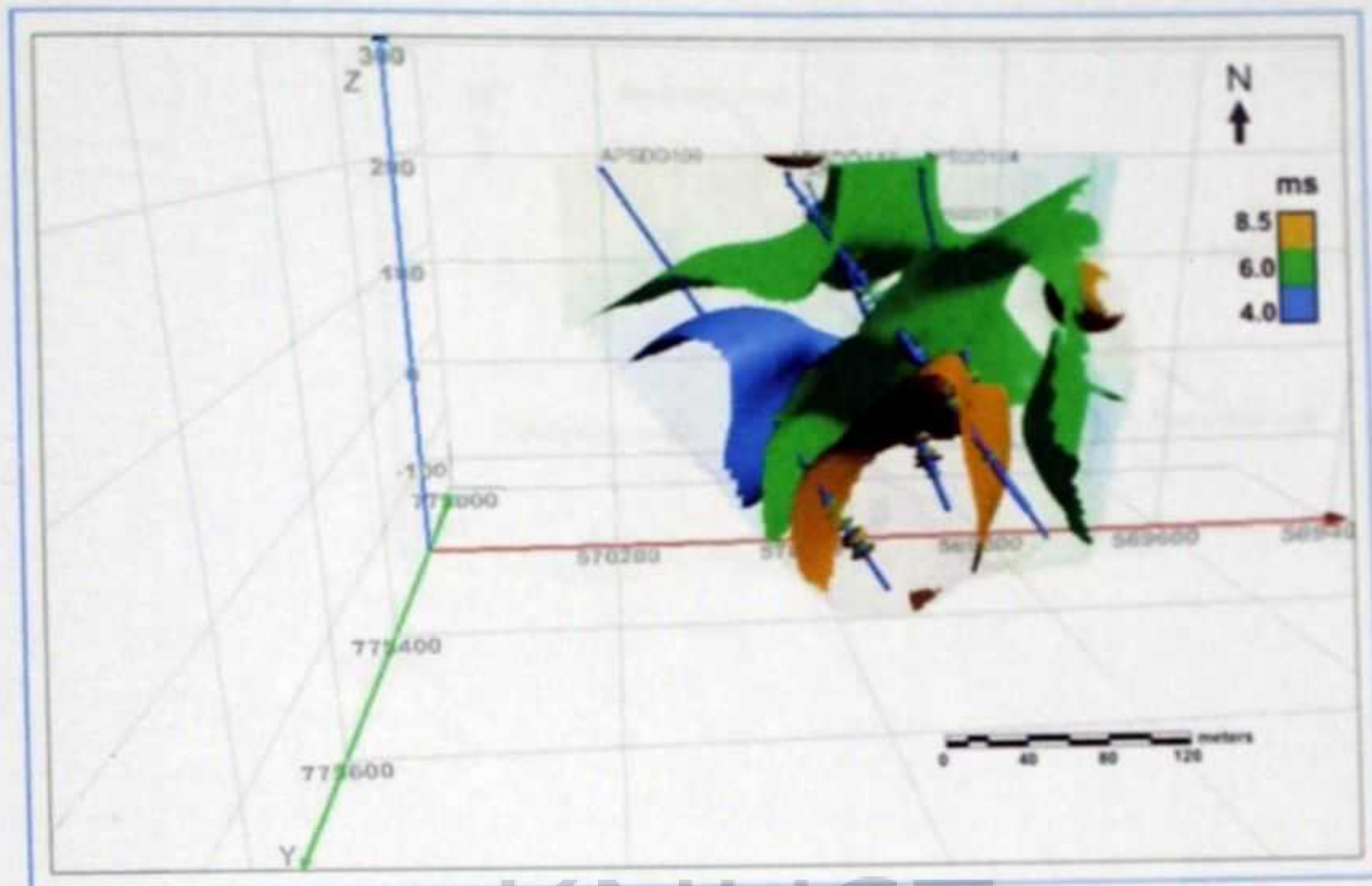
84

Figure 4.16: Iso-surface of chargeability data between 4 ms and 8.5 ms with gold values in drill holes.

It can be observed that, the three chargeable zones mapped from the block model; one at near surface, at depth which mapped the mineralized zone and one to the east of the model was clearly also mapped in the iso-surface in figure 4.17. The less chargeable zones at depth and at the surface were the areas mapped as the highly resistive zones in the resistivity model which makes sense since the reverse of conductivity is resistivity.

The data range was between 1 and 13 ms with a threshold value of 8.5ms. Taking the data through the drill hole gold values greater than 8.5 ms of the area made an interesting observation.
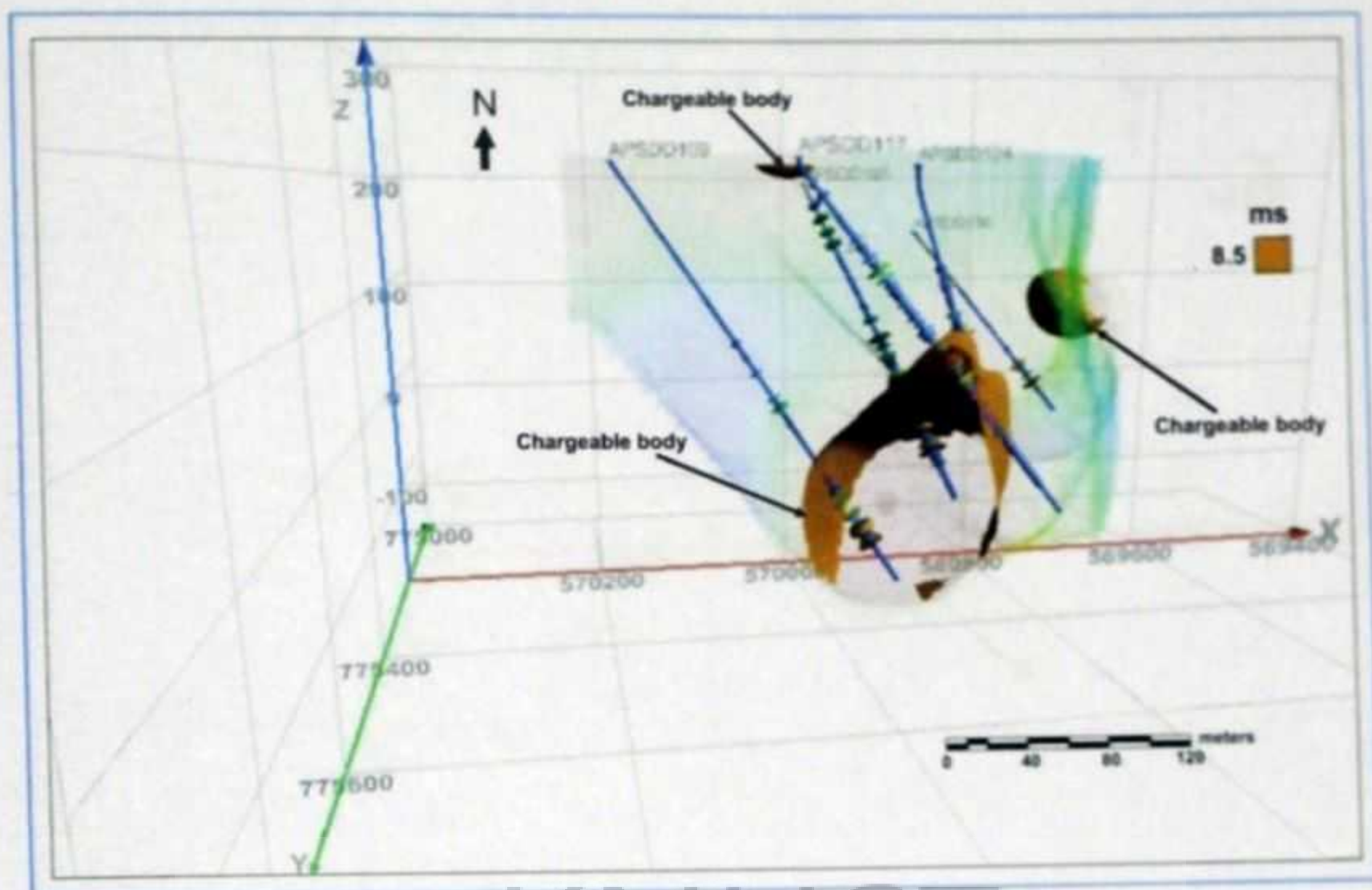
Figure 4.17: Iso-surface of chargeability data greater than 8.5 ms with drill holes and gold values.

The three distinct chargeable areas mapped out is also shown in the transparent plot in figure 4.18. It clearly showed a chargeable zone at depth, at the surface and around the mid-section with the largest chargeable body at depth. This really confirmed what the pyrite logging showed in all the drill holes as they all had some pyrite and gold values right from the near surface to the end of all the holes. Plotted on it are the drill holes with the gold values in them with most of it falling on the largest chargeable body at depth. This is clearly seen on the transparent plot.
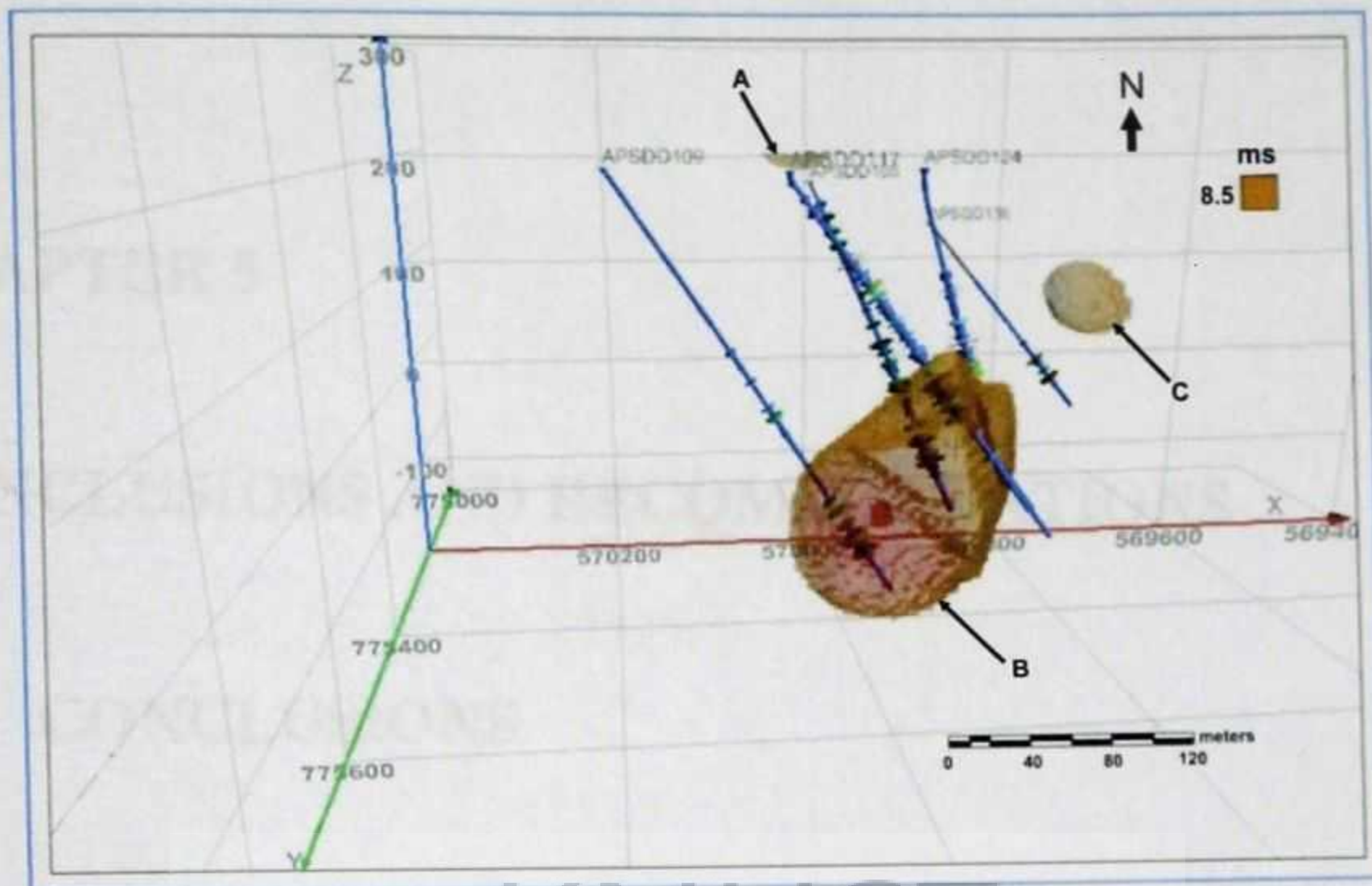
Figure 4.18: Transparent iso-surface of chargeability data greater than 8.5 ms with drill holes and gold values.

A clearer view of the good gold values in the drill holes falling inside the chargeable zone is clearly seen in the transparent plot. Most of the gold assays in all the drill holes except hole APSDD136 fell in the chargeable body labeled 'B' at depth of about 300 m below the earth surface. The round like shape on the drill holes is the gold values most of which can be seen inside the biggest chargeable body labelled 'B'. The good gold values in drill hole APSDD136 which lies out of any of the chargeable bodies but close to the one labeled 'C' is probably due to that chargeable body which will have to be tested. A closer drill hole to APSDD136 would have mapped the mineralized zone very well.

CHAPTER 5

CONCLUSIONS AND RECOMMENDATIONS

5.1   CONCLUSIONS

Hole to hole IP/resistivity down hole survey was carried out on Apensu-South concession of Newmont Ghana Gold Limited with the aim of delineating zone of gold mineralized zones at depth on the property. Petrophysical analyses such as laboratory chargeability measurement and pyrite logging were carried out on the drilled samples obtained from these holes. The pyrite logging established the presence of pyrite (disseminated sulphide) in all the drill holes used in the survey, an important source of the chargeable signature in this area. The laboratory chargeability measurements carried out on the drill core gave a positive correlation between chargeability and gold grade with a correlation co-efficient of 0.83. The hole-to-hole survey results revealed that the survey area has a chargeable signature which can be traced at depth. The 3D model of the chargeability signature using a threshold value of 8.5 ms produced a chargeability model that coincided well with the delineated gold reserve on the property. The IP method was successful in delineating the gold mineralized zone at a depth of about 300 m. This could be attributed to the presence of disseminated sulphides, one of the major pathfinders of gold in the Birimian Super group (Kesse, 1985; Griffs et al., 2002).

The laboratory based resistivity measurements on the selected cores on the other hand

showed very weak correlation between gold assay and resistivity values with coefficient of correlation of -0.37. This was confirmed by the various 3D resistivity models which did not produce any distinctive signature that could delineate the gold mineralized zone due to the presence of the disseminated sulphide associated with the mineralized zone.

5.2 RECOMMENDATIONS

The following recommendations are made:

- Surveys should be carried out right after drilling as much as possible since most of the holes would be fresh and will not cave in as being the case for most of the drill holes which are closer to mining pit.

- The drill holes should be cased with PVC pipes from the surface to the end of the saprolite zone to prevent the holes from caving in thereby keeping the holes open.

- A heavier dummy probe is recommended to prevent the stacking of the probe in the drill holes which was one of the major problems encountered during the probing stage.

- The pyrite logging should be carried out on all the drill holes to be surveyed to establish the presence of pyrite in this area which will give much impetus for this method.

- Drilling to test the other mapped chargeable zone to the west of the major delineated zone at depth is also recommended.

- It is also strongly recommended that the survey is carried on a large strike length with more holes as the previous two surveys have been on small scales with fewer drill holes.

89

- A survey on a different terrain and geology with probably graphite and other pathfinder minerals will help in the full understanding of this method in exploring for gold in the Birimian in general.

REFERENCES

Abitibi Geophysics report on Newmont Subika project, 2011

Abitibi Geophysics report on Regcourt project, 2011

Ahafo Feasibility Study, 1997.

Ahafo Gold Mine Environmental report to EPA, 2006.

Ahafo Gold mine Environmental report to EPA, 2007.

Ahafo, mineral reserve and resources report, 2008.

Ahafo Gold Mine Environmental report to EPA, 2009.

Allibone, A. H., McCuaig, T. C., Harris, D., Etheridge, M., Munroe, S., Byrne, D., & Gyapong, W. (2002). Structural controls on gold mineralization at the Ashanti deposit, Obuasi, Ghana. Special Publication-Society of Economic Geologists, 9, 65-94.

Advanced Geosciences, Inc., 2003.

Berube, Pierre, Eng., & Wasylechko, Roman (2010). Ontario Mineral Exploration review.

Daniels, J. J., & Dyck, A. V. (1984). Borehole resistivity and electromagnetic methods applied to mineral exploration. Geoscience and Remote Sensing, IEEE Transactions on, (1), 80-87.

EAGE 69th Conference & Exhibition — London, UK, 11 - 14 June 2007

Eisenlohr, B. N. (1989). The Structural Geology of Birimian and Tarkwaian Rocks of Southwest Ghana. Rep. Arch. BGR, 106448, 66.

Eisenlohr, B.N., & Hirdes, W. (1992). The structural development of the early Proterozoic Birmian and Tarkwaian rocks of southwest Ghana.

Griffis, J.R, & Agezo, F.L. (2000). Gold deposits of Ghana, 7-14.

Grow, L. M. (1982). Induced polarization for geophysical exploration. The Leading Edge, 1(1), 55-70.

Cook, Kim. (2010). Geological interpretation of Ahafo District.

Hirdes, W., Davis, D. W., and Eisenlohr.B.N. (1992). Reassessment of Proterozoic granitoid ages in Ghana on the basis of U/Pb zircon and monazite dating. Precambian Research, 56, 89-96.

John, M. (1939). Field Geophysics–a handbook of geophysical society of London.

91

Junner, N. R. (1935). Gold in the Gold Coast. Gold Coast Geol. Surv. Mem. 4, 67.

Junner, N. R. (1940). Geology of the Gold Coast and Western Togoland (with revised geological map). Gold Coast Geological Survey Bulletin. 11, 40, Accra.

Keller, G. V., & Frischknecht, F. C. (1966). Electrical methods in geophysical prospecting.

Kemna, A., Binley, A., & Slater, L. (2004). Crosshole IP imaging for engineering and environmental applications. *Geophysics*, *69*(1), 97-107.

Kesse, G.O. (1985). The mineral and rock resources of Ghana. Balkema, Rotterdam.

Leube, A., and Hirdes,W. (1986). The Birimian Supergroup of Ghana – depositional environment, structural development and conceptual model of an Early Proterozoic suite. Rept No 99529, Arch. BGR: 260 , Hannover (unpubl.).

Leubes A, Hirdes, Mauer, W. R, Kesse. G.O. (1990). The early Proterozoic Birimian Supergroup of Ghana and some aspects of its associated gold mineralization, Precamb Res: 139-165.

Loke, M.H. (2004). 2-D and 3-D Electrical Imaging Surveys.

Loke, M. H., & Barker, R. D. (1996). Practical techniques for 3D resistivity surveys and data inversion1. Geophysical Prospecting, 44(3), 499-523

Manu, E. (2011). Application of Ground Penetrating Radar in Delineating Zones of Gold Mineralization at the Subenso-North Concession of Newmont Ghana Gold Limited.

Marshall, D.J., & Madden, T.R. (1995). Induced polarization, a study of its causes. Geophysics, 24(4), 790-816.

Mwenifumbo, C. J. (1997). Electrical methods for ore body delineation. In Proceedings of Exploration, 97, 667-676.

Newmont Ahafo Gold Mine report to EPA, 2006-2009.

Olivar, A., de Lime, L. and Sharma, M.M. (1990). A grain conductivity approach to shaly sandstones. Geophysics, 55(10), 1347-1356.

Patella, D., & Schiavone, D. (1977). Comparative Analysis of Time Domain and Frequency Domain in the Induced Polarization Prospecting Method. Geophysical Prospecting, 25(3), 496-511.

Pelton, W. H., Ward, S. H., Hallof, P. G., Sill, W. R., & Nelson, P. H. (1978). Mineral discrimination and removal of inductive coupling with multifrequency IP. Geophysics, 43(3), 588-609.

Reynolds, J. M. (1997). An introduction to applied and environmental geophysics. State the publishes

Takyi-kyeremeh, K. (2010). Integrated Geophysical Study of the Subika Deposit of Newmont Ghana Ahafo Project, Thesis work submitted to the Department of Physics, KNUST, for the award of MSc. Geophysics.

Taylor. P.N., Moorbath, S., and Hirdes,W. (1992). Paleoproterozoic crustal evolution in the Birimian of Ghana; constraints from geochronology and isotope geochemistry Precambrian Research, 56, 97-111.

Telford, W.M., Geldart, L.P., Sheriff, R.E. and Keys, D.A. (1990). Applied Geophysics. (Second Edition), Cambridge University Press, Cambridge, 770.

93

Appendix A

A.1 Used Softwares

• LATEX: typesetting and layout

• Coral Draw X5: graphics

• Oasis Montaj (Geosoft): data processing and enhancing

• ArcGIS Desktop 10